Characterization of the epigenetical inactivation of the tumor suppressor gene *RASSF1A* in human mammary epithelial cells

Dissertation

zur Erlangung des akademischen Grades

doctor rerum naturalium (Dr.rer.nat.)

vorgelegt der

Mathematisch-Naturwissenschaftlich-Technischen Fakultät
(mathematisch-naturwissenschaftlicher Bereich)
der Martin-Luther-Universität Halle-Wittenberg

von Frau Maria Hahn, geb. Strunnikova
geboren am 01.02.1977 in Sankt-Petersburg

Gutachter:

1. Prof. Dr. G. Reuter

2. Prof. Dr. B. Horsthemke

Halle (Saale), den 10.Oktober 2005

Contents

Abbreviations

µ	micro
5-Aza-CdR	5-aza-2'-deoxycytidine
Aprt	adenine phosphoribosyltransferase
APC	anaphase-promoting complex
ATM	ataxia telangiectasia-mutated kinase
ATP	adenosine triphosphate
BSA	albumin bovine, fraction V
bp	base pair
cDNA	complementary deoxyribonucleic acid
ChIp	chromatin immunoprecipitation
CNK	connector enhancer of KSR
COBRA	combined bisulfite restriction analysis
dATP	deoxyadenosine triphosphate
dCTP	deoxycytosine triphosphate
dGTP	deoxyguanosine triphosphate
dNTP$_S$	deoxyribonucleoside triphosphates
DMEM	Dolbecco's MEM
DNA	deoxyribonucleic acid
DNMT	DNA methyltransferase
Dntt	terminal deoxynucleotidyltransferase
DTT	dithiothretol
dTTP	deoxythymidine triphosphate
GSTP1	glutathione-S-transferase
E.coli	*Escherichia coli*
EDTA	ethylene diamine tetraacetic acid 2Na
EGTA	ethylene glycol tetraacetic acid
Electro mobility-shift assay	EMSA
EtOH	ethanol
h	hour
HAT	histone acetyltransferase
HDAC	histone deacetylase
HF	human fibroblasts
HMF	human mammary fibroblasts
HMEC	human mammary epithelial cell

IDS	*iduronate-2-sulfatase* gene
IGFBP-3	insulin-like growth factor-binding protein-3
kb	kilobase pair
l	liter
LM-PCR	ligation-mediated polymerase chain reaction
LOH	loss of heterozygosity
M	mole
MBD	methyl-CpG binding domain protein
MCAF	MBD1-containing chromatin-associated factor
min	minute
MSP	methylation specific polymerase chain reaction
NME	normal mammary epithelium
NP-40	Nonindet P- 40
PBMC	peripheral blood mononuclear cells
PBS	phosphate buffered saline
PCR	polymerase chain reaction
PD	population doublings
PMSF	phenylmethylsylfonil fluoride
RB	retinoblastoma
RASSF1	Ras-association domain family 1
RNA	ribonucleic acid
rpm	rotations per minute
RT	room temperature
RT-PCR	reverse transcription PCR
SDS	sodium lauryl sulfate
s	second
SA-β-gal	senescence-associated β-galactosidase
Tan	annealing temperature
Tm	measurement temperature
TBE	Tris-borate-EDTA buffer
TRF	telomere restriction fragment
Tris-HCL	tris
UV	ultra violet light

1 Introduction

1.1 Epigenetics

The malignant program of the cancer cells is associated with altered function of genes or its inactivation. This can be mediated by disruption of coding sequences and epigenetical alterations. Two epigenetical modifications are critical for transcription regulation: DNA methylation and chromatin modification. Recent studies showed that epigenetical changes have a central role in neoplastic progression.

1.1.1 DNA methylation

Mammalian genomic DNA contains four bases. In addition to these, a fifth base, methylated cytosine is found (reviewed by Laird, 1999; Herman and Baylin, 2003). The cytosine methylation is a post-replicative event occurring symmetrically on both DNA strands at CpG sites and provided by DNA methyltransferases (*DNMT*). The pattern and content of CpG methylation is cell specific. In the genome, CpGs are mostly clustered in CpG islands (reviewed by Herman and Baylin, 2003). As supposed, methylated cytosine can be deaminated with subsequent replacement by thymidine (reviewed by Laird, 1999). Hence, most of the CpGs without any regulatory role were eliminated in evolution to prevent these mutations. The localization of CpG islands is often associated with the promoter regions (reviewed by Jones and Laird, 1999; Esteller and Herman, 2002). In the transcribed genes, upstream regions of the CpG islands are usually unmethylated. The DNA methylation in the 5' end of the promoter CpG island mostly leads to inactivation of transcription. Imprinted genes, germ-specific genes, tissue-specific genes and X chromosome are examples of the transcriptional inactivation by DNA methylation (reviewed by Rountree *et al.*, 2001; Esteller and Herman, 2002; Herman and Baylin, 2003). The control of the mechanism, which protects promoter from DNA methylation, can be lost during aging, since gradual increase of the *de novo* DNA methylation takes place in non-imprinted genes during senescence (reviewed by Jones and Laird, 1999). In cancer cells, hyper- and hypomethylation of DNA are found (reviewed by Herman and Baylin, 2003). Aberrant DNA hypomethylation is identified in normally imprinted genes and chromosome pericentromeric regions of malignant cells. DNA hypomethylation of pericentromeric

regions leads to chromosome instabilities and mistakes in replication. *De novo* DNA methylation of the promoters and the following gene silencing were observed in several tumor suppressor genes in cancer cells. In some cases, the DNA methylation can mediates gene inactivation even when CpG island is located outside the promoter (reviewed by Jones and Laird, 1999). However, aberrant DNA methylation of the CpG islands does not always lead to transcriptional inactivation and also the genes inactivated by DNA methylation in cancer cells are not always tumor suppressor genes.
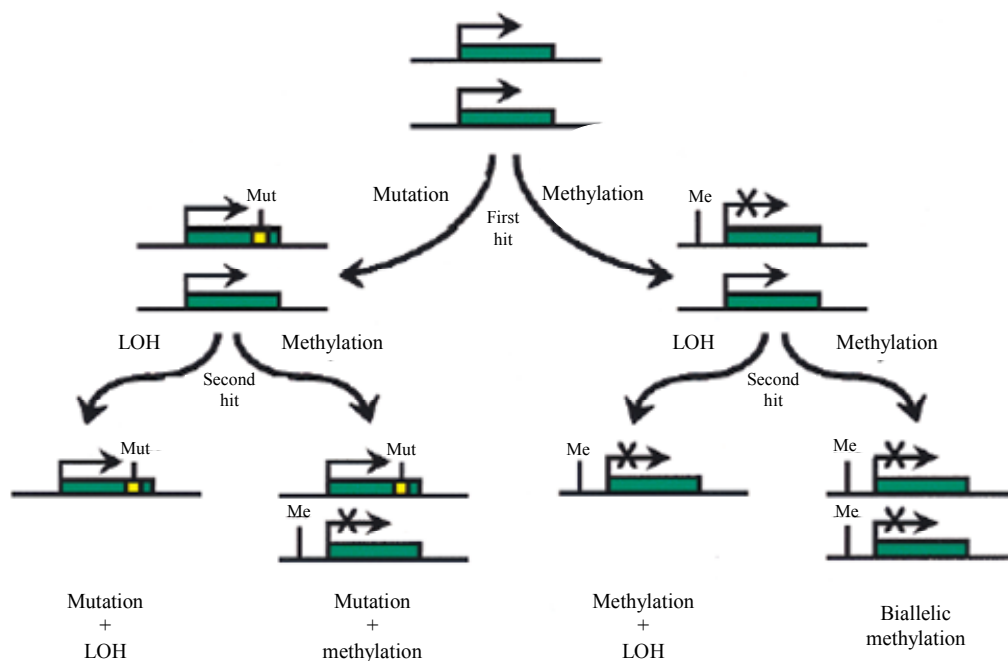
Figure 1-1. Knudson's two-hit hypothesis revised. Two active alleles of a tumor suppressor gene are indicated by the two green boxes shown at the top. The first step of gene inactivation is shown as a localized mutation on the left or by transcriptional repression by DNA methylation on the right. The second hit is shown by either LOH or transcriptional silencing (Adopted from Jones and Laird, 1999).

The inactivation mechanism of the tumor suppressor gene by DNA methylation was proposed by Jones and Laird (Figure 1-1) using Knudson's two-hits model (Jones and Laird, 1999). Knudson's model defines that the inactivation of both alleles is necessary for the loss of gene function (Figure 1-1). According to Jones and Laird, the first and second inactivation hits can be mediated by aberrant DNA methylation in promoter region of the tumor suppressor gene (Figure 1-1). Using DNA demethylating drug 5-aza-2'-deoxycytidine (5-Aza-CdR), the importance of promoter DNA hypermethylation in gene expression was illustrated (reviewed by Herman and Baylin,

2003). The mechanism of the DNA methyltransferase (*DNMT*) inactivation by 5-Aza-CdR can be explained as an analog of cytosine, 5-Aza-CdR integrating in the DNA sequence by replication. In contrast to cytosine, 5-Aza-CdR can not be methylated by *DNMT*, while it contains nitrogen in place of carbon at fifth position of cytosine. DNA methylation is not only involved in transcription control and chromosome stability, but also in the replication time of DNA (reviewed by Herman and Baylin, 2003). The level of the DNA methylation is correlated with time of replication i.e., heavy methylated DNA replicates late as compared to unmethylated DNA regions containing active genes. DNA methylation alone does not repress transcription, since only addition of proteins to the methylated DNA and following organization of chromatin lead to transcriptional inactivation (reviewed by Rountree *et al.*, 2001; Herman and Baylin, 2003). Thus, both DNA methylation and chromatin structure are involved in regulation of transcriptional activity.

1.1.2   Chromatin

In the eukaryotic nuclei, the genomic DNA is highly folded and compacted by proteins in a dynamic structure termed chromatin. The unit of chromatin is termed nucleosome and contains 146 bp of DNA wrapped around nucleosome core (reviewed by Jenuwein and Allis, 2001; Rountree *et al.*, 2001; Ehrenhofer-Murray, 2004). The nucleosome core is formed by octamer of four core histone proteins: H2A, H2B, H3 and H4. Histone H1 is located between nucleosomes and responsible for the DNA folding in high-order chromatin structure, 30 nm fiber. Chromatin is a dynamic structure, which controls access of transcription regulators to DNA (reviewed by Herman and Baylin, 2003). When DNA is heavy methylated, nucleosomes are closely compacted. At such state, chromatin is inaccessible (heterochromatic) for the transcription regulators. In contrast, nucleosomes are spaced with wide and irregular intervals at the sites of transcribing genes. At this state, chromatin is accessible (euchromatic) for other proteins. Euchromatic and heterochromatic states have own chromatin modifications. These modifications are post-translation modifications of the histones such as histone acetylation, methylation, phosphorylation and ubiquitylation (reviewed by Ehrenhofer-Murray, 2004). Except ubiquitylation, most of the histone modifications are observed in N-terminal tails of histones. Recent studies demonstrate the importance of histone modifications in the gene regulation. Transcriptionally active chromatin is marked by

histone H3 with acetylated lysine 9, 14 and histone H3 with methylated lysine 4 (Figure 1-2) (reviewed by Jenuwein and Allis, 2001; Sarraf and Stancheva, 2004). Methylation at lysine 9 of histone H3 is associated with transcriptionally silenced gene promoters and inactive chromatin (Figure 1-2). This histone modification is found in the inactivated X chromosome and pericentromeric chromosome regions (reviewed by Nguyen *et al.*, 2002; Santoro *et al.*, 2002).
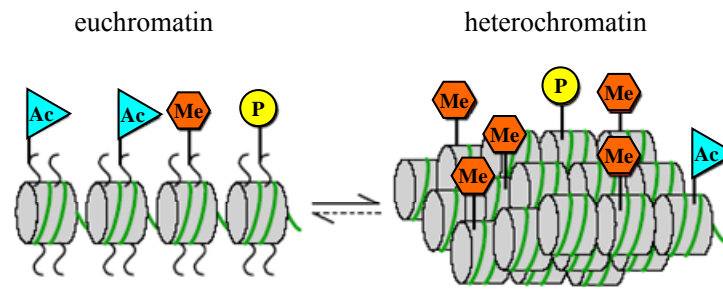
Figure 1-2. Euchromatin and heterochromatin. Schematic representation of euchromatin and heterochromatin as accessible or condensed nucleosome fibers containing acetylated (AC), phosphorylated (P) and methylated (Me) histone NH$_2$-termini (Adopted from Jenuwein and Allis, 2001).

Histone acetylation is carried out by histone acetyltransferases (*HATs*) (reviewed by Ehrenhofer-Murray, 2004). *HATs* as *p300* and *CREB-binding protein* play a role in the initiation of transcription. Removal of the acetyl groups from histone H3 by histone deacetylases (*HDACs*) leads to transcriptional inactivation, which is mediated by increasing of the chromatin compactization (reviewed by Rountree *et al.*, 2001; Herman and Baylin, 2003). Formation of inaccessible chromatin is also mediated by interaction partner of *HDAC*, histone H3 lysine 9 methyltransferase (*SU(VAR)3-9*) (Czermin *et al.*, 2001). *DNMTs* can repress gene transcription by binding of *HDACs* and transporting it to the gene promoters (Fuks *et al.*, 2000; Robertson *et al.*, 2000; Rountree *et al.*, 2000). Moreover, *HDACs* can be recruited by proteins, which specifically bind to methylated CpGs (Fuks *et al.*, 2000; Suzuki *et al.*, 2003; reviewed by Rountree *et al.*, 2001; Esteller and Herman, 2002; Herman and Baylin, 2003). These proteins are termed Methyl-CpG binding domain proteins (*MBDs*). *MBDs* have the ability to repress transcription by itself (reviewed by Herman and Baylin, 2003) and interact with histone H3 lysine 9 methyltransferase (Fuks *et al.*, 2003; Sarraf and Stancheva, 2004). Moreover, *DNMT1* is identified in complexes with *MBDs* (*MBD2*, *MBD3 and MeCP2*) (Tatematsu *et al.*, 2000; Kimura and Shiota, 2003). Out of six

mammalian *DNMTs* (*DNMT1*, *DNMT1o*, *DNMT2*, *DNMT3a*, *DNMT3b* and *DNMT3L*), *DNMT1* methylates DNA with hemi-methylated CpGs and is responsible for maintaining of DNA methylation after each round of replication; whereas other *DNMTs* are only specific for the development or methylate *de novo* DNA or have no catalytic activity (reviewed by Robertson, 2002; Jaenisch and Bird, 2003). In addition, absence of *DNMT1* in cancer cells leads to disorganization of nuclear structure, increasing in acetylation and decreasing in methylation at lysine 9 of histone H3 (Espada *et al.*, 2004). In concordance with this observation, Fuks and colleagues identified *SUV39H1* histone H3 lysine 9 methyltransferase in a complex with *DNMT1* and *DNMT3a* (Fuks *et al.*, 2003).
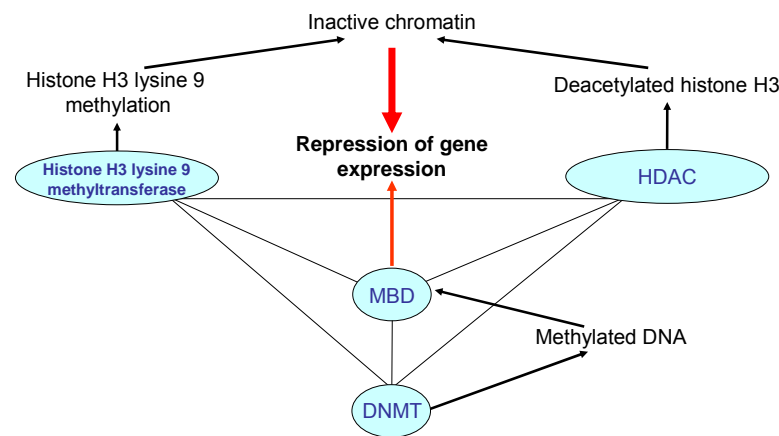
Figure 1-3. Maintaining of inactive chromatin. Connecting lines indicate interaction partners. Arrows indicate functions or following effect.

Furthermore, after 5-Aza-CdR treatment of cancer cells with the epigenetically inactivated $p16^{INK4}$ promoter, the following changes were observed: the upregulation of $p16^{INK4}$ expression, reduction of levels of methylated histone H3 lysine 9 and *MBD* (*MeCP2*), increasing levels of acetylated histone H3 and methylated histone H3 lysine 4 (Nguyen *et al.*, 2002). Thus, histone modifications and DNA methylation are related events, which play a role in the promoter inactivation (Figure 1-3).

1.1.3   Specificity protein 1 (*Sp1*)

Many housekeeping, tissue-specific and viral genes contain functionally important GC- and related GT/CACC-boxes. The proteins from *Sp* family recognize and bind to

these motifs. The *Sp* family includes four isoforms: *Sp1*, *Sp2, Sp3* and *Sp4* (Hagen *et al.*, 1992; reviewed by Suske, 1999; Samson and Wong, 2002). Three of them: *Sp1*, *Sp3* and *Sp4* recognize and bind to GC boxes as well as to GT/A-rich motifs with similar affinity (Hagen *et al.*, 1992; reviewed by Suske, 1999; Samson and Wong, 2002). *Sp1* and Sp3 are expressed in a wide variety of mammalian cells. *Sp2* binds preferentially to GT/A-rich sequences and is detected predominantly in neuronal tissues. *Sp* proteins belong to a family of transcription regulators known as the mammalian *Sp/XKLF* or "Krüppel-like" factors. *Sp/XKLF* proteins are characterized by a highly-conserved DNA-binding domain containing three Krüppel-like C_2H_2 zinc fingers. Homological proteins to the *Sp/XKLF* were identified in *Drosophila melanogaster*, *Caenorhabdidtis elegans* and yeast (reviewed by Philipsen and Suske, 1999; Suske, 1999; Turner and Crossley, 1999; Samson and Wong, 2002). *Sp1* was one of the first eukaryotic transactivators to be isolated. In 1983, using *Sp1* isolated from HeLa cell extracts, Dynan and Tjian performed *in vitro* transcription from the *SV40* viral early promoter (Dynan and Tjian, 1983). *Sp1* may form tetramers by interaction of glutamine-rich domains (Figure 1-4) (reviewed by Samson and Wong, 2002). Formation of these tetramers can be involved in a DNA loop formation. The carboxyl-terminal domain of *Sp1* may play an important role in the *Sp1* synergistic activation by the stacking of tetramers (Figure 1-4) (Matsushita *et al.*, 1998). By direct interactions with DNA or via interactions with other transcription regulators, *Sp1* mediates activation and repression of different promoters (reviewed by Kavurma and Khachigian, 2004).

Figure 1-4. Structural features of the *Sp1* protein. The *Sp1* length is indicated on the right. Red boxes indicate 2 glutamine rich regions and blue box represents a carboxyl-terminal domain. The black boxes label the zinc fingers.

Sp1 and its isoform *Sp3* bind to the same motif. *Sp3* protein was originally found as a repressor of the *Sp1*-mediated activation by binding to the same site (Hagen *et al.*, 1994). Analysis of different promoters showed that *Sp1* and *Sp3* may display parallel or opposing transcription activities (reviewed by Samson and Wong, 2002). *Sp1*

interacts with *TAFII130*, which is a subunit of the general transcription factor *TFIID* (Pugh and Tjian, 1990; Tanese *et al.*, 1996). There are speculations that *Sp1* may play a role as TATA box in the TATA less promoters, since *Sp1* can recruit *TFIID* (Kaufmann and Smale, 1994; Tanese *et al.*, 1996). Also, *Sp1* can interact with other proteins such as the early growth response factor *Egr-1*, octamer transcription factor *Oct-1* and nuclear receptors for estrogens or androgens (reviewed by Samson and Wong, 2002). Furthermore, *Sp1* interacts with *E2F1*, *c-Myc*, *p53* and *HDAC1* (Karlseder *et al.*, 1996; Doetzlhofer *et al.*, 1999; Gartel *et al.*, 2001; Lagger *et al.*, 2003). Importance of *Sp1* was shown by Marin and colleagues. They demonstrated that *Sp1 null* embryos are severely retarded in growth and die after day 10 of embryonic development (Marin *et al.*, 1997). The *Sp1* sites appear to play a critical role in the maintenance of the methylation-free CpG islands, since the removal or mutation of the *Sp1* motif exposes DNA methylation of the CpG-rich regulator regions (Macleod *et al.*, 1994; Brandeis *et al.*, 1994; Gazzoli and Kolodner, 2003). The open question is still: is the *Sp1* binding sensitive to the DNA methylation at the *Sp1* site or not? Several reports demonstrated that *Sp1* is insensitive to the DNA methylation (Holler *et al.*, 1988; Harrington *et al.*, 1988; Mancini *et al.*, 1999). Whereas in other studies, methylated CpGs variably reduce the *Sp1* binding (Gazzoli and Kolodner, 2003; Chang *et al.*, 2004; Butcher *et al.*, 2004). However, Wei-Guo Zhu and colleagues demonstrated that methylation at CG sites outside of the consensus *Sp1*-binding site may directly reduce the ability of *Sp1/Sp3* to bind (Zhu *et al.*, 2003). In summary, *Sp1* plays an important role in transcription regulation by recruiting *RNA polymerase II* via *TFIID*, by interacting with DNA, transcriptional factors and *HDAC1* and also by protecting the promoters from aberrant DNA methylation.

1.2 *RASSF1A*

In 2000, Dammann and colleagues discovered and cloned a new gene, *RASSF1* from common homozygous deletion area at 3p21.3 (Dammann *et al.*, 2000). This gene is termed <u>Ras</u>- <u>association</u> domain <u>family</u> 1 (*RASSF1*) gene because of the predicted *Ras*-association domain and homology to the murine *Ras*-effector *NORE1*. Homology search and cDNA screening identified 7 alternatively spliced transcripts: *RASSF1A*, *RASSF1B* (minor form), *RASSF1C*, *RASSF1D* (cardiac-specific), *RASSF1E* (pancreas-specific), *RASSF1F* and *RASSF1G* (reviewed by Dammann *et al.*, 2003). *RASSF1A*

and *RASSF1C* are major transcripts, which are expressed in normal tissues (Dammann *et al.*, 2000). Both isoforms have four common exons, which encode the *RAS*-association domain (Figure 1-5). The transcription of *RASSF1A* and *RASSF1C* starts from two different CpG islands, which are approximately 3.5 kb apart (Figure 1-5). The *RASSF1A* transcript is frequently missing in human cancer cells in contrast to *RASSF1C*, which is identified in all analyzed malignant cells except cells containing homozygous deletion of this region (reviewed by Dammann *et al.*, 2003). To identify mutations of *RASSF1A*, sequences of its exons were analyzed in cancer cells. Only two confirmed somatic mutations were identified in more than 200 different carcinoma samples. Thus, mechanism of the *RASSF1A* inactivation is other than mutagenesis. Analysis of the *RASSF1A* CpG island identified frequent methylation of the *RASSF1A* promoter in cancer cells. Further research showed that DNA hypermethylation of the *RASSF1A* CpG island is the most frequent event in primary human cancer. In lung tumor, DNA hypermethylation of the *RASSF1A* promoter is correlated with advanced tumor stages and impaired survival of patients. Methylation of the *RASSF1A* promoter corresponds also with LOH frequency in several types of cancer. Furthermore, the *RASSF1A* inactivation is associated with viral infections of *SV40* and *EBV*. Expression of exogenous *RASSF1A* inhibits tumor growth *in vitro* and *in vivo* (Dammann *et al.*, 2000; Li *et al.*, 2004; Song *et al.*, 2004; reviewed by Dammann *et al.*, 2003). Moreover, the *RASSF1A* knockout mice are prone to spontaneous and induced carcinogenesis (Tommasi *et al.*, 2005). Thus, *RASSF1A* plays a role as tumor suppressor gene.
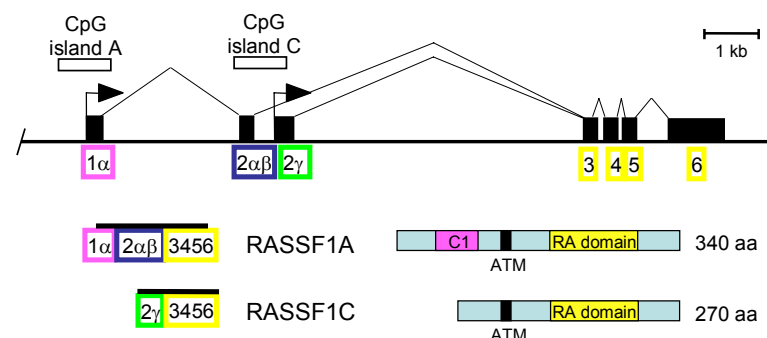
Figure 1-5. Map of the *RASSF1* gene with two main isoforms. Two promoters of *RASSF1* (arrows) are located in the CpG islands (open squares). *RASSF1A* and *RASSF1C* are made by alternative promoter usage und RNA splicing of exons (black boxes). The encoded protein length is indicated in amino acid (aa) and domains are marked as: C1 - diacylglycerol/phorbol ester binding domain; RA - RAlGDS/AF6 *Ras*-association domain; ATM - putative ATM phosphorylation site consensus sequence (Adopted from Dammann *et al.*, 2003).

Several different groups reported that *RASSF1A* is a microtubule-binding protein (Figure 1-6) (Liu *et al.*, 2003; Dallol *et al.*, 2004; Rong *et al.*, 2004; Vos *et al.*, 2004), which can directly interact with tubulins and microtubule-associated proteins (Dallol *et al.*, 2004; Rong *et al.*, 2004). *RASSF1A* stabilizes microtubules and induces growth arrest in G2/M and G1/S phases (Figure 1-6) (Shivakumar *et al.*, 2002; Liu *et al.*, 2003; Rong *et al.*, 2004). Its association with microtubules was observed at interphase; whereas in mitosis, *RASSF1A* colocalizes with spindles and centrosomes (Figure 1-6) (Liu *et al.*, 2003). Additionally, control of the cell cycle can be mediated by the *RASSF1A* interaction with *Cdc20*, an activator of anaphase-promoting complex (*APC*) (Song *et al.*, 2004). After interaction with *RASSF1A*, *Cdc20* will not activate *APC* and the cell cycle is blocked at prometaphase. The other interaction partner of *RASSF1A* is *p120^{EAF}* (Fenton *et al.*, 2004). *p120^{EAF}* interacts with *retinoblastoma* (*RB*) and *p53* and is involved in the control of entering the S-phase (Fenton *et al.*, 2004). Furthermore, *RASSF1A* negatively regulates cyclin *D1* (Shivakumar *et al.*, 2002), which mediates phosphorylation of *RB* and controls the exit from G1 phase (reviewed by Sherr, 1996).
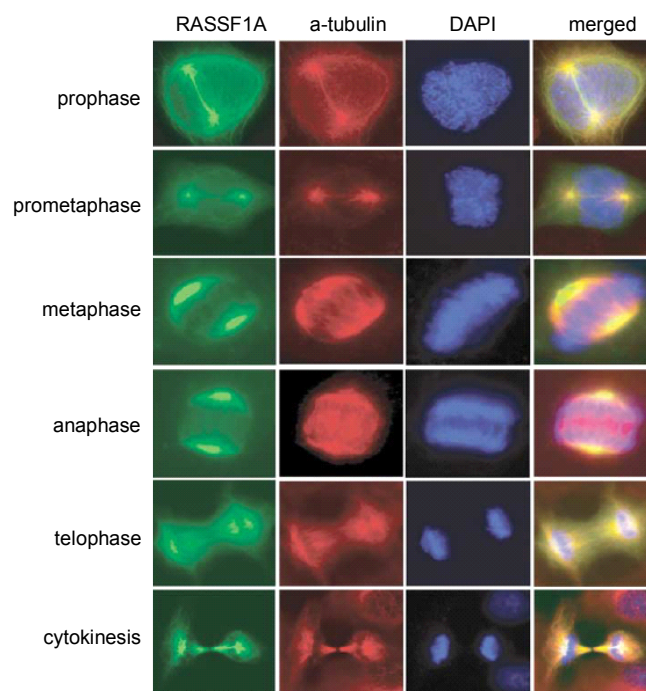
Figure 1-6. *RASSF1A* localizes to the mitotic apparatus during mitosis. COS-7 cells transfected with *GFP-RASSF1A* (green) were fixed, permeabilized and co-stained with an anti-a-tubulin antibody (red) and DAPI (blue). Cells at each mitotic stage are as indicated (Adopted from Liu *et al.*, 2003).

RASSF1 as *NORE1* can bind the serine/threonine kinase *MST1* (*mammalian sterile twenty-like*), which mediates the *Ras*-apoptotic effect (Khokhlatchev *et al.*, 2002). *RASSF1* and *NORE1* can form heterodimers, therefore, as supposed, *RASSF1* is also involved in the *Ras*-signaling (Ortiz-Vega *et al.*, 2002). However, the *RASSF1C-NORE1* interaction is weaker compared to the *RASSF1A-NORE1* binding. Furthermore, *RASSF1C* can stabilize microtubules but not as effective as *RASSF1A* (Rong *et al.*, 2004; Vos *et al.*, 2004). *RASSF1C* induces cell cycle arrest (Rong *et al.*, 2004). The inactivation of *RASSF1C* and *RASSF1A* leads to the *Ras*-induced genomic instability (Vos *et al.*, 2004). Moreover, Li and colleagues identified that *RASSF1C* may play a role as a tumor suppressor gene, since *RASSF1C* can repress the growth of cancer cells *in vitro* and *in vivo* and the mutations or loss of expression of *RASSF1C* were observed in tumors (Li *et al.*, 2004). The connector enhancer of *KSR* (*CNK*) is a *c-Raf* binding protein mediating *Ras*-induced *Raf* activation (Rabizadeh *et al.*, 2004). *CNK1* is an interaction partner of *RASSF1*. *CNK* can repress division of cancer cells and initiate apoptosis via complex *RASSF1A-MST1* (*or MST2*). Hence, *RASSF1A* supports the *CNK1* apoptotic effect in contrast to *RASSF1C*, which does not influence the *CNK1* induced apoptosis. In addition, both isoforms contain a consensus of phosphorylation site for ataxia telangiectasia-mutated kinase (*ATM*) (Dammann *et al.*, 2000), which plays a role in cycle arrest, apoptosis and maintaining of the genomic instability (reviewed by Shiloh and Kastan, 2001). Mutation of this site in *RASSF1* leads to significant reduction in the protein phosphorylation level compared to wildtype (Shivakumar *et al.*, 2002). Moreover, cancer cell transfected with mutated *RASSF1A* at position for *ATM* phosphorylation could enter the synthesis phase in contrast to cells transfected with the *RASSF1A* construct without mutation. Additionally, mutations at this site were observed in cancer cells. The binding of *RASSF1* to *Ras* is still an open question. Ortitz-Vega and colleagues described this binding as weak (Ortiz-Vega *et al.*, 2002). From other side, Vos and colleagues demonstrated the *RASSF1* binding to a *Ras* in GTP-dependent manner *in vivo* and *in vitro* and the *RASSF1A* induced apoptosis (Vos *et al.*, 2000). Taken together, both *RASSF1* isoforms are associated with microtubules and can mediate cell cycle arrest and prevent *Ras*-induced genomic instability. In contrast to *RASSF1A*, *RASSF1C* shows weak or no characteristic related with cell cycle control. This could be revealed to the absence of diacylglycerol/phorbol ester binding domain in *RASSF1C*. The

frequent epigenetical inactivation of *RASSF1A* in cancer cells is associated with the function of *RASSF1A* as a tumor suppressor in cell proliferation.

1.3   Human mammary epithelial cells (HMECs)

Detection of breast cancer at early stage may save lives of patients. Hence, to study the mechanism of malignant transformation of breast cells is very important. There are evidences that inactivation of $p16^{INK4}$ tumor suppressor by its promoter methylation occurs in histological normal breast tissues (Holst *et al.*, 2003) and it may promote a premalignant cell program (Crawford *et al.*, 2004). In addition to the $p16^{INK4}$ promoter methylation in breast carcinomas, an epigenetical inactivation of $p16^{INK4}$ was identified during HMEC senescence (Brenner *et al.*, 1998; Foster *et al.*, 1998; Esteller *et al.*, 2001; Dominguez *et al.*, 2003). Analogous to $p16^{INK}$, high rate of the *RASSF1A* promoter methylation was observed in breast carcinomas (Dammann *et al.*, 2001; Dulaimi *et al.*, 2004). Moreover, histological normal breast tissues contain cells with aberrant methylation of the *RASSF1A* CpG island (Yan *et al.*, 2003; Lewis *et al.*, 2005). Thus, *RASSF1A* may be epigenetically inactivated in HMECs analogous to $p16^{INK4}$.

In tissue culture, human mammary fibroblasts (HMF) proliferate for a limited number of population doublings (PD) and then enter a plateau termed replicative senescence or Hayflick limit (reviewed by Figueroa *et al.*, 2000). It is believed that the reason for the Hayflick limit is the telomeres shortening (reviewed by Sandhu *et al.*, 2000). The shortening of telomeres is mediated due to the instability of DNA polymerase in the replication of the outermost ends of the lagging strand DNA (reviewed by Figueroa *et al.*, 2000). This instability results in a lost of approximately 50-200 bp of telomeres in each round of replication. In stem cells and some cancer cell lines, the telomere shortening is overcome by telomerase, a ribonucleoprotein complex that adds *de novo* telomeric sequences. At Hayflick limit, HMF have a mean telomere restriction fragment (TRF) of approximately 6-8 kb (reviewed by Romanov *et al.*, 2001). HMF, which reached Hayflich limit, are large vacuolated cells with a flat form and expressing senescence-associated β-galactosidase (SA-β-gal) (reviewed by Tlsty *et al.*, 2001). These cells persist to stay at this stage. After 15-30 PD, HMECs attain senescence morphology i.e., large, flat and becomes vacuolated (Figure 1-7) (reviewed by Romanov *et al.*, 2001). Similar to HMF, HMECs express SA-β-gal and have a

mean TRF of approximately 6-8 kb. At this phase, HMECs and HMF have elevated levels of the *p16^{INK4}* expression (Alcorta *et al.*, 1996; Brenner *et al.*, 1998; Foster *et al.*, 1998). In contrast to HMF obtained from the same mammary tissue, HMECs escape from this proliferation block with a high frequency of spontaneous emergence (Romanov *et al.*, 2001). After senescence selection, HMECs enter a second period of exponential growth (Brenner *et al.*, 1998; Foster *et al.*, 1998). At the post-selection stage, HMECs are characterized by heavy DNA methylation of the *p16^{INK4}* promoter followed by the absence of the *p16^{INK4}* expression (Brenner *et al.*, 1998; Foster *et al.*, 1998). After 25-45 PD, HMECs go back to senescence phenotype associated with SA-β-gal expression and enter a new plateau termed agonescence (Romanov *et al.*, 2001). Cells at agonescence are characterized by high levels of chromosome abnormalities compared to cells at senescence proliferation state. At five PD before agonescence, these abnormalities are detected in 66-100% metaphases and are mediated by critically shortened telomeres with a mean TRF of approximately 5 kb (Tlsty *et al.*, 2001; Romanov *et al.*, 2001). As proposed, the proliferative barrier at agonescence is a telomere-dependent proliferative barrier (reviewed by Stampfer and Yaswen, 2003).
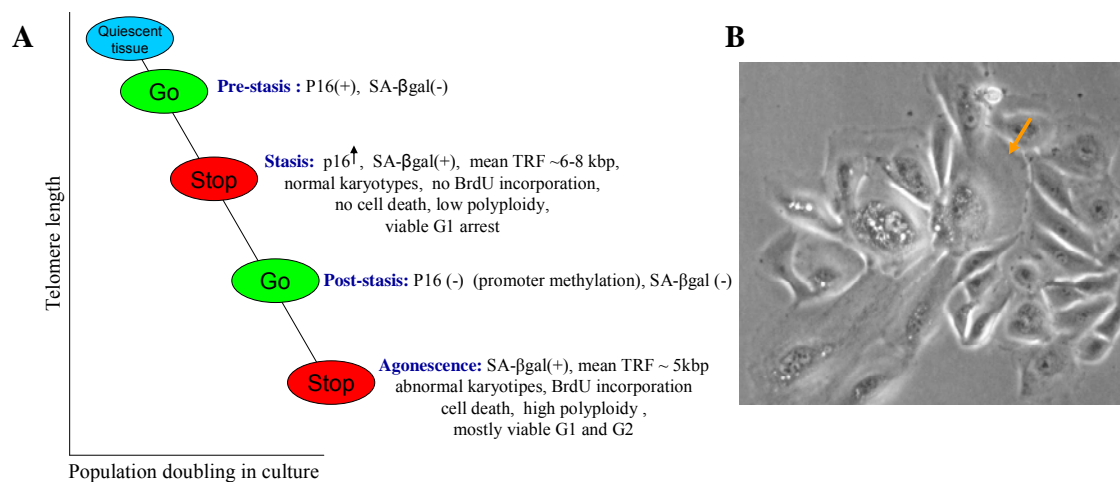
Figure 1-7. HMECs in culture. A. A model of HMEC proliferation in cell culture. **B.** HMECs in post-stasis proliferation phase (100x). Yellow arrow indicates cell in agonescence proliferation phase.

Yaswen and Stampfer suggest that the generation of chromosomal abnormalities during post-stasis may lead to telomerase reactivation (Yaswen and Stampfer, 2002). This reactivation can be a preferential way of tumor progressing of epithelial cells.

When escaping from stasis by HMECs was observed, researchers speculated that first proliferation barrier is associated with short length of telomeres (Hayflick limit)

(Romanov *et al.*, 2001). However, studies of the last years show that the elevated level of *p16^{INK4}* is responsible for this proliferation plateau via *RB* using following mechanism: *p16^{INK4}* interacts and inhibits cyclin *D1* dependent protein kinases; as a result of this interaction, *RB* can not be phosphorylated by these kinases; therefore, cells go to G1 arrest (reviewed by Sherr, 1996; Stampfer and Yaswen, 2003). Recent studies showed that the upregulation of *p16^{INK4}* is stress associated. Ramirez and colleagues found that HMECs, which were grown on feed layers, do not enter the proliferation plateau and do not show any change in the *p16^{INK4}* expression (Ramirez *et al.*, 2001; Herbert *et al.*, 2002). Furthermore, evaluation of the *p16^{INK4}* expression can be mediated by other stress types, such as high level of O_2 and inadequate medium; therefore, changing of incubation conditions can delay senescence (reviewed by Drayton and Peters, 2002). Thus, the *p16^{INK4}* inactivation in an inadequate culture environment is an event, which is necessary for proliferation. Interestingly, that researcher could not identify gross chromosome abnormalities in mouse embryo cells, which avoid stasis (Loo *et al.*, 1987). Basis on new knowledge's, the new term, stasis (stress or aberrant signaling induced senescence) had been introduced to refer to stress-associated senescence (Drayton and Peters, 2002). Stasis was identified in experiments with culture of mouse embryo cells, keratinocytes, skin fibroblast, oligodendrocyte precursor cells and normal rodent glia (Loo *et al.*, 1987; Mathon *et al.*, 2001; Tang *et al.*, 2001; Ramirez *et al.*, 2001). Shortly, HMECs in culture enter two proliferation plateaus; first is mediated by *p16^{INK4}* via *RB* and second is telomere-dependent proliferative barrier. The post-stasis cells are characterized by the epigenetically inactivated *p16^{INK4}* promoter.

1.4   Aim of study

Aim of the present study was localization and analysis of the regulatory elements in the *RASSF1A* promoter. Moreover, mechanism of epigenetical inactivation of the *RASSF1A* promoter should be elucidated in present research. In concordance with this aim, mechanism of methylation of the *RASSF1A* promoter should be analyzed. Furthermore, roles of chromatin state and transcription regulatory elements in epigenetical inactivation of the *RASSF1A* promoter should be investigated. Additionally, hypothesis about epigenetical inactivation of the *RASSF1A* promoter during senescence of HMECs should be verified.

2 Materials and methods

2.1 Materials

2.1.1 Plasmids

pGEM-T vector	Promega, Heidelberg, Germany
pGL3-promoter vector	Promega, Heidelberg, Germany
pRL-null vector	Promega, Heidelberg, Germany

2.1.2 Antibodies

Acetyl-H3 antibodies	Biomol, Hamburg, Germany
H3-trimethyl lysine 9 antibodies	Abcam, Cambridge, UK
Sp1 antibodies	Santa Cruz Biotechnology, Inc., Santa Cruz, Calif., USA
XPA antibodies	Santa Cruz Biotechnology, Inc., Santa Cruz, Calif., USA

2.1.3 Biological materials

Human MTC Panel I	Clontech Laboratories, Inc., USA
TOP 10F' E. coli competent cells	Clontech Laboratories, Inc., USA
Total RNA of normal mammary gland	BD Biosciences, Erembodegem, Belgium

2.1.4 Cell medium

DMEM 1x	Biochrom AG, Berlin, Germany
Fetal calf serum	Biochrom AG, Berlin, Germany
Epith-o-ser	C-C-Pro, Neustadt, Germany
Mammary epithelial cell growth medium	MEGM; PromoCell, Heidelberg, Germany
Opti-MeM I Reduced Serum Medium	Invitrogen, Groningen, Netherlands
RPMI 1640 with glutamine	Biochrom AG, Berlin, Germany

2.1.5 Enzymes

Alkaline phosphatase, *Shrimp*	Roche Diagnostic GmbH, Mannheim, Germany
Proteinase K	Promega, Heidelberg, Germany
RNAsin, RNAse inhibitor	Promega, Heidelberg, Germany
Restriction enzymes	New England BioLabs, Beverly, USA

SssI methylase	New England BioLabs, Beverly, USA
T4 DNA ligase	Promega, Heidelberg, Germany
T4 polynucleotide kinase	New England BioLabs, Beverly, USA
Taq$^\alpha$ I	Roche Diagnostic GmbH, Mannheim, Germany

2.1.6   Equipment

Ultrasound homogenizator, Sonicator, Bandelin Sonopuls HD2070	Bandelin Electronics, Berlin, Germany
UV spectrometer, GeneQuant pro RNA/DNA Calculator	Amersham Biosciences, Freiburg, Germany
Hybridizer HB-1D	Techne Inc., Duxford, Cambridge, USA
LightCycler "Rotor Gene 2000"	Corbett Research, Sydney, Australia
Gel Dryer, Model 583	BioRad, Muenchen, Germany
Model SA gel electrophoresis unit	Invitrogen, Groningen, Netherlands
Nylon membrane, Hybond N+	Amersham Biosciences, Freiburg, Germany
PCR cycler – Perkin Elmer DNA thermal cycler (for radioactive labelling)	Perkin Elmer, Norwalk, USA
Thermocycler, Mastercycler gradient	Eppendorf, Hamburg, Germany
Power supply, Powerpak 200	BioRad, Muenchen, Germany
Power supply, Powerpak 3000	BioRad, Muenchen, Germany
Electroblotter, the Panther Semidry Electroblotter HEP3	PeqLab- Owl Separation Systems, Biotechnologie GmbH, Erlangen, Germany
UV Stratalinker 1800	Stratagene, La Jolla, CA, USA
Vacuum concentrator, model 5301	Eppendorf, Hamburg, Germany
Phosphoimager, Storm 860	Molecular Dynamics, Inc., Sannyvale, CA, USA

2.1.7   Kits

Dual-Luciferase Reporter Assay system	Promega, Heidelberg, Germany
iScript cDNA Synthesis kit	Bio-Rad, Muenchen, Germany
QIAamp DNA kit	Qiagen, Hilden, Germany
QIAfilter plasmid Maxiprep kit	Qiagen, Hilden, Germany
QIAprep spin kit	Qiagen, Hilden, Germany
QIAquick Gel Extraction kit	Qiagen, Hilden, Germany
QuickChange XL Site-Directed Mutagenesis kit	Stratagene, La Jolla, CA, USA

Wizard DNA Clean-Up system   Promega, Heidelberg, Germany

2.1.8   Polymerases

Exo⁻ Pfu DNA polymerase   Stratagene, La Jolla, CA, USA

Expand Long Template PCR system   Roche Diagnostic GmbH, Mannheim, Germany

Fast Taq polymerase   Roche Diagnostic GmbH, Mannheim, Germany

Taq polymerase, Invitaq   InViTek, Berlin, Germany

2.1.9   Reagents

$[\alpha\text{-}^{32}P\ CTP]$ MP Biomedicals, Co., Irvine, Ca, USA

$[\gamma\text{-}^{32}P\ ATP]$ MP Biomedicals, Co., Irvine, Ca, USA

2-mercaptoethanol   Sigma, Deisenhofen, Germany

5-Aza-CdR   Sigma, Deisenhofen, Germany

Ammonium acetate   Merck, Darmstadt; Germany

ATP, lithium salt   Roche Diagnostic GmbH, Mannheim, Germany

Betain   Sigma, Deisenhofen, Germany

Boric acid   Roth, Karlsruhe, Germany

Bromphenol blue   Merck, Darmstadt; Germany

BSA   Roth, Karlsruhe, Germany

Chloroform   Roth, Karlsruhe, Germany

Deoxycholate   Sigma, Deisenhofen, Germany

Dimethyl sulfate   Fluka Biochemica, Ulm, Germany

dNTP$_S$ InViTek, Berlin, Germany

DTT   Roth, Karlsruhe, Germany

EDTA   Roth, Karlsruhe, Germany

Ethanol 96%   Merck, Darmstadt; Germany

Ficoll-Plague^{TM} Plus   Amersham Pharmacia Biotech AG, Uppsala, Sweden

Formaldehyde 37%   Roth, Karlsruhe, Germany

Formamide 99%   Serva Electrophoresis GmbH, Heidelberg, Germany

Formic acid 95%   Sigma, Deisenhofen, Germany

Glycogen   Roche Diagnostic GmbH, Mannheim, Germany

Hydrazine (64%)   Sigma, Deisenhofen, Germany

Hydroquinone	Sigma, Deisenhofen, Germany
Interleukin-2 for cell cultures	Pharma Biotechnologie Hannover, Hannover, Germany
KCl	Merck, Darmstadt, Germany
LiCl	Sigma, Deisenhofen, Germany
Lipofectamine 2000	Invitrogen, Groningen, Netherlands
$MgCl_2$	InViTek, Berlin, Germany
Na-cacodylate	Sigma, Deisenhofen, Germany
NaOH	Merck, Darmstadt, Germany
NP-40	Fluka Biochemica, Ulm, Germany
PBS 1x	Invitrogen, Groningen, Netherlands
Phenol	Merck, Darmstadt; Germany
Phytohemagglutinin	Biochrom AG, Berlin, Germany
Penicillin/streptomycin	Biochrom AG, Berlin, Germany
Piperidine 99%	Sigma, Deisenhofen, Germany
PMSF	Sigma, Deisenhofen, Germany
Protease inhibitor coctail tablets, Complete Mini	Roche Diagnostic GmbH, Mannheim, Germany
S-adenosylmethionine	New England BioLabs, Beverly, USA
Salmon sperm DNA/protein A agarose	Upstate, Charlottesville, USA
Salmon Sperm DNA	Sigma, Deisenhofen, Germany
SDS	Roth, Karlsruhe, Germany
Sephadex G-50	Pharmacia Biotech AB, Uppsala, Sweden
Sodium acetate	Merck, Darmstadt; Germany
Sodium bisulfite	Sigma, Deisenhofen, Germany
Sucrose	Merck, Darmstadt; Germany
$Sybr^{TM}$ Green I	BioWhittaker, Belgium
TBE 1x	100 mM tris, 100 mM boric acid, 2 mM EDTA pH 8.0
Tris	Invitrogen, Groningen, Netherlands
Triton X-100	Roth, Karlsruhe, Germany
Trizol reagent	Invitrogen, Groningen, Netherlands
tRNA E.coli	Roche Diagnostic GmbH, Mannheim, Germany
Urea	Roth, Karlsruhe, Germany
Water, Ampuwa	Fresenius Kabi, Bad Homburg, Germany
Xylene cyanole	Merck, Darmstadt, Germany

2.1.10 Cell cultures

Four breast cancer cell lines (T47D, MDA-MB-231, MCF7 and ZR75-1), HeLa S3 and the A549 lung cancer cell line were obtained from American Type Culture Collection and cultured in the recommended medium. Human mammary epithelial cells (HMEC-184 and HMEC-48R) were obtained from reduction mammoplasty and provided by Martha Stampfer (Lawrence Berkeley Laboratories, Berkeley CA, USA). Additional mammary epithelial cells (HMEC-219 and HMEC-1001) were purchased from Clonetics (Clonetics, BioWhittaker, Verviers, Belgium) or isolated from normal mammary epithelium (NME), which was obtained from healthy women of the Universtätsfrauenklinik Halle by reduction mammoplasty and cultivated in epith-o-ser up to a passage 4 (HMEC-141). Clonetics cell lines (HMEC-219 and HMEC-1001) were available only at post-stasis stadium and sub-cultured until they reached agonescence. HMECs were cultivated in serum free mammary epithelial cell growth medium (Epith-o-ser) to no more than 80% confluence. Cells were grown at 37°C in 5% CO_2 and medium was changed every 3 days. To determine the population doublings, the cells were counted at each passage.

2.1.11 Cultivation of the peripheral blood mononuclear cells (PBMC)

For cultivation, mononuclear cells from blood were isolated from healthy person according to the following protocol. Blood was collected using syringe containing Li-heparin (Sarstedt AG & Co., Nümbrecht, Germany). Five ml of blood was diluted with 5 ml of RPMI medium. Further, 10 ml of blood mix was overlayered onto 3 ml Ficoll-Plague™ Plus and spun without a brake for 30 min at 1400 rpm at 10°C. Interphase containing PBMC was collected and washed twice with PBS. Isolated cells were incubated for 5 h at 37°C in 5% CO_2 in RPMI medium supplemented with 10% fetal calf serum, 100 units/ml penicillin and 100 µg/ml streptomycin. Further, the non-adherent cells were transferred into new flask and cultivated in RPMI medium supplemented with 10% fetal calf serum, 100 units/ml penicillin, 100 µg/ml streptomycin and 4.8 µg/ml phytohemagglutinin at 37°C in 5% CO_2. Separation of adherent cells from non-adherent cells was performed to remove monocytes; therefore cultivated cells were mainly lymphocytes. After 72 h, medium was changed to RPMI supplemented with 10% fetal calf serum, 100 units/ml penicillin, 100 µg/ml streptomycin and 25 units/ml interleukin-2. After 4 days of cell incubation at 37°C in

5% CO_2, cells were spun for 5 min at 1500 rpm at RT, washed with PBS and used for DNA and RNA isolations.

2.1.12 Oligonucleotides

All primers were generated by Oligo 4.0 software (National Bioscience, Inc. Plymouth, USA) and produced desalted by Invitrogen (Invitrogen, Groningen, Netherlands). Linker primers for LM-PCR were produced and purified by high pressure liquid chromatography by Qiagen (Qiagen, Hilden, Germany).

2.2   Methods

2.2.1   Treatment of cells with 5-aza-2'-deoxycytidine (5-Aza-CdR)

For expressional analysis by RT-PCR (see below chapters 2.2.8 and 2.2.9), cells of HMEC-184 passage 13 and the breast carcinomas (T47D, MDA-MB-231, MCF7 and ZR75-1) were grown for 4 days in the presence or absence of 10 µM 5-Aza-CdR.

2.2.2   DNA isolation from tissues and cultured cells

Genomic DNA was extracted according to Sambrook and colleagues (Sambrook *et al.*, 1989). Briefly, DNA was isolated by cell lysis with *Proteinase K* (0.375 mg/ml) digestion at 55°C for 6 – 8 h and by extraction with phenol/chloroform. After precipitation with EtOH, DNA was dissolved in H_2O and quantified by UV spectrometry.

2.2.3   DNA isolation from blood

DNA from blood was isolated using *QIAamp DNA* kit according to the manufacturer's instructions (Qiagen), eluated with water and quantified by UV spectrometry.

2.2.4   I*n vitro* methylation of the HeLa DNA

For *in vitro* methylation, 20 µg of the HeLa DNA was treated with 60 units of *SssI* methylase (New England BioLabs) at 37°C in 200 µl of reaction mix containing 160 µM S-adenosylmethionine. After 4 h of incubation, an S-adenosylmethionine was added to a final concentration of 320 µM and the incubation was continued overnight. Further, the DNA was purified with phenol/chloroform, precipitated and dissolved at 1 µg/µl in H_2O.

2.2.5   Bisulfite treatment of the DNA

Bisulfite treatment of the DNA was carried out according to the protocol of Clark and colleagues (Clark *et al.*, 1994). Two µg of genomic DNA was denatured by adding NaOH to a final concentration of 0.3 M and incubating at 37°C for 15 min. Sodium bisulfite, to a final concentration of 3.2 M, and hydroquinone, to a final concentration

of 0.5mM, were added to the denatured DNA; samples were carefully mixed and incubated at 55°C for 16 h. The modified DNA was purified through the *Wizard DNA Clean-Up* system (Promega). NaOH, to a final concentration of 0.3 M, was added and DNA was incubated for 10 min at 37°C. After adding of 2 μg of glycogen and one volume of 7.5 M ammonium acetate, the bisulfite-treated DNA was precipitated and dissolved in 100 μl of H_2O.

2.2.6   Methylation specific PCR (MSP)

DNA methylation pattern of the *p16* CpG island was determined by MSP using primers pairs *p16*-M and *p16*-U (Table 2-1) and the conditions as described by Herman and colleagues (Herman *et al.*, 1996). Briefly, 100 ng of bisulfite-treated genomic DNA was amplified in 25 μl of reaction volume using the following final concentrations: 1x *Taq* buffer, 2 units of *Taq* polymerase (InViTek), 0.2 mM dNTPs, 1.5 mM $MgCl_2$, 4% formamide and 10 pmoles of specific primers to methylated or unmethylated DNA (Table 2-1). After an initial denaturation step at 95°C for 2 min, the cycling conditions were as follows: 92°C for 30 s, annealing temperature (Tan) (Table 2-1) for 30 s and 72°C for 30 s for 40 cycles. The last elongation step was performed at 72°C for 5 min. To prevent degradation of primers and template by 3'→5' exonuclease activity of *Taq* polymerase at low temperature (http://www1.qiagen.com/products/pcr/ proofstartsystem /default.aspx), the polymerase was added to PCR mix at 65°C (Hot Start). PCR products were resolved on a 2% TBE agarose gel.

Table 2-1. P16 gene: primers and PCR conditions for MSP

	Primers (5'→3')	T_{an}, °C	Size of PCR product, bp
P16-M[1]	U: TTATTAGAGGGTGGGGCGGATCGC L: GACCCCGAACCGCGACCGTAA	65	150
P16-U[2]	U: TTATTAGAGGGTGGGGTGGATTGT L: CAACCCCAAACCACAACCATAA	60	148

[1]Primer pair for amplification of the methylated DNA. [2]Primer pair for amplification of the unmethylated DNA.

2.2.7 Methylation analysis of the *RASSF1* locus

2.2.7.1 Combined bisulfite restriction analysis (COBRA)
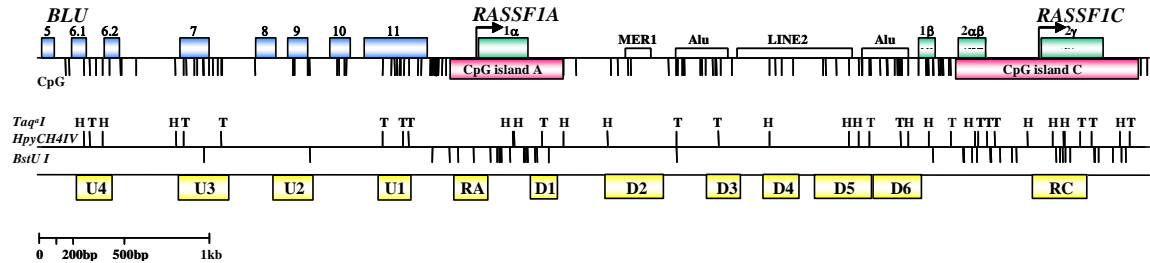
Figure 2-1. Map of the *RASSF1* locus. The arrows indicate the transcriptional start sites of the *RASSF1* isoforms. The *RASSF1* and *BLU* exons are marked by the green and blue boxes, respectively. Red boxes represent the *RASSF1A* and *RASSF1C* CpG islands. The localizations of the CpG islands were determined by CpGplot (http://www.ebi.ac.uk). Obs/Exp. sets the minimum average observed to expected ratio of C plus G to CpG in a set of 10 windows that are required before a CpG island is reported. Additional DNA elements (*Alu, MER1 and LINE2*) were located by RepeatMasker (ftp.genome.washington.edu/RM/RepeatMasker.html) and marked by white boxes. CpGs are marked by bars. The coding DNA strand was deaminated *in silicio*. The indicated 12 PCR fragments (yellow boxes) of the 7 kb locus were analyzed by COBRA. The restriction cutting sites of CpG containing sequence are shown (*HpyCH4IV, TaqᵅI and BstUI*).

The DNA methylation status of the *RASSF1* locus was determined by COBRA (Xiong and Laird, 1997). For this analysis, the primers for 12 fragments (U4, U3, U2, U1, RA, D1, D2, D3, D4, D5 and D6) of the *RASSF1* locus were generated (Figure 2-1 and Table 2-2).

For the first PCR of COBRA, 100 ng of bisulfite-treated genomic DNA was amplified in 25 µl of the reaction volume using the following final concentrations: 1x *Taq* buffer, 2 units of *Taq* polymerase (InViTek), 0.2 mM dNTPs, 1.5 mM $MgCl_2$, formamide (Table 2-2) and 10 pmoles of each primer (Table 2-2). After an initial denaturation step at 95°C for 5 min, the cycling conditions were as follows: 95°C for 20 s, T_{an} (Table 2-2) for 30 s and 72°C for 50 s (number of cycles is shown in Table 2-2). The final elongation step was performed at 72°C for 5 min.

For the nested PCR of COBRA, 5 µl of the first PCR products was amplified in 50 µl of the reaction volume using the following final concentrations: 1x *Taq* buffer, 4 units of *Taq* polymerase (InViTek), 0.2 mM dNTPs, 1.5 mM $MgCl_2$, formamide (Table 2-2) and 10 pmoles of each primer (Table 2-2). After an initial denaturation step at 95°C for 5 min, the cycling conditions were as follows: 95°C for 20 s, T_{an} (Table 2-2) for 30 s and 72°C for 40 s (number of cycles is shown in Table 2-2). The final elongation step was performed at 72°C for 5 min.

Twenty to fifty ng of the nested PCR products was digested with 2 units of restriction enzyme in 10 µl of reaction mix as described in Table 2-2. PCR product of *in vitro* methylated HeLa DNA was used as a control for complete digestion. The restriction products were resolved on a 2% TBE - agarose gel and analyzed by ImageJ 1.28V software (NIH, USA).

2.2.7.2   Bisulfite sequencing

Amplified bisulfite PCR products were subcloned into the *pGEM-T* vector according to the manufacturer's instructions (Promega). Briefly, 2 µl of PCR products was ligated with 25 ng of *pGEM-T* vector using 1.5 units of *T4 DNA* ligase (Promega) in 10 µl of reaction mix for 4 h at RT. After ligation, the DNA was transformed in *TOP 10F' E. coli* competent cells according to the manufacturer's instructions (Clontech). After "Blue/White" screening, the plasmid DNA from 5 white clones was isolated by the *QIAprep spin* kit (Qiagen) and sequenced by automated DNA sequencers (SeqLab, Göttingen, Germany) using T7B (5' TAATACGACTCACTATAGGG) and M13RL (5' GGAAACAGCTATGACCATGAT) primers.

2.2.8   RNA isolation and reverse transcription

Total RNA was extracted from cells using the Trizol reagent according to the manufacturer's instructions (Invitrogen), dissolved in water solution of *RNAsin* (1u/µl) and quantified by UV spectrometry.

cDNA was synthesized from 0.5 µg of RNA using the *iScript cDNA Synthesis* kit (BioRad) in a total volume of 20 µl which consisted of 4 µl of 5x iScript reaction mixture, 1 µl of reverse transcription mix and RNA in a nuclease-free water. cDNA synthesis conditions were as follows: 5 min at 25°C, 30 min at 42°C, 5 min at 85°C. For real time PCR experiments, ready cDNA was diluted thrice in water.

For expression analysis in normal human mammary gland, total RNA from this tissue was obtained from Clontech. To analyze gene expression in different human tissues (heart, whole brain, placenta, lung, liver, skeletal muscle and kidney), ready cDNA from the Human MTC panel I was utilized (Clontech).

Table 2-2. COBRA: PCR and restriction conditions

		First PCR			Nested PCR			Restriction	
		Primers (5'→3')	T_{an}, ºC (cycles[1]; FA[2],%)		Primer (5'→3')	T_{an}, ºC (cycles[1]; FA[2],%)	Size[3], bp	Restriction enzyme	Product
RC	CU	GTTTTTTGTGGTAGGTGGGGTTTG	57 (25; 0)	CU2	GGTGGGGTTTGTGAGTGGAGTTT	57 (40; 0)	311	*Hpy CH4*	4, 66, 117, 124
	CL	AATCCRAATCCTCTTAACTACAATAACCAC		CL2	ACTACTCRTCRTACTACTCCAAATCATTTC				
D6	5U	GGGGTGAGAATGGAGAATGGAATAT	57 (25; 2)	5U	GGGGTGAGAATGGAGAATGGAATAT	57 (40; 2)	282	*Bstu I*	142, 184
	5L	AAAACCACAAACAAAAAAACCTACTCAAC		6L2	CCAAACTAATCTCAAACTCCTAATCTCA				
D5	5U	GGGGTGAGAATGGAGAATGGAATAT	57 (25; 2)	5U2	GGGTGGATTATTTGAGATTAGGAGTTT	55 (40; 2)	368	*Hpy CH4*	58, 106, 204
	5L	AAAACCACAAACAAAAAAACCTACTCAAC		5L	AAAACCACAAACAAAAAAACCTACTCAAC				
D4	4U	GTGAGGTTGAAGAAAAGGGAATTAAATTT	58 (36; 2)				245	*Hpy CH4*	49, 196
	4L	CCCCCTACAACTCCTACTCAACTCCTT							
D3	2U	TTTTTTTTGATTTAGTGAATTAGATGTTAAA	54 (20; 2)	3U2	GGGGGGGAGTATAAAGTTGTGATAGAAT	57 (40; 2)	256	*Taq$^{\alpha}$ I*	48, 208
	2L	CTATATTCAAACAATTCTCCCACCTCA		2L	CTATATTCAAACAATTCTCCCACCTCA				
D2	2U	TTTTTTTTGATTTAGTGAATTAGATGTTAAA	54 (20; 2)	2U	TTTTTTTTGATTTAGTGAATTAGATGTTAAA	56 (40; 2)	380	*Hpy CH4*	39, 341
	2L	CTATATTCAAACAATTCTCCCACCTCA		2L2	CCCCCCAACTAAATTTATAATATCCTC				
D1	1U	GAGGGGAAGGGGTAGTTAAGGGGTA	57 (25; 2)	1U2	GGAAGGGGTAGTTAAGGGGTAG	54 (40; 2)	185	*Bstu I*	12, 32, 72, 79
	1L	TTCCCTTCACCCTAAAAATTCTAAAAAA		1L2	AACAACCACCTCTACTCATCTATAACCC				
RA	AU	GTTTTGGTAGTTTAATGAGTTTAGGTTTTTT	55 (20; 0)	AU	GTTTTGGTAGTTTAATGAGTTTAGGTTTTTT	54 (40; 6)	184	*Taq$^{\alpha}$ I*	21, 82, 92
	AL	ACCCTCTTCCTCTAACACAATAAAACTAACC		AL2	CCCCACAATCCCTACACCCAAAT				
U1	u1U	TGGGAAAAGTATGGAAAGATTTGTGTT	57 (25; 2)	u12	TAAATGAGGGTTGTAGTTGTTGAGGGT	57 (35; 2)	237	*Taq$^{\alpha}$ I*	27, 55, 122
	u1L	TACTAAAAAAAAAAAAATCCCCACATCC		u1L2	TAAAACAACACACTTAACCTACCCACTAAA				
U2	u2U	TGGTTTATTTGTAGAGTTTTTTGGTTTATTTG	59 (25; 2)	u2U2	GAAGGATTTGGTGTTGGAATAGGTAGG	59 (40; 2)	254	*Bstu I*	33, 221
	u2L	CCACCCACATCCATACCTCCTCCTACA		u2L2	CCTCCCTACCATTTCCACAAACCT				
U3	u3U	GTGTGTTGGTTTTTTTTTTTAGGTAAGTTG	58 (25; 2)	u3U	GTGTGTTGGTTTTTTTTTTTTAGGTAAGTTG	57 (35; 2)	331	*Bstu I*	151, 180
	u3L	AAAATACCTATAAAAACCCATATCCCACTAA		u3L2	ATCACCTAAAACCCAAAAACTAAAAAAAA			*Taq$^{\alpha}$ I*	37, 79, 215
U4	u4U	GTGAATATTGTGTGATTTTTTAGGAGTTGTA	56 (25; 2)	u4U2	TTGATGGAATTTGAGATTGTATTGAAGG	57 (35; 2)	283	*Hpy CH4*	41, 132, 110
	u4L	AATAAAAAAAAAACCCTACCTCCTTCCC		u4L	AATAAAAAAAAAACCCTACCTCCTTCCC			*Taq$^{\alpha}$ I*	77, 206

[1]Number of cycles. [2]Formamide concentration in PCR mix. [3]Size of PCR product

2.2.9   Quantification of transcription level by real time RT-PCR

2.2.9.1   Real time PCR

Real time PCR was carried out in a LightCycler "Rotor Gene 2000" using $Sybr^{TM}$ *green I* detection. Reactions were set up in 25 µl of volume using the following final concentrations: 1x *Taq* buffer (1.5 mM $MgCl_2$), 1 unit of *Fast Taq* polymerase (Roche), 0.25 mM dNTPs each, 10 pmoles of each primer (Table 2-3), 0.2x $Sybr^{TM}$ *Green I* (BioWhittaker), formamide (Table 2-3) and 2 µl of cDNA. After an initial denaturation step at 95°C for 5 min, the cycling conditions were as follows: 95°C for 20 s, T_{an} (Table 2-3) for 30 s, 72°C for 30 s and a fluorescence measurement after 15 s of the appropriate measurement temperature (Tm) (Table 2-3) for 50 cycles. The final elongation step was performed at 72°C for 5 min. The melting temperature of the PCR products were analyzed by a fluorescence measurement at every 1°C step after 5 s from 70°C up to 99°C. All measurements were independently repeated three times with several cDNA preparations. The amplification of PCR products was verified using melting curve option and subsequent gel electrophoresis using 2% TBE agarose gel.

Table 2-3. RT-PCR: Primers and conditions.

	Primers (5'→3')	T_{an}, °C	Tm, °C	FA[1], %	Size of PCR product, bp
RASSF1A	U: GGCTGGGAACCCGCGGTG	60	83	2	239
	L: TCCTGCAAGGAGGGTGGCTTCT				
RASSF1C	U: AGCTCGAGCAGTACTTCACCGC	64	83	2	261
	L: TCCTGCAAGGAGGGTGGCTTCT				
p16	U: GCTGCCCAACGCACCGAATAGT	60	88	2	157
	L: CTCCCGGGCAGCGTCGTG				

[1]Formamide concentration.

Data analysis was performed by Rotor Gene Software version 4.6 using comparative method (see chapter 2.2.9.3). In experiments with cDNA from different tissues, the *RASSF1A* and *RASSF1C* expression levels were plotted relative to the transcription levels in the pancreas (=100%). For analysis of the *RASSF1A* and *RASSF1C* expressions in PBMC, HeLa, HF, mammary gland, HMECs and breast cancer cell lines, the expression levels were plotted relative to transcription levels in HF (=100%). To verify the *RASSF1A* and *RASSF1C* expressions in HMEC-184 after 5-Aza-CdR

treatment, the expression levels were plotted relative to transcription level in untreated cells (=100%). For analysis of the $p16^{INK4}$ transcription in HeLa, HF, HMECs, A549, T47D, ZR75-1, MCF7 and MDA-MB-231, the expression levels of $p16^{INK4}$ were plotted relative to expression levels in HeLa (=100%).

2.2.9.2   Analysis of melting curve

Real time PCR method is based on the quantification of DNA amount at every cycle. A special fluorophor $Sybr^{TM}$ $green$ I is utilized for this analysis. $Sybr^{TM}$ $green$ I is sensitive to low amount of DNA in contrast to ethidium bromide (Schneeberger et $al.$, 1995). The fluorescence of double stranded DNA and $Sybr^{TM}$ $green$ I is at least eleven folds higher than with single stranded DNA (Zipper et $al.$, 2004).
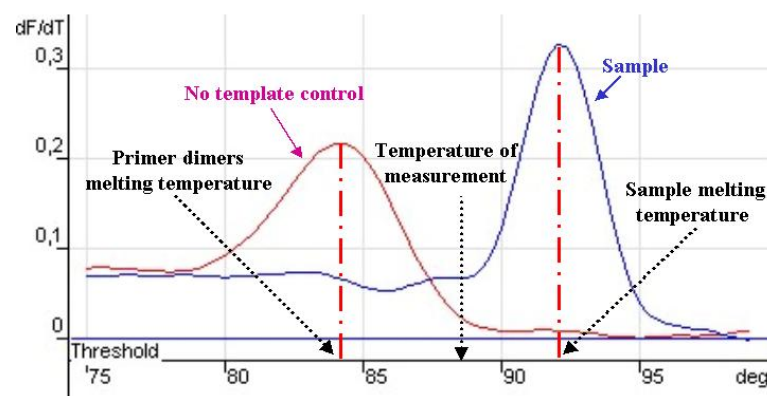
Figure 2-2. Melting data of double stranded DNA. Melting data of a sample (blue line) and of a non template control (pink line) are present as a first derivation of fluorescence level (dF/dT) versus temperature. The peaks of the graph represent the melting temperature of probes. The optimal temperature for the fluorescence measurement of the specific PCR product is indicated.

In real time PCR experiments with $Sybr^{TM}$ $green$ I, the measurement of DNA amount is performed after every elongation step at specific temperature for every primer pair. This temperature is determined using melting curve analysis (Figure 2-2). To perform this analysis, the fluorescence measurement of PCR products at every 1°C step after 5 s from 70°C up to 99°C takes place as a last step of real time PCR. Further, these raw data are presented as the first derivation of fluorescence level (dF/dT) versus temperature (Figure 2-2) (Rotor Gene Software version 4.6). The peaks of this derivation present temperature when maximal changing of fluorescence occurs during melting (Figure 2-2). Using this derivation, it is possible to identify the temperature

(Tm) when primer dimers are already melting and PCR products are double stranded (Figure 2-2). At this Tm, the amount of DNA is measured at every cycle of PCR.

2.2.9.3 Comparative method

Comparative quantification of gene expression was performed using the Rotor Gene Software version 4.6 in comparative quantification mode. This quantification is a real time PCR analysis technique, which allows the estimation of relative expressions of genes without requiring a standard curve (Herrmann and Corbett_Research, 2002). Comparative quantitation is used to compare a certain sample to any other in the same experiment (Rotor Gene Software version 4.6). The method evaluates the amplification of each sample, and then calculates an average with error coefficient. The average of the amplification is required to compare the reaction of samples by analysis the relative Take-Off points of each sample (Herrmann and Corbett_Research, 2002). To calculate the Take-off point, the second derivative of the raw data of fluorescence measurements at every cycle is taken (Rotor Gene Software version 4.6) (Figure 2-3). A peak of this derivative is a time point when the reaction increases most rapidly. The peak occurs shortly after Take-off of the reaction (Figure 2-3). The Take-Off is the last point before which the fluorescence signal emerges from the background (Herrmann and Corbett_Research, 2002). In different experiments, different probes were used as standard reaction and the DNA (cDNA) amount in these samples were defined as 100%. The comparative concentrations were calculated only for probes with amplification rate from 1.6 up to 2.0. Variabilities of reactions were about 5%.
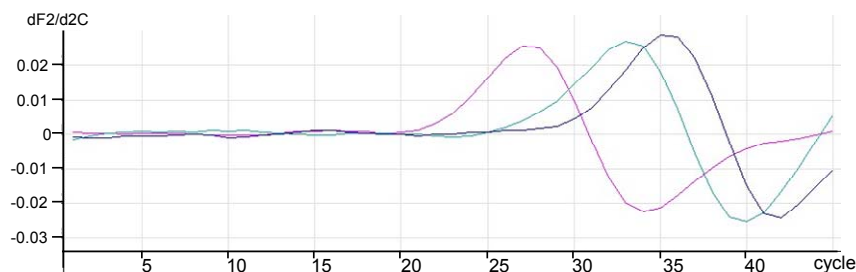
Figure 2-3. The second derivative of the raw data. Lines on the graph are the second derivative of the raw data of the reactions with cDNA of HF (pink), HMEC-48R p15 (green) and HMEC-48R p16 (violet). The peaks of this function determinate a time when reaction increases most rapidly. Take-off reactions are 23.2 for HF and 28.4 for 48R p16, 31.1 for 48R p17.

2.2.10 Luciferase assay

2.2.10.1 Amplification of the *RASSF1A* and *RASSF1C* promoter fragments

To clone fragments of the *RASSF1A* and *RASSF1C* promoters (Figure 2-4), 50 ng of the human fibroblasts genomic DNA was amplified in 50 µl of reaction volume using the following final concentrations: 1x *Taq* buffer, 0.2 mM dNTPs, 1.5 mM MgCl$_2$, 1.5 M betain and 3.75 units of proof reading *Taq* polymerase from *Expand Long Template PCR* system (Roche) and 20 pmoles of each primers (Table 2-4). After an initial denaturation step at 94°C for 2 min, the cycling conditions were as follows: 94°C for 20 s, T$_{an}$ (Table 2-4) for 30 s and 68°C for 2 min for 30 cycles. The final elongation step was at 68°C for 7 min. All primers harbored a new *EcoRI* site (5'GAATTC) (Table 2-4).
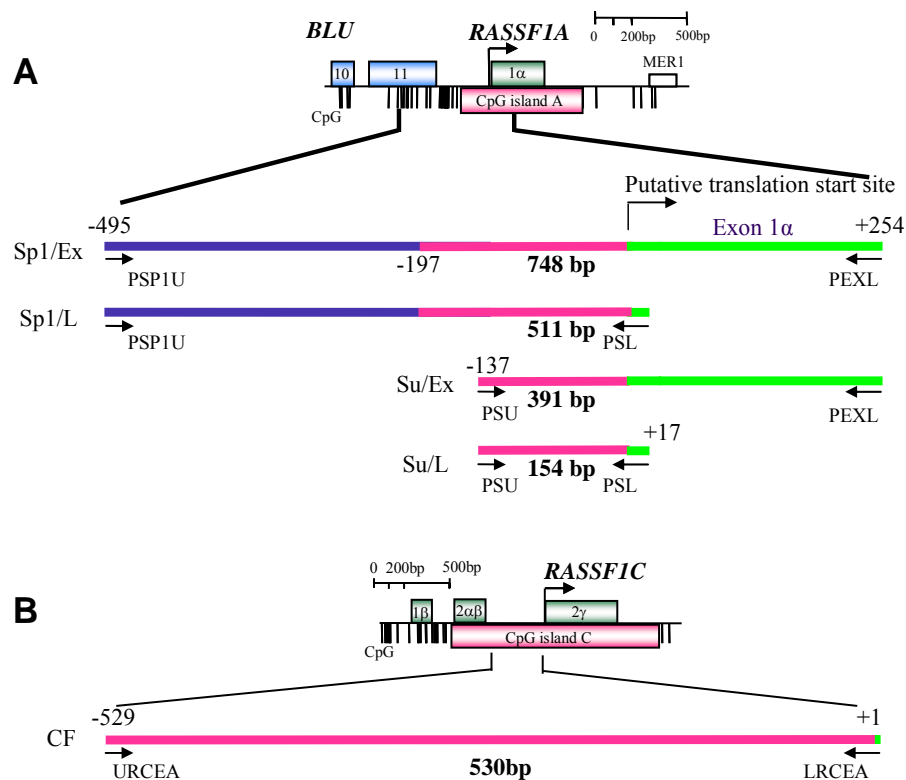
Figure 2-4. Amplification of fragments of the *RASSF1A* and *RASSF1C* promoters. A. A map of the *RASSF1A* promoter region is shown. For further details see Figure 2-1. The four DNA fragments of the *RASSF1A* CpG island were amplified using several primer combinations (Table 2-4). Green line indicates a sequence of the exon 1α. The red line represents a sequence of the *RASSF1A* CpG island fragment located upstream from the putative translation start. Blue line shows a sequence of the putative *RASSF1A* promoter fragment located upstream from the *RASSF1A* CpG island. **B.** A map of the *RASSF1C* promoter region is shown. DNA fragment of the *RASSF1C* CpG island was amplified using URCEA and LRCEA primers (Table 2-4). Green line indicates a sequence of the exon 2γ of *RASSF1C*. Red line represents a sequence the *RASSF1C* CpG island fragment located upstream from the putative *RASSF1C* translation start.

Table 2-4. Conditions for amplification of the *RASSF1A* and *RASSF1C* promoter fragments

	Fragment	Primers	T_{an}, ºC	PCR/fragment[1]	Primers (5'→3')
Prom.A	Sp1/L	PSP1U+ PSL	64	535/512 bp	**PSP1U:**GAATTC[2]ATTAATTGGAGAGCAGAGCGGGCGGTA
	Sp1/Ex	PSP1U+ PEXL	64	772/749 bp	**PSU:**GAATTC[2]ATTAATCGCGGCTCTCCTCAGCTCCTTC
	Su/L	PSU+ PEXL	64	178/154 bp	**PSL:**GAATTC[2]*ACCGGT*[3]TCAGGCTCCCCCGACATGGC
	Su/Ex	PSU+ PSL	64	415/391 bp	**PEXL:**GAATTC[2]*ACCGGT*[3]TCACGCGCGCACTGCAGGC
Prom.C	CF	URCEA+LRCEA	65	537/530 bp	**URCEA:** GGAATTC[2]TCGAGGGCTGCCTGGGTG
					LRCEA: GGAATTC[2]TAGCCGTACCCGCCCGTCCC

[1]Size of PCR product / size of the *RASSF1* fragment in PCR product. [2]*EcoRI* restriction site (5'GAATTC). [3]*AgeI* restriction site (5'ACCGGT).

2.2.10.2 Cloning of the *RASSF1* promoter fragments into the *pGEM-T* vector

PCR products were gel purified using the *QIAquick Gel Extraction* kit (Qiagen) and cloned into the *pGEM-T* vector (Promega) using for transformation *TOP 10F' E. coli* competent cells (Clontech). Ligation and transformation were performed according to the manufacturer's instructions (Promega, Clontech). After "Blue/White" screening, the plasmid DNA from 5 white clones was isolated by the *QIAprep spin* kit (Qiagen) and dissolved in 50 µl of elution buffer. To determine the presence of the PCR products in the *pGEM-T* vectors, 4 µl of plasmid DNA from each clone was analyzed by restriction analysis with 10 units of *EcoRI* (New England BioLabs) in 10 µl of reaction mix at 37ºC for 2 h. The restriction products were resolved on a 1% TBE agarose gel. The sequences of plasmids were verified (see chapter 2.2.10.3).

30 µg of the verified plasmid was treated with 80 units of *EcoRI* (New England BioLabs) in 100 µl of reaction mix at 37ºC for 4 h. After resolving the restriction products on a 1% TBE agarose gel, promoter fragments were isolated using the *QIAquick Gel Extraction* kit according to the manufacturer's instructions (Qiagen).

2.2.10.3 Sequencing

DNA sequence analysis was carried out by automated DNA sequencers (SeqLab, Göttingen, Germany) using T7B and M13RL primers (see chapter 2.2.7.2).

2.2.10.4 Cloning of the *RASSF1* promoter fragments in the *pRL-null* vector

Five µl of *pRL-null* vector (Promega) was treated with 30 units of *EcoRI* (New England BioLabs) in 100 µl of reaction mix at 37ºC for 4 h. The plasmid DNA was

precipitated and dissolved in 50 µl of H₂0. Two µl of digested DNA was used as negative control for the dephosphorylation reaction; whereas 48 µl of DNA was treated at 37ºC for 15 min with 11 units of *Shrimp* alkaline phosphatase (Roche) in 100 µl of reaction mix. After precipitation DNA was dissolved in 45 µl of H₂0 and then used for ligation.

One µl of the dephosphorylated *pRL-null* vector was ligated with 2 µl of the *EcoRI* digested *RASSF1* promoter fragment using 1.5 units of *T4 DNA* ligase (Promega) in a 10 µl reaction mix for 4 h at RT. After ligation, the DNA was transformed in *TOP 10F' E. coli* competent cells according to the manufacturer's instructions (Clontech). DNA of 5 clones was isolated by the *QIAprep spin* kit according to the manufacturer's instructions (Qiagen), treated with diagnostic restriction enzymes to determine the orientation of the insert (Table 2-5) and analyzed by sequencing (see chapter 2.2.10.3).

Table 2-5. Analysis of orientation of the *RASSF1* promoter fragments in the *pRL-null* vector

Construct	Restriction enzyme	Right orientation[1]	Wrong orientation[2]
CF-pRLnull	*XmaI*	110 bp, 278 bp, 3.5 kb	156 bp, 278 bp, 3.4 kb
	XhoI	53 bp, 3.8 kb	584 bp, 3.3 kb
Sp1/L-pRLnull	*AgeI, HindIII*	570 bp, 3.3 kb	49 bp, 3.8 kb
Sp1/Ex-pRLnull	*AgeI, HindIII*	807 bp, 3.3 kb	49 bp, 4 kb
Su/L-pRLnull	*AgeI, HindIII*	213 bp, 3.3 kb	49 bp, 3.5 kb
	BamHI	1.6 kb, 1.9 kb	1.5 kb, 2 kb
Su/Ex-pRLnull	*AgeI, HindIII*	450 bp, 3.3 kb	49 bp, 3.7 kb
	BamHI	1.8 kb, 1.9 kb	1.5 kb, 2.3 kb

[1]Sizes of restriction products of constructs containing the right orientated promoter fragment. [2]Sizes of restriction products of constructs containing the wrong orientated promoter fragment.

2.2.10.5 *In vitro* methylation of the Sp1/L-pRLnull construct

Twenty µg of Sp1/L-pRLnull DNA was treated with 60 units of *SssI* methylase (New England BioLabs) and 160 µM S-adenosylmethionine 37°C overnight in 200 µl of reaction mix. In parallel, a mock methylation was performed with 20 µg of Sp1/L-pRLnull plasmid DNA. After DNA purification with phenol/chloroform, 1 µg of glycogen was added. The DNA was precipitated and dissolved in H₂O at a concentration of 1µg/µl and quantified by UV spectrometry. In the luciferase assays, expression of the *in vitro* methylated Sp1/L-pRLnull plasmid was compared to the mock methylated Sp1/L-pRLnull.

2.2.10.6 Generation of constructs containing the mutated *RASSF1A* promoter
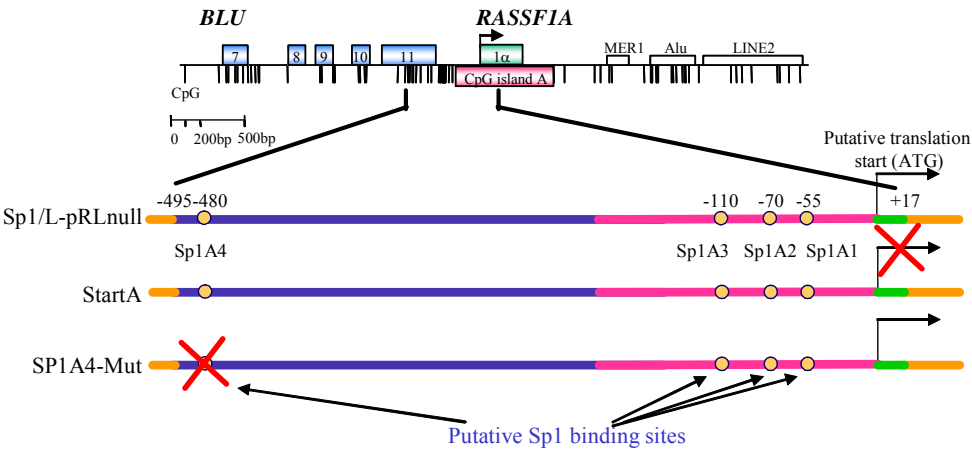
Figure 2-5. Mutations of the *Sp1* and translation start sites in the *RASSF1A* promoter. A map of the *RASSF1A* promoter region is shown. For further details see Figure 2-1. Constructs StartA and Sp1A4 were generated by site-directed mutagenesis of the Sp1/L-pRLnull plasmid. The crosses indicate new mutations in the putative *RASSF1A* translation start site and the putative *Sp1* site. Yellow and green lines represent sequences of the *pRL-null* vector and the exon 1α of *RASSF1A*, respectively. Red and blue line indicate sequences of the *RASSF1A* CpG island fragment located upstream from the putative translation start site and the putative *RASSF1A* promoter fragment located upstream from the *RASSF1A* CpG island, respectively.

Plasmids Sp1A4-Mut and StartA were generated by the *QuickChange XL Site-Directed Mutagenesis* kit using the Sp1/L-pRLnull vector (Figure 2-5) with primers listed in Table 2-6 according to the manufacturer's instructions (Stratagene). After transformation and "Blue/White" screening, the plasmid DNA was isolated from 5 white clones by the *QIAprep spin* kit and analyzed by sequencing.

Table 2-6. Primers used for site-directed mutagenesis of the *Sp1* and translation start sites in the *RASSF1A* promoter

Construct	Original sequence→ mutated sequence	Primers (5'→3')
StartA	ATG → CTG	CTGMTU:CCCAACCGGGCC<u>CTG</u>TCGGGGGAGCC CTGMTL:GGCTCCCCCGA<u>CAG</u>GGCCCGGTTGGG
Sp1A4-Mut	GGGCGG→ AAGCGA	ASP1MTU:GAGAGCAGAGC<u>AAGCGA</u>TAAAGCTGCTGAC ASP1MTL:GTCAGCAGCTTTA<u>TCGCTT</u>GCTCTGCTCTC
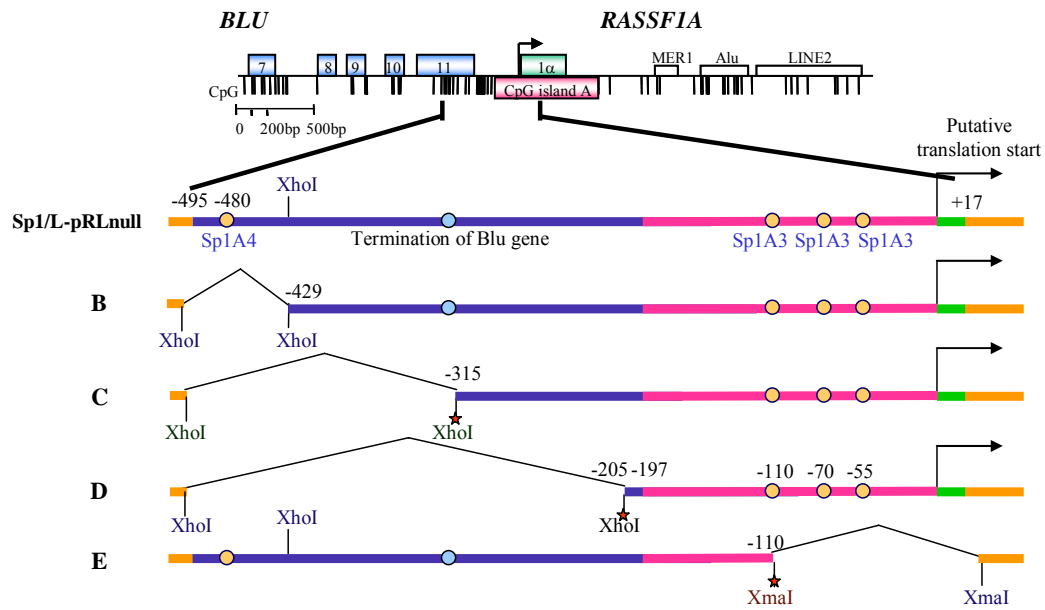
Figure 2-6. Deletions in the *RASSF1A* promoter. A map of the *RASSF1A* promoter region is shown. For further details see Figure 2-1. Plasmids B, C, D and E were generated by deletions in the *RASSF1A* promoter fragments of Sp1/L-pRLnull plasmid using *XhoI* and *XmaI* restriction sites. A red star symbols indicate the restriction sites generated by site-directed mutagenesis. Yellow and green lines represent sequences of the *pRL-null* vector and the exon 1 α of *RASSF1*A, respectively. Red and blue lines outline sequences of the *RASSF1A* CpG island fragment located upstream from the putative *RASSF1A* translation start site and the *RASSF1A* promoter fragment located upstream from CpG island, respectively.

To generate the B construct (Figure 2-6), 11 µg of Sp1/L-pRLnull plasmid was restricted with 30 units of *XhoI* enzyme (New England BioLabs) at 37ºC for 4 h. The digested DNA was resolved on a 1% TBE agarose gel and DNA fragments with 3.7 kb size were isolated from gel using the *QIAquick Gel Extraction* kit (Qiagen). The DNA fragments were selfligated using 1.5 units of *T4 DNA* ligase (Promega) in 10 µl of reaction mix for 4 h at RT. The ligated DNA was transformed in *TOP 10F' E. coli* competent cells according to the manufacturer's instructions (Clontech). Plasmid DNA from two clones was isolated by the *QIAprep spin* kit (Qiagen) and analyzed by sequencing. To generate C, D and E (Figure 2-6) constructs, new restriction sites in Sp1/L-pRLnull plasmid were created using the *QuickChange XL Site-Directed Mutagenesis* kit and primers listed in Table 2-7 according to the manufacturer's instructions (Stratagene). After DNA transformation and "Blue/White" screening, the plasmid DNA from two positive clones was isolated by the *QIAprep spin* kit (Qiagen). Further, 5 µg of plasmid DNA was treated with 60 units of *XhoI* (New England BioLabs) (for the C and D constructs) or 30 units of *XmaI* (New England BioLabs) (for the E construct) in 100 µl of reaction mix at 37ºC for 4 h. After resolving the

digested DNA on a 1% TBE agarose gel, the DNA fragments with 3.6 kb size were isolated using the *QIAquick Gel Extraction* kit (Qiagen). Further, the DNA fragments were selfligated using 1.5 units of *T4 DNA* ligase (Promega) in 10 µl of reaction mix for 4 h at RT and transformed in *TOP 10F' E. coli* competent cells according to the manufacturer's instructions (Clontech). Plasmid DNA from 5 clones was isolated by the *QIAprep spin* kit (Qiagen). Sizes of the *RASSF1A* inserts in the constructs were analyzed by restriction (see Table 2-8) and sequencing analysis.

Table 2-7. Primers used for site-directed mutagenesis of the *RASSF1A* promoter

Construct	Fragment size[1]	Restriction site [2]		Primers (5'→3')
		enzyme	position	
C	330 bp	*XhoI*	-315	UMXC1: GTAAAGCTGGC<u>CTCGAG</u>[3]AAACACGGGTATC
				LMXC1: GATACCCGTGTTT<u>CTCGAG</u>[3]GCCAGCTTTAC
D	220 bp	*XhoI*	-205	UMXD1: GCGGGGGGGGGCT<u>CTCGAG</u>[3]AGCGCGCCCAG
				LMXD1: CTGGGCGCGCT<u>CTCGAG</u>[3]AGCCCCCCCCGC
E	393 bp	*XmaI*	-110	UMXE1: CAGCTCCTTCCC<u>GGGCCC</u>[4]AGTCTGGATCC
				LMXE1: GGATCCAGACT<u>GGGCCC</u>[4]GGGAAGGAGCTG

[1]Size of the *RASSF1A* fragment in construct after deletion. [2]New generated restriction site. [3]*XhoI* restriction site (5'CTCGAG). [4]*XmaI* restriction site (5'GGGCCC).

Table 2-8. Restriction analysis of the C, D and E constructs

Construct	Restriction enzyme	Construct with deletion[1]	Construct without deletion[2]
C-pRLnull	*XhoI, EcoRI*	330 bp, 3.3 kb	53 bp, 63 bp, 115 bp, 330 bp, 3.3 kb
D-pRLnull	*XhoI, EcoRI*	220 bp, 3.3 kb	53 bp , 63 bp, 220 bp, 225 bp, 3.3 kb
E-pRLnull	*PstI, EcoRI*	393 bp, 3.3 kb	19 bp, 535 bp, 3.3 kb

[1]Restriction products of plasmid with successfully deleted fragment. [2]Restriction products of the mutated Sp1/L-pRLnull vector without deletion.

2.2.10.7 Generation of the constructs containing the mutated *RASSF1C* promoter
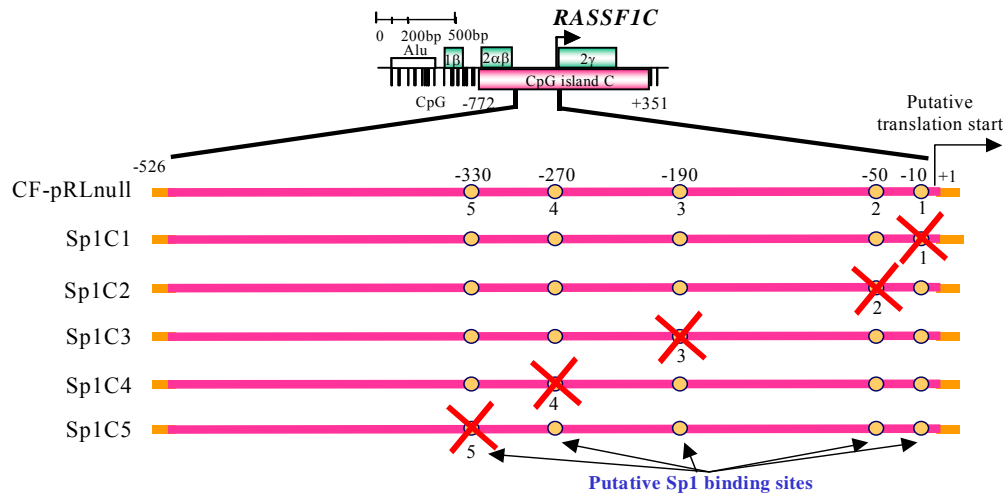
Figure 2-7. Mutations of the *Sp1* sites in the *RASSF1C* promoter. A map of the *RASSF1C* promoter region is shown. For further details see Figure 2-1. Plasmids Sp1C1, Sp1C2, Sp1C3, Sp1C4 and Sp1C5 were generated by site-directed mutagenesis of the putative *Sp1* sites in the *RASSF1C* promoter using the CF-pRLnull construct. The crosses indicate mutations in the putative *Sp1* sites. Yellow and pink lines indicate sequences of the *pRL-null* and the *RASSF1C* CpG island fragment, respectively. Green line represents a sequence of the exon 2γ of *RASSF1C*.

Plasmids Sp1C1, Sp1C2, Sp1C3, Sp1C4 and Sp1C5 were generated by the *QuickChange XL Site-Directed Mutagenesis* kit using the CF-pRLnull construct (Figure 2-7) with primers listed in Table 2-9 according to the manufacturer's instructions (Stratagene). After transformation and "Blue/White" screening, the plasmid DNA from 5 white clones were isolated by the *QIAprep spin* kit (Qiagen) and analyzed by sequencing.

Table 2-9. Primers used for site-directed mutagenesis of the *RASSF1C* promoter

Construct	Original sequence→ mutated sequence	Primers (5'→3')
Sp1C1	CCGCCC→TCGCTT	Sp1C1U: TCCCGCACCTTC<u>TCGCTT</u>TCGCCTCCGGCC Sp1C1L: GGCCGGAGGCGA<u>AAGCGA</u>GAAGGTGCGGGA
Sp1C2	CCGCCC→TCGCTT	Sp1C2U: GGACGCTGGCAC<u>TCGCTT</u>CCGTTCCCTGTG Sp1C2L: CACAGGGAACGG<u>AAGCGA</u>GAGCCAGCGTCC
Sp1C3	CCGCCC→TCGCTT	Sp1C3U: GCGTGCGTGTCC<u>TCGCTT</u>CGGCGTTCCTGC Sp1C3L: GCAGGAACGCCG<u>AAGCGA</u>GGACACGCACGC
Sp1C4	GGGCGG→AAGCGA	Sp1C4U: CGCACGCGACCG<u>AAGCGA</u>TGGTTGGCGGCT Sp1C4L: AGCCGCCAACCA<u>TCGCTT</u>CGGTCGCGTGCG
Sp1C5	GGGCGG→AAGCGA	Sp1C5U: GGACTGGGGGAC<u>AAGCGA</u>GTACGGCTATGG Sp1C5L: CCATAGCCGTAC<u>TCGCTT</u>GTCCCCCAGTCC

2.2.10.8 Cell transfection and *Dual - Luciferase Reporter Assay* system

For transfection, the plasmid DNA was isolated by the *QIAfilter plasmid Maxiprep* kit (Qiagen) and quantified by UV spectrometry.

In 6-well plates, 3 μg of vector containing the *RASSF1* promoter and 120 ng of *pGL3-promoter* vector were co-transformed in HeLa S3 cells. To determine the background, 3 μg of *pRL-null* vector (Promega) and 120 ng *pGL3-promoter* vector (Promega) were co-transformed in cells grown in one of the wells. *Lipofectamine 2000* was used for transfection according to the manufacturer's instructions (Invitrogen). After 6 h of transfection, Opti-MeM I Reduced Serum was replaced by appropriate culture medium. After 18 h, cells were washed with PBS and rocked with passive lysis buffer (*Dual-Luciferase Reporter Assay* system) for 15 min at RT. Expression of constructs was analyzed by *Dual-Luciferase Reporter Assay* system according to the manufacturer's instructions (Promega).

2.2.10.9 Analysis of *Dual - Luciferase Reporter Assay* data

To determine the transfection efficiency, *pGL3-promoter* vector containing the *Firefly Luciferase* gene under the *SV40* promoter was used for co-transfection. In every experiment, transfection of the *pRL-null* vector was performed to determine the *Renilla Luciferase* expression in a vector without insert.

For every sample, reaction was performed with substrates for both luciferases, thus every sample had two raw data:

A - raw data with *Renilla Luciferase* substrate

B - raw data with *Firefly Luciferase* substrate = transfection efficiency

Reactions with *Renilla Luciferase* substrate were normalized for the reaction with *Firefly Luciferase* substrate in the same sample by formula: $C = A / B$. Normalized reaction with the *pRL-null* vector ($C_0 = A_0 / B_0$) was defined as a background and expression of vector containing the *RASSF1* promoter fragment was calculated by formula: $D = C - C_0$. Expression of one of the constructs containing the *RASSF1* (A or C) promoter fragments was defined as 100% ($S_{tandard} = 100\%$) and expression of the *pRL-null* vector was defined as 0% ($D_{pRL-null} = 0\%$). On the basis of there formulas, D and the average of D with standard deviations were calculated for all samples.

2.2.11 The electro mobility-shift assay (EMSA).

2.2.11.1 Isolation of nuclear extract

Nuclear extract was isolated as described by Tommasi and Pfeifer with some modifications (Tommasi and Pfeifer, 1995). To isolate nuclei, HeLa S3 cells were washed twice with cold PBS and incubated in lysis buffer (10 mM hepes-KOH pH 7.9, 10 mM KCL, 0.3 M sucrose, 1.5 mM $MgCl_2$, 0.2 mM EDTA, 0.1 mM EGTA, 2.0 mM 2-mercaptoethanol, 0.5 mM PMSF, 1% NP-40) on ice for 20 min. The nuclei were scraped, spun for 10 min at 4000 rpm at 4ºC, transferred into Eppendorf tube and pelleted. Further, the nuclei were resuspensed and gently extracted in 2.5 volume (volume of nuclei) of cold nuclei extraction buffer (20 mM Hepes-KOH pH 7.9, 0.42 M NaCl, 1.5 mM $MgCl_2$, 0.2 mM EDTA, 0.1 mM EGTA, 2.0 mM 2-mercaptoethanol, 0.5 mM PMSF, 20% Glycerol). After centrifugation for 30 min at 12000g at 4ºC, the supernatant was dialyzed against 50 volumes (volumes of supernatant) of dialysis buffer (20 mM Hepes-KOH pH 7.9, 100 mM KCL, 0.2 mM EDTA, 2.0 mM 2-mercaptoethanol, 0.5 mM PMSF, 20% glycerol) overnight at 4ºC. After measuring the protein concentration by Bradford method (Bradford, 1976), the nuclear extract was stored at -80ºC in aliquots.

2.2.11.2 Labelling of oligos

Labelling of oligos was carried out as previously described by Latchman with some modifications (Latchman, 1995). Two complementary single stranded oligonucleotides (Table 2-10) with concentrations 50 pmol/µl were mixed in equimolar amounts, annealed by heating for 5 min at 80ºC and gradually cooled to RT over a period of 5 h.

For labelling of double stranded oligos, reaction was set up in 20 µl of volume using the following final concentrations: 1x buffer *T4 polynucleotide* kinase, 100 pmol of double stranded annealed oligonucleotides, 20 µCi [γ-[32] P ATP] and 10 units of *T4 polynucleotide* kinase (New England BioLabs). After incubation for 30 min at 37ºC and adding of 20 µg of glycogen, oligos were precipitated and dissolve in 20 µl of H_2O.

Table 2-10. Oligonucleotides for EMSA

Upper oligo (5'→3')	Lower oligo (3'→5')	ds oligo[1]
AGCAGAGCGGGCGGTAAAGCTG	TCGTCTCGCCCGCCATTTCGAC	Sp1A4
AGCAGAGCGttCGGTAAAGCTG	TCGTCTCGCaaGCCATTTCGAC	Sp1A4-m
CTCCTTCCCGCCGCCCAGTCTG	GAGGAAGGGCGGCGGGTCAGAC	Sp1A3
CTCCTTCCCGttGCCCAGTCTG	GAGGAAGGGCaaCGGGTCAGAC	Sp1A3-m
GTCGGGGCCCGCCCTGTGGCCC	CAGCCCCGGGCGGGACACCGGG	Sp1A2
GTCGGGGCCCGaaCTGTGGCCC	CAGCCCCGGGCttGACACCGGG	Sp1A2-m
CTGTGGCCCCGCCCGGCCCGCG	GACACCGGGGCGGGCCGGGCGC	Sp1A1
CTGTGGCCCCGaaCGGCCCGCG	GACACCGGGGCttGCCGGGCGC	Sp1A1-m

[1]Double stranded oligonucleotides

2.2.11.3 EMSA

The DNA-binding assays were carried out as described by Tommasi and Pfeifer with some modifications (Tommasi and Pfeifer, 1995). Binding reactions were set up on ice in 20 µl volume using the following final concentrations: 13 mM Hepes-KOH pH 7.9, 64 mM KCL, 0.5 mM $MgCl_2$, 0.13 mM EDTA, 0.3 mM PMSF, 13% glycerol, 1.5 µg of *Salmon* sperm DNA, 2 µg of antibodies (*Sp1* or *XPA*, both from Santa Cruz Biotechnology) and 5 µg of nuclear extract proteins. In some experiments, a 250 pmol (2500 pmol in case with SpA4) of the double stranded unlabelled oligonucleotides listed in Table 2-10 was included as competitor. After incubation of the binding mix for 10 min on ice, 2 µl of the radioactive labelled oligos was added and incubation was continued for 1 h. The DNA – protein complex was mixed with 2 µl of EMSA loading buffer (0.2% xylene cyanol, 0.2% bromophenol blue) and resolved on a 6% polyacrylamide gel in TBE 0.25x at 100 Volt for 4 h. The gel was dried under vacuum using gel dryer (BioRad) for 1 h at 80ºC and analyzed by a phosphoimaging.

2.2.12 Ligation-mediated PCR (LM-PCR)

LM-PCR is a method of genomic analysis to determine primary DNA nucleotide sequences, methylation patterns, DNA lesion formation and repair, and *in vivo* protein–DNA footprints (reviewed by Dai *et al.*, 2000). This technique is based on the ligation of an oligonucleotide linker onto the 5'-end of each DNA molecule, where 5'-end was generated by chemical cleavage of the strand. The presence of linker on all 5'-ends allows the exponential PCR, which results in amplification of the signal. The general LM-PCR steps are outlined in Figure 2-8. LM-PCR of the cleaved DNA was performed as previously described by Dammann and Pfeifer with some modification (Dammann and Pfeifer, 1997).
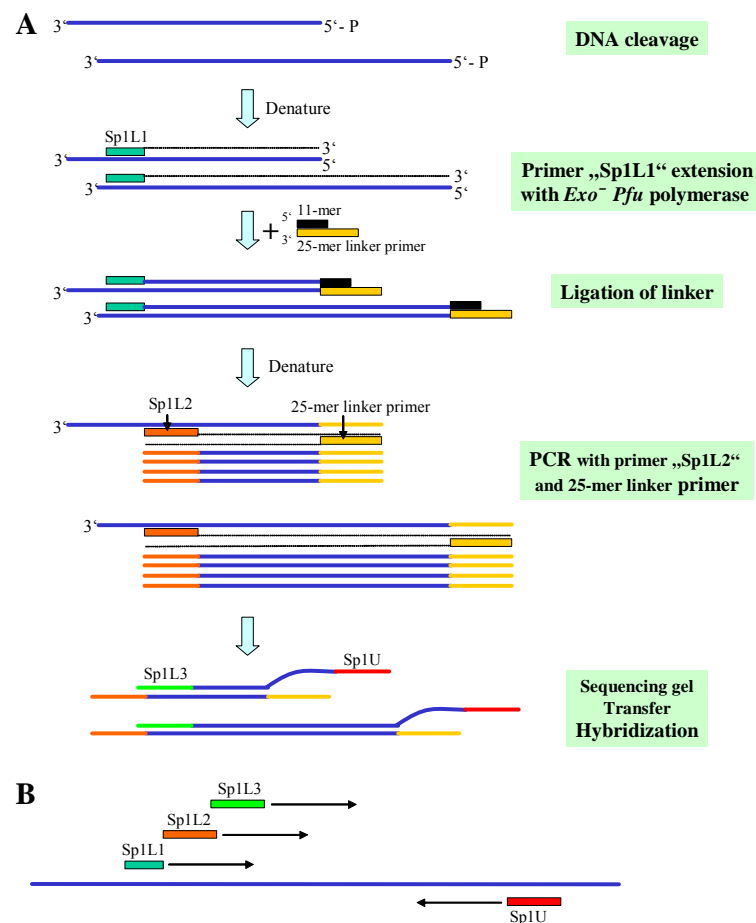
Figure 2-8. Outline of the ligation–mediated PCR procedure. A. LM-PCR procedure. The first step of the technique is a cleavage of the DNA. Next step is a generation of blunt end on one side using primer extension of a gene-specific oligonucleotide (primer Sp1L1). Third step is a ligation of linkers to the blunt ends. Next step is an expontial PCR amplification using the longer oligonucleotide of the linker (25-mer linker primer) and a second gene-specific primer (primer Sp1L2). After amplification, the DNA fragments were separated on the sequencing gel, electroblotted onto nylon membranes and hybridized with gene specific probe to visualize the sequence ladders. **B.** Arrangement of primers in a LM-PCR.

2.2.12.1 *In vivo* footprinting using dimethyl sulfate

For genomic footprinting experiments, HeLa S3 cells were treated with medium containing 0.2% dimethyl sulfate for 5 min at RT. Further, cells were washed with cold PBS, scraped, spun for 5 min at 1000 g at 4ºC and washed once more with cold PBS.

2.2.12.2 DNA isolation

The following DNA isolation method was used to prevent single and double stranded DNA breaks, which can be produced by the isolation procedure. The quality of DNA, which was obtained, allows high amplification efficiencies.

DNA from cells for chemical cleavage was isolated according the following procedure: $1x10^7$ to $1x10^8$ cells were washed with cold PBS, scraped and spun for 5 min at 1000 g at 4ºC. Cells were resuspensed in 4 ml of cold buffer A (0.3 M sucrose, 60 mM KCl, 15 mM NaCl and 2 mM EDTA pH 8.0). After adding of 4 ml of cold buffer A containing 1% NP-40, cells were incubated for 5 min on ice and spun for 5 min at 100 g at 4ºC. The nuclei pellet was washed in cold buffer A without nonindet P - 40 and resuspensed in 3 ml of buffer B (150 mM NaCl, 5 mM EDTA pH 7.8). After adding of 3 ml of buffer C (20mM tris pH 8.0, 20 mM NaCl, 20 mM EDTA pH 8.0, 1% SDS, 600 µg/ml *Proteinase K*), nuclei were incubated at 45ºC for 3 h. Further, DNA was extracted using phenol/chloroform, precipitated and dissolved in water.

2.2.12.3 Chemical cleavage of DNA

DNA was cleaved according to the Maxam Gilbert procedure (Maxam and Gilbert, 1977). Using vacuum concentrator, 50 µg of genomic HeLa S3 DNA were dried and dissolved in water volume according to the base-specific reaction protocol. All chemical cleavages were performed on ice.

G reaction: Five µl of DNA was dissolved in 200 µl of dimethyl sulfate buffer (50 mM Na-cacodylate, 1 mM EDTA pH 8.0). Further, 1 µl of dimethyl sulfate was added (99%) and DNA was incubated for 5 min at RT. The reaction was stopped by adding of 50 µl of dimethyl sulfate stop buffer (1.5 M Na-acetate pH 7.1, 1 M 2-mercaptoethanol). After adding of 100 µg of glycogen, DNA was precipitated by 750 µl of precooled 96% ethanol.

G+A reaction: 25 µl of 100% formic acid was added to 11 µl of DNA and incubated for 10 min at RT. After stopping the reaction by 50 µl of dimethyl sulfate stop buffer, 5 µl of 20 mg/ml glycogen was added. DNA was precipitated with 750 µl of precooled 96% ethanol.

T+C reaction: 47 µl of 64% hydrazine was added to 20 µl of DNA and incubated for 20 min at RT. After stopping the reaction by 200 µl of hydrazine stop buffer (0.3 M Na-acetate pH 7.5, 0.1 M EDTA pH 8.0), 5 µl of 20 mg/ml glycogen was added. DNA was precipitated with 750 µl of precooled 96% ethanol.

C reaction: 47 µl of 64% hydrazine and 15 µl of 5 M NaCl were added to 5 µl of DNA and incubated for 20 min at RT. After stopping the reaction by 200 µl of hydrazine stop buffer, 5 µl of 20 mg/m glycogen was added. DNA was precipitated with 750 µl of precooled 96% ethanol.

Samples from four reactions (G, G+A, C, T+C) were further treated together as described below. After incubation for 30 min at -70°C, DNA was precipitated and dissolved in 225 µl of water. Further, DNA was precipitated once more and dissolved in 50 µl of water.

For piperidine treatment, 50 µl of 2 M piperidine was added to DNA and incubated for 30 min at 90°C. After cooling on ice for 5 min and adding of 40 µg of glycogen, DNA was precipitated, dried overnight in vacuum concentrator and dissolved in 50 µl of water.

2.2.12.4 Primer extension

For primer extension *Exo⁻Pfu DNA* polymerase was used (Stratagene). Reactions were set up in 30 µl of volume using the following final concentrations: 1x cloned *Pfu* reaction buffer, 0.25 mM dNTPs each, 1 pmol Sp1L1 primer (5'GGAGGCCAGCTTTACTGTGCTA), 1.5 units of *Exo⁻ Pfu DNA* polymerase, 2 µg of cleaved DNA. After an initial denaturation step at 95°C for 5 min and following annealing at 56°C for 2 min 30 s, the reaction mix was gradually heated from 57°C up to 74°C with 1°C step for 3 s. The final elongation step was done at 72°C for 15 min.

2.2.12.5 Linker preparation

Linker was prepared by annealing a 25-mer linker primer 20 pmol/µl (5'GCGGTGACCCGGGAGATCTGAATTC) to 11-mer linker primer 20 pmol/µl (5'GAATTCAGATC). For annealing, primer mix was heated at 95°C for 3 min and gradually cooled to RT over a period of 5 h.

2.2.12.6 Ligation

45 µl of a ligation mix (13.33 mM $MgCl_2$, 30 mM DTT, 1.1 mM ATP, 16.7 mg BSA, 100 pmol linker, 50 mM tris pH 7.7, 3.25 units of *T4 DNA* ligase (Promega)) was added to primer extension mix on ice. After 24 h of incubation at 16°C, the ligation was stopped by heating for 10 min at 70°C and adding of 30 µl of stop-mix (7.2 M ammonium acetate, 4 mM EDTA pH 8.0, 20 µg glycogen). Ligated fragments were precipitated and dissolved in 50 µl of H_2O.

2.2.12.7 PCR amplification

For PCR amplification, 50 µl of PCR mix (2 x Fast *Taq* buffer, 3 mM $MgCl_2$, 0.5 mM dNTPs each, 10 pmol/µl 25-mer linker primer (5'GCGGTGACCCGGGAGATCTGAATTC), 10 pmol/µl Sp1L2 primer (5'TAGAGGAAGAGGGTCCCCACATCCG) and 4 units of *Fast Taq* polymerase (Roche)) was added to ligated fragments. After denaturation for 5 min at 95°C, the PCR cycling conditions were as follows: 95°C for 30 s, 66°C for 30 s and 72°C for 1 min for a total of 25 cycles. The last elongation step was performed for 10 min at 72°C. After amplification, 25 µl of PCR-stop mix (1.56 M sodium acetate, 60 mM EDTA pH 7.7, 10 mg tRNA) was added. The DNA was extracted using 250 µl of phenol/chloroform (92 µl phenol + 158 µl chloroform), precipitated and dissolved in 6 µl of formamide loading dye (62.6% formamide, 1.33 mM EDTA pH 7.7, 0.03% xylene cyanole, 0.03% bromphenol blue).

2.2.12.8 Gel electrophoresis and electroblotting.

Three µl of PCR products was denatured at 95°C for 3 min and separated on 8% polyacrylamide gel containing 7 M urea in TBE 1x for 4 h with the following parameters: 3000 Volt, 75 Watt, 50°C (glass temperature). Further, DNA fragments

were electroblotted onto nylon membrane using electroblotter at 17 Volt and 2 Ampere for 40 min in TBE 1x.

2.2.12.9 Preparation of a single stranded PCR probe

PCR products were used as a template to synthesize a single strand probe. These PCR products were generated as follow: 100 ng of genomic HeLa S3 DNA was amplified in 25 µl of reaction mix (1x *Taq* buffer, 2 units of *Taq* polymerase (InViTek), 0.2 mM NTPs, 1.5 mM $MgCl_2$, 20 pmoles of primers Sp1L2 (5'TAGAGGAAGAGGGTCCCCACATCCG) and Sp1U (5'CTGCAGTTGCTGAGGGCCGACC)). After the first denaturation for 5 min at 95°C, DNA was amplified for 40 cycles with following conditions: 95°C for 30 s, 66°C for 30 s and 72°C for 30 s. The last elongation step was performed for 10 min at 72°C. After gel purification using the *QIAquick Gel Extraction* kit (Qiagen), PCR products were dissolved in 30 µl of water.

For probe labelling, 3 µl of PCR product was amplified in 100 µl of reaction mix (1x *Taq* buffer, 5 units of *Taq* polymerase (InViTek), 1 mM dATP, 1 mM dGTP, 1 mM dTTPs, 30 µCi [α-^{32}P CTP], 1.5 mM $MgCl_2$, 50 pmoles Sp1L3 primer (5'CCTGGCCCTCCTGGTCCGGTTT)). After the first denaturation for 5 min at 95°C, DNA was amplified for 30 cycles with following conditions: 95°C for 1 min, 64°C for 2 min and 72°C for 3 min. PCR products were clean from radioactive nucleotides using a Sephadex G-50 column, 400 µl of probe was used for hybridization.

2.2.12.10 UV cross linking, hybridization and exposure

DNA was UV cross linked to membrane with UV Stratalinker at 1.2 mjoules after electroblotting (see chapter 2.2.12.8). The membrane was prehybridizated at 64°C for 4 h in hybridization buffer (0.25 M Na_2HPO_4 pH 7.2, 1 mM EDTA pH 7.7, 7% SDS, 1% BSA) and hybridized with a single stranded gene specific PCR probe overnight at 64°C. The membrane was washed twice with a 64°C warm washing buffer 1 (20 mM Na_2HPO_4 pH 7.2, 1mM EDTA pH 7.7, 2.5% SDS, 0.25% BSA) and twice with a 64°C warm washing buffer 2 (20 mM Na_2HPO_4 pH 7.2, 1 mM EDTA pH 7.7, 1% SDS). Signals were analyzed by a phosphoimaging.

2.2.13   Chromatin Immunoprecipitation (ChIP)

2.2.13.1   Cell treatment and DNA shearing

ChIp was performed as described in the Upstate protocol for the *Chromatin Immunoprecipitation Assay* kit (http://www.upstate.com/img/coa/17-295-27400.pdf) with some modifications. In order to perform ChIP analysis, histones and other proteins were crosslinked to the DNA in cells by adding formaldehyde to a final concentration of 1% to the culture medium and by incubating for 10 min at 37°C. The cells were washed twice with cold washing buffer (PBS, 1 tablet protease inhibitor cocktail pro 50 ml, 1 mM PMSF), scraped into conical tube and spun for 4 min at 2000 g at 4˚C. The cell pellet was resuspensed in a SDS lysis buffer (1% SDS, 10 mM EDTA pH 8.0, 50 mM tris pH 8.1, 1 mM PMSF, 1 tablet protease inhibitor cocktail pro 10 ml) with cell concentration of $1x10^6$ cells pro 200 μl of SDS lysis buffer and incubated for 10 min on ice. Further, cell lysate was sonicated to shear DNA to lengths between 200 and 500 bp using ultrasound homogenizator and spun for 10 min at 13000 g at 4˚C. After centrifugation, 200 μl of supernatant fraction was transferred into a new tube and diluted in 1800 μl of cold ChIp dilution buffer (0.01% SDS, 1.1% Triton X-100, 1.2 mM EDTA pH 8.0, 16.7 mM tris pH 8.1, 167 mM NaCl, 1 mM PMSF, 1 tablet protease inhibitor cocktail pro 10 ml). Twenty microliters (1/100 volume) of this solution was kept to quantitate the DNA amount in different lysates and this probe was considered to be the "input" control.

2.2.13.2   Immunoprecipitation

To reduce nonspecific background, the diluted cell supernatant was pre-cleared with 80 μl of *salmon sperm DNA/protein A agarose* using following protocol: 80 μl of *salmon sperm DNA/protein A agarose* was added to the 2 ml of cell lysate. After incubation for 1 h on ice, the cell lysate was spun for 1 min at 1000 rpm and supernatant fraction was transferred to a new tube for immunoprecipitation.

After adding of 2 μg of antibodies (*H3-trimethyl lysine 9* or a*cetyl-H3* or *Sp1*), cell lysate was incubated overnight at 4°C. Further, the antibody/chromatin complex was isolated by adding of 60 μl of *salmon sperm DNA/protein A agarose,* incubating for 1 h on ice and pelleting for 1 min at 1000 rpm. For a negative control, a no antibody immunoprecipitation was utilized.

The protein A agarose/antibody/protein complex was washed with 1 ml of low salt immune complex wash buffer (0.1% SDS, 1% Triton X-100, 2 mM EDTA pH 8.0, 20 mM tris pH 8.1, 150 mM NaCl), 1 ml of high salt immune complex wash buffer (0.1% SDS, 1% Triton X-100, 2 mM EDTA pH 8.0, 20 mM tris pH 8.1, 500 mM NaCl), 1 ml of LiCl immune complex wash buffer (0.25 M LiCl, 1% NP-40, 1% deoxycholate, 1 mM EDTA pH 8.0, 10 mM tris pH 8.1) and 2 ml of TE buffer (10 mM tris pH 8.0, 1 mM EDTA pH 8.0).

2.2.13.3 Extraction of immunoprecipitated DNA

For quantitative PCR analysis, the DNA was eluted from agarose beads as follows. The protein A agarose/antibody/protein complex was incubated in 250 µl of elution buffer (1% SDS, 0.1 M $NaHCO_3$) for 15 min at RT. After pulse centrifugation, the eluate was collected. The elution step was performed twice.

Reverse protein-DNA crosslinking was performed by adding of 20 µl of 5 M NaCl to the combined eluates (500 µl) and incubating overnight at 65°C. Analogously, "Input" sample was treated in 0.2 M NaCl overnight at 65°C. After this treatment, the following solutions: 10 µl of 0.5 M EDTA pH 8.0, 20 µl of 1 M tris pH 7.0 and 2 µl of 10 mg/ml *Proteinase K* were added to DNA in "input" sample and to immunoprecipitated DNA. The DNA was incubated for 3 h at 45°C. After phenol extraction and precipitation, the DNA was dissolved in 50 µl of water. The histone modifications and *Sp1* binding were quantified by real time PCR using the primers listed in Table 2-11. "Input" sample and "no antibody" probe were used as positive (100%) and background (0%) controls, respectively.

2.2.13.4 Real time PCR of immunoprecipitated DNA

Real time PCR was carried out in the LightCycler "Rotor Gene 2000" using *Sybr*[TM] *green I* detection. Reactions were set up in 25 µl of volume with the following final concentrations: 1x *Taq* buffer (1.5 mM $MgCl_2$), 1 unit of *Fast Taq* polymerase (Roche), 0.25 mM dNTPs each, 10 pmoles of each primer (Table 2-11), 0.2 x *Sybr*[TM] *Green I,* formamide (Table 2-11) and 2 µl of DNA. After an initial denaturation step for 5 min at 95°C, the cycling conditions were as follows: 95°C for 20 s, T_{an} (Table 2-11) for 30 s 72°C for 30 s and a fluorescence measurement after 15 s of appropriate

Tm (Table 2-11) for a total of 50 cycles. The last elongation step was performed for 5 min at 72°C. Further, the melting temperatures of the PCR products were analyzed by a fluorescence measurement at every 1°C step after 5 s from 70°C up to 99°C. The amplification of PCR products was verified using the melting curve option (see chapter 2.2.9.2) and subsequence electrophoresis in 2% TBE agarose gel. All measurements were performed thrice. Data analysis was performed using the comparative method described in a chapter 2.2.9.3. (Rotor Gene Software version 4.6). The amount of DNA in analyzed samples was plotted relative to DNA amount in "input" sample (100%) using comparative method. A DNA amount in "no antibody" probe was defined as background control (0%).

Table 2-11. ChIp: Primers and conditions.

	Primers (5'→3')	T_{an}, ºC	Tm, ºC	FA[1], %	PCR product size, bp
A2	U: GATCACGGTCCAGCCTCTG L: CTCGAGCCTTCACTTGGGGT	62	85	2	109
A1	U: CTGGGGGAGGCGCTGAAGTC L: GCTCAGGCTCCCCCGACATG	62	85	4	115
C1	U: CGATTTCCCGGCGGCACA L: CCAGCGTCCGGGCAAGCG	60	85	4	200

[1]Formamide concentration in PCR mix.

3   Results

The *RASSF1A* tumor suppressor is frequently inactivated in cancer cells by DNA methylation of its CpG island (reviewed by Dammann *et al.*, 2003). However, the mechanisms of transcriptional regulation and epigenetical inactivation of this gene are not identified. *Sp1* protein is a transcription regulator (Dynan and Tjian, 1983), which is associated with promoter protection from *de novo* DNA methylation (Macleod *et al.*, 1994; Brandeis *et al.*, 1994). Four putative *Sp1* binding sites were identified in the *RASSF1A* promoter by *in silicio* analysis. To verify this putative *Sp1* sites, the electro mobility-shift assay (EMSA), luciferase assay, ligation mediated PCR (LM-PCR) and chromatin immunoprecipitation (ChIp) were performed. To identify additional regulatory elements, the *RASSF1A* promoter was analyzed by luciferase assay and *in vivo* footprinting. Further, expressional and epigenetical states of the *RASSF1A* promoter were investigated in consecutive passages of HMECs by quantitative RT-PCR, combined bisulfite restriction analysis (COBRA) and chromatin immunoprecipitation (ChIp) and these data were compared to cells with the active and inactive *RASSF1A* promoter. In summary, in the present study, regulatory elements in the *RASSF1A* promoter were identified and analyzed; the functional relationships between DNA methylation, histone modifications, *Sp1* binding and the *RASSF1A* expression were examined in proliferating HMECs.

3.1   Characterization of regulatory sequences in the *RASSF1A* promoter

In the *RASSF1A* promoter, four putative *Sp1* site were identified by *in silicio* analysis using the Transcription Element Search System (http://www.cbil.upenn.edu/tess). Three putative *Sp1* sites are located in the *RASSF1A* CpG island, which was determined by CpGplot (http://www.ebi.ac.uk). The fourth putative *Sp1* site is located upstream, in the exon 11 of *BLU* gene (Figure 3-1). To analyze mechanism of the *RASSF1A* transcription regulation, four fragments of the *RASSF1A* promoter were cloned in a luciferase reporter vector (*pRL-null*) and verified by *Dual-Luciferase Reporter Assay* system (Figure 3-1). In the Sp1/Ex-pRLnull construct, a 749 bp fragment of the *RASSF1A* promoter including exon 1α and the four putative *Sp1* sites was cloned (Figure 3-1). Sp1/L-pRLnull plasmid contained a 511 bp fragment of the *RASSF1A* promoter including the putative translation start site and four putative *Sp1*

sites (Figure 3-1). For generation of the Su/Ex-pRLnull construct, a 391 bp fragment of the *RASSF1A* promoter containing the three putative *Sp1* sites located in the *RASSF1A* CpG island and exon 1α was used (Figure 3-1). In Su/L-pRLnull construct, a 154 bp fragment of the *RASSF1A* promoter including the putative translation start codon and three putative *Sp1* sites was cloned (Figure 3-1).
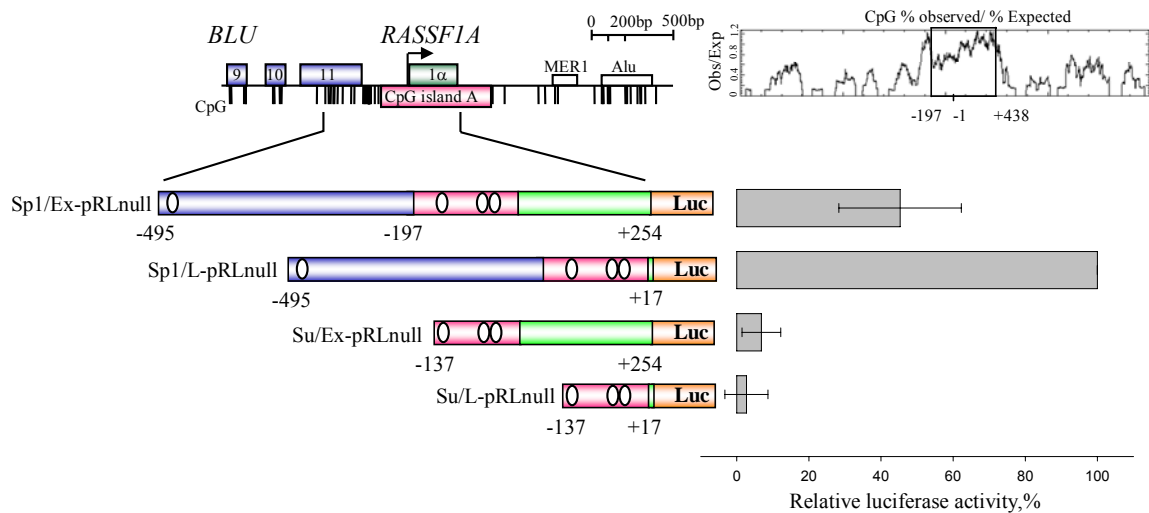
Figure 3-1. Analysis of the *RASSF1A* promoter fragments by *Dual-Luciferase Reporter Assay* system. A map of the *RASSF1A* promoter region is shown. CpG island was determined by CpGplot (http://www.ebi.ac.uk). For further details see Figure 2-1. The four *RASSF1A* fragments (Sp1/EX, Sp1/L, Su/Ex and Su/L) were cloned in the *pRL-null* vector and analyzed by *Dual-Luciferase Reporter Assay* system. The promoter activities of the constructs were compared to the Sp1/L-pRLnull plasmid (=100%). The relative activities of the *RASSF1A* promoter fragments were determined relative to the promoter less *pRL-null* vector (=0%) in three independent assays (standard deviations are indicated). Green and red lines indicate sequences of the exon 1α and the *RASSF1A* CpG island fragment located upstream from the putative translation start, respectively. Blue and yellow lines represent sequences of the putative *RASSF1A* promoter fragment located upstream from CpG island and the *pRL-null* vector, respectively. White dots label the putative *Sp1* sites.

Analysis of luciferase assay data identified that Sp1/L-pRLnull plasmid containing the *RASSF1A* promoter fragment located from -494 up to +17 had the highest transcriptional activity compared to Sp1/Ex-pRLnull, Su/Ex-pRLnull and Su/L-pRLnull in transfected HeLa cells (Figure 3-1). Adding of the *RASSF1A* exon 1α to Sp1/L-pRLnull resulted in two times downregulation of reporter gene activity (Figure 3-1). In Su/Ex and Su/L constructs, absence of the fragment located between -494 and -137 led to 97% and 93% reduction of the promoter activity compared to Sp1/L-pRLnull, respectively (Figure 3-1). Thus, Sp1/L-pRLnull construct had presumably all necessary regulatory elements for transcription.
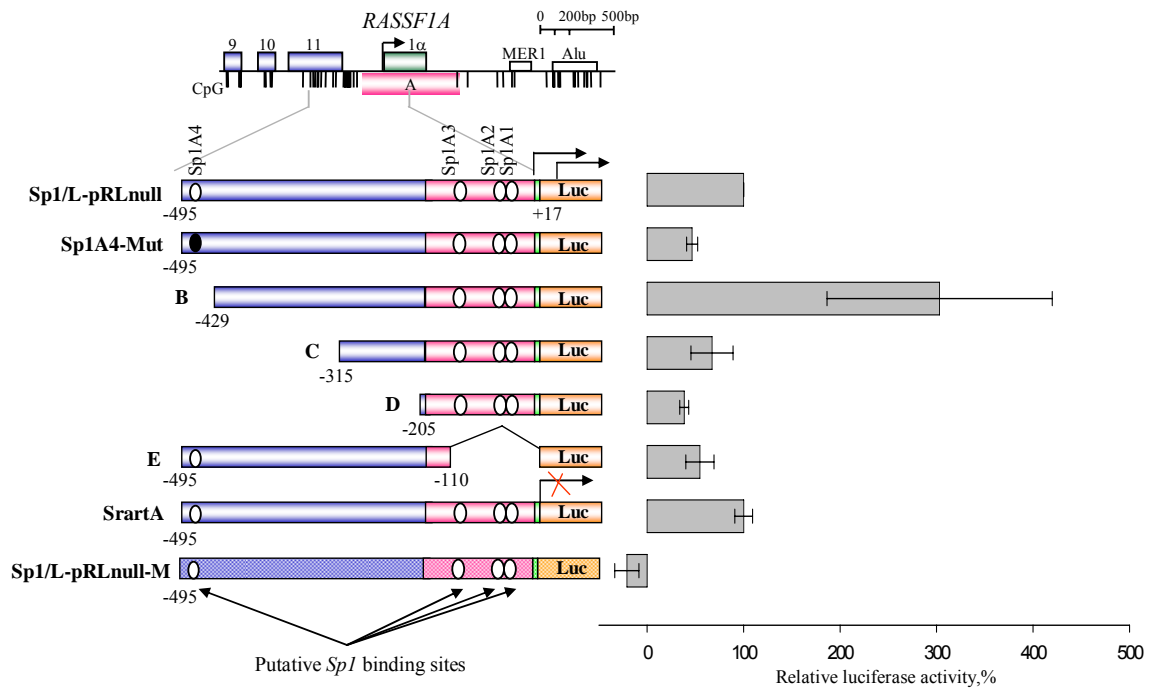
Figure 3-2. Deletion and functional analysis of the *RASSF1A* promoter. A map of the *RASSF1A* promoter region is shown. For further details see Figure 2-1. Using *Dual-Luciferase Reporter Assay* system, the promoter activities of the indicated constructs containing promoter deletions (B, C, D, E) and mutations (StartA and Sp1A4-Mut) were compared to Sp1/L-pRLnull plasmid (=100%). The Sp1/L-pRLnull construct was used for generation analyzed plasmids by mutagenesis. The relative activities of constructs and the *in vitro* methylated plasmid (Sp1/L-pRLnull-M) were determined relative to the promoter less *pRL-null* vector (=0%) in three independent assays (standard deviations are indicated). Black and white dots represent mutated and non-mutated *Sp1* sites, respectively. Green and red lines indicate sequences of the exon 1α and the *RASSF1A* CpG island fragment located upstream from putative translation start, respectively. Blue and yellow lines label sequences of the putative *RASSF1A* promoter fragment located upstream from CpG island and the *pRL-null* vector, respectively.

To identify the localization of the regulatory elements in the *RASSF1A* promoter, several constructs were generated by mutations of the Sp1/L-pRLnull plasmid (Figure 3-2). Mutation of the upstream located *Sp1* site (Sp1A4) resulted in two times downregulation of the transcription activity compared to intact construct (Figure 3-2). In contrast, deletion of a 63 bp fragment containing this *Sp1* site (Sp1A4) resulted in 3 times increasing of the promoter activity compared to intact construct (Figure 3-2). Further deletions of 3' end of the *RASSF1A* promoter fragment led to the downregulation of the luciferase activity compared to intact construct, since the constructs with 180 bp (C) and 290 bp (D) deletions had 23% and 61% decrease in the promoter activity, respectively, compared to intact plasmid (Sp1/L-pRLnull) (Figure 3-2). Deletion of the *RASSF1A* CpG island fragment containing the three putative *Sp1* sites resulted in 45% reduction of promoter activity compared to intact construct (Sp1/L-pRLnull) (Figure 3-2). However, this diminishment is not due to the deletion of

the Kozak consensus, since mutation of ATG to CTG (StartA) showed no significant changes compared to the intact sequence (Sp1/L-pRLnull) (Figure 3-2). *In vitro* methylation of the Sp1/L-pRLnull plasmid (Sp1/L-pRLnull-M) reduced the luciferase expression completely (Figure 3-2).

Shortly, the four putative *Sp1* binding sites located in the *RASSF1A* promoter were analyzed by luciferase assay. According to this analysis, mutation of the upstream putative *Sp1* site (SP1A4) and deletion of the CpG island fragment containing three putative *Sp1* sites led to decreased promoter activities.

3.2   Characterization of regulatory sequences in the *RASSF1C* promoter

Ras associated domain family 1 gene (*RASSF1*) has two main transcript isoforms: *A* and *C* (Dammann *et al.*, 2000). The *RASSF1A* and *RASSF1C* transcriptions initiate at two different CpG islands, which lie 3.5 kb apart. *RASSF1A* is frequently epigenetically inactivated in cancer cells; whereas *RASSF1C* is expressed in cancer cells and its inactivation is detected only in cells containing LOH of this region (reviewed Dammann *et al.*, 2003). The five putative *Sp1* sites were identified upstream from the putative translation start codon of *RASSF1C*. These *Sp1* sites were detected in the *RASSF1C* CpG island, which was determined by CpGplot (http://www.ebi.ac.uk) (Figure 3-3). These sites were the only significant transcription binding positions revealed by *in silicio* analysis of the *RASSF1C* promoter with the Transcription Element Search System (http://www.cbil.upenn.edu/tess). To compare promoter activities of the *RASSF1A* and *RASSF1C* promoters, a 531 bp fragment of the *RASSF1C* CpG island containing the five putative *Sp1* sites was cloned in the *pRL-null* vector (CF-pRLnull) and analyzed by *Dual-Luciferase Reporter Assay* system(Figure 3-3). Analysis of Sp1/L-pRLnull and CF-pRLnull constructs identified that the CF-pRLnull transcription activity was three times higher compared to Sp1/L-pRLnull plasmid (Figure 3-3).

To identify localization of the *RASSF1C* regulatory elements, five constructs with mutations at the putative *Sp1* sites were generated using the CF-pRLnull plasmid (Figure 3-3). Analysis of constructs by the luciferase assay identified that sequential mutation of the four putative *Sp1* sites (Sp1C1, Sp1C2, Sp1C3 and Sp1C4) in the *RASSF1C* promoter resulted in significant reduction of the promoter activity compared to intact construct (CF-pRLnull) (Figure 3-3). Transcription activities of the constructs

with *Sp1* site mutations at position -12 and -52 were 62% and 80% decreased, respectively, compared to intact plasmid (CF-pRLnull) (Figure 3-3). The promoter activity of the construct with mutated *Sp1* site at position -187 was completely abolished and 97% reduction of promoter activity was identified in the construct with the mutated *Sp1* site at position -273 compared to intact plasmid (CF-pRLnull) (Figure 3-3). In contrast, mutation of the *Sp1* site located at -327 had only minor effects on activity of the reporter gene (Figure 3-3).

In summary, the *RASSF1C* promoter fragment containing the five putative *Sp1* sites had three times elevated level of promoter activity compared to the *RASSF1A* promoter fragment containing the four putative *Sp1* sites. In the *RASSF1C* promoter, mutations in the four putative *Sp1* sites led to decrease or inactivation of transcription activity.
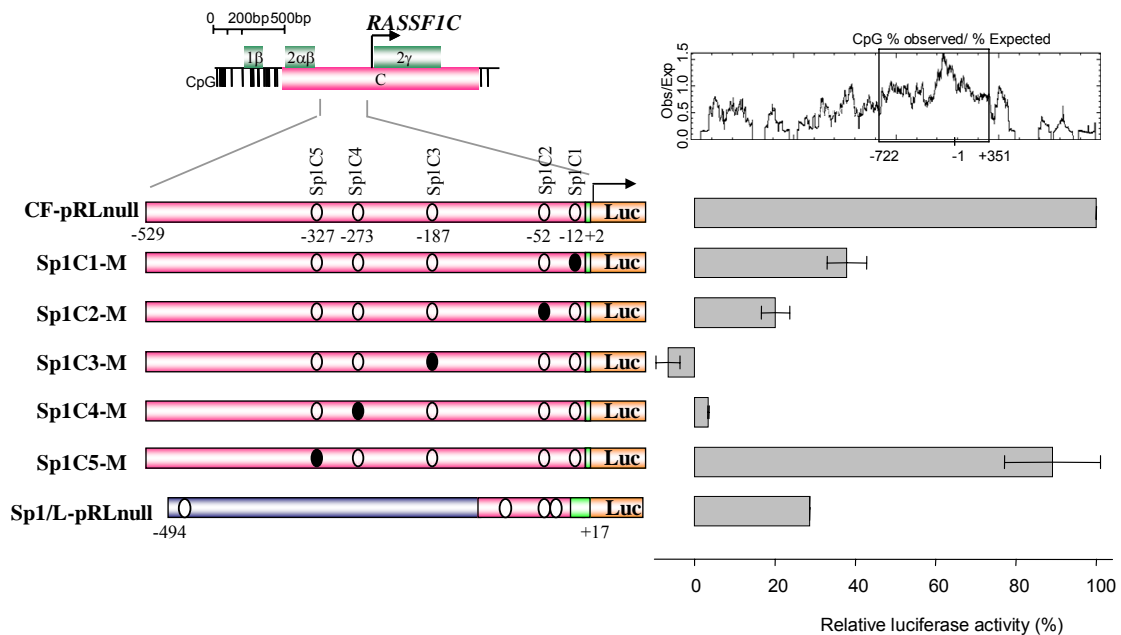
Figure 3-3. Promoter analysis of *RASSF1C* by *Dual-Luciferase Reporter Assay system*. A map of the *RASSF1C* promoter region is shown. The *RASSF1C* CpGs island was determined by CpGplot (http://www.ebi.ac.uk). For further details see Figure 2-1. Using the CF-pRLnull construct, five plasmids were generated by mutagenesis at the putative *Sp1* sites and analyzed by *Dual-Luciferase Reporter Assay* system. The promoter activities of indicated constructs (Sp1C1-M, Sp1C2-M, Sp1C3-M, Sp1C4-M, Sp1C5-M, Sp1/L-pRLnull) were compared to CF-pRLnull promoter activity (=100%). The relative activities of the constructs were determined relative to the promoter less *pRL-null* vector (=0%) in three independent assays (standard deviations are indicated). Green and red lines indicate sequences of the *RASSF1* exons and the CpG island fragments located upstream from translation start, respectively. Blue and yellow lines represent sequences of the putative *RASSF1A* promoter fragment located upstream from CpG island and the *pRL-null* vector, respectively. Black and white dots represent mutated and non-mutated putative *Sp1* sites, respectively.

3.3 Electro mobility-shift assay of the *Sp1* sites located in the *RASSF1A* promoter

To verify the *Sp1* binding to the *RASSF1A* promoter, electro mobility-shift assay (EMSA) was performed (Figure 3-4). For EMSA, eight double stranded oligos were generated. The four of them were 22 bp DNA fragments of the *RASSF1A* promoter containing one from the four putative *Sp1* sites (Sp1A1, Sp1A2, Sp1A3 and Sp1A4). Other four oligos were generated by mutations of the *Sp1* sites (5'GTTCGG) in Sp1A1, Sp1A2, Sp1A3 and Sp1A4 (Sp1A1-m, Sp1A2-m, Sp1A3-m and Sp1A4-m). After incubation of radioactive labelled wildtype oligos with HeLa nuclear protein extract, a shift was detected with Sp1A1, Sp1A2, Sp1A3 and Sp1A4 (Figure 3-4 B, C, D and E). A super-shift was identified when *Sp1* antibodies were added (Figure 3-4 B, C, D and E). In contrast, supershifts were not identified after incubation with *XPA* antibodies (Figure 3-4 B, C, D and E). The cold *Sp1* probes competed for the *Sp1* binding of radioactive labelled oligos (Figure 3-4 B, C, D and E). However, the cold competitors containing the mutated *Sp1* sites (5'GTTCGG) were not able to compete significantly (Figure 3-4 B, C, D and E). Moreover, shifts were found with the methylated in *vitro* oligos containing the *Sp1* sites. In summary, the four *Sp1* sites in the *RASSF1A* promoter were identified according to EMSA analysis.
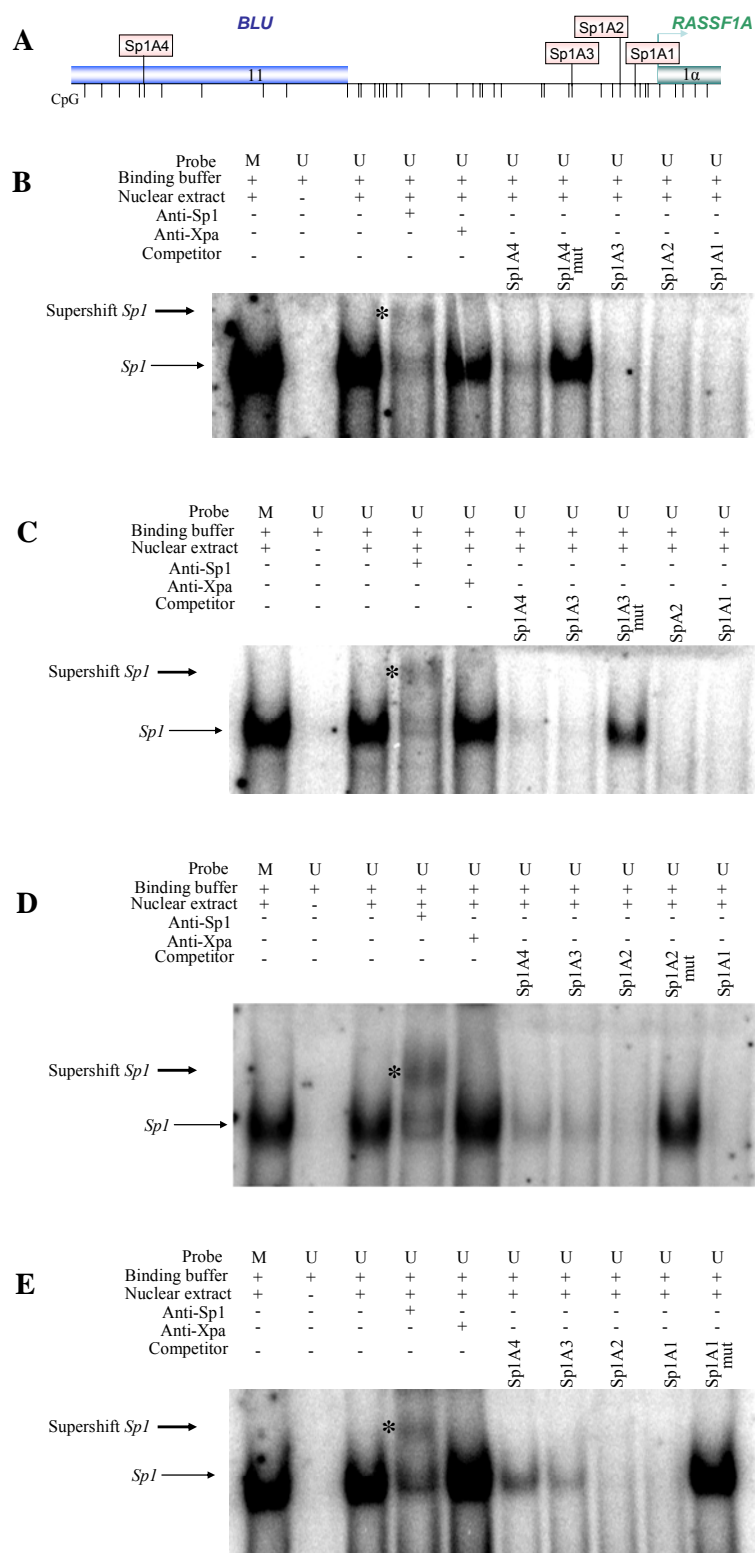
Figure 3-4. EMSA of the four *Sp1* sites located in the *RASSF1A* promoter. A. Map of the *RASSF1A* promoter. Localizations of the four putative *Sp1* sites of the *RASSF1A* promoter, CpGs and exons of *RASSF1A* and *BLU* gene are shown. The arrow indicates the putative start site of the *RASSF1A* translation. **B.** EMSA with labelled Sp1A4 oligo. 22 bp labelled unmethylated (U) and *in vitro* methylated (M) oligos were incubated with HeLa nuclear extract and analyzed by EMSA. Additionally, the oligos were incubated with *Sp1* or *XPA* antibody (supershift is indicated by arrow and asterisk) and competitor oligos. Mutated (mut) competitors were included in the assays. **C.** EMSA with labelled Sp1A3 oligo. **D.** EMSA with labelled Sp1A2 oligo. **E.** EMSA with labelled Sp1A1 oligo.

3.4 Analysis of the *RASSF1A* promoter fragment by *in vivo* footprinting

To verify the *Sp1* binding to the *RASSF1A* promoter, *in vivo* footprinting was performed using the ligation-mediated PCR method (LM-PCR) (Figure 3-5). In the analyzed DNA fragment of the *RASSF1A* promoter, the four hyperreactive Gs were identified at the positions: -481, -468, -461 and -433 relative to the putative translation start codon of *RASSF1A* (Figure 3-5 B and C). The hyperreactive G located at the position -481 belongs to sequence of the upstream *Sp1* site.

Thus, the upstream *Sp1* site (Sp1A4) in the *RASSF1A* promoter was verified by *in vivo* footprinting analysis, EMSA and luciferase assay. An *in vivo* footprinting analysis of *Sp1* sites located in the *RASSF1A* CpG island should be performed in next future.
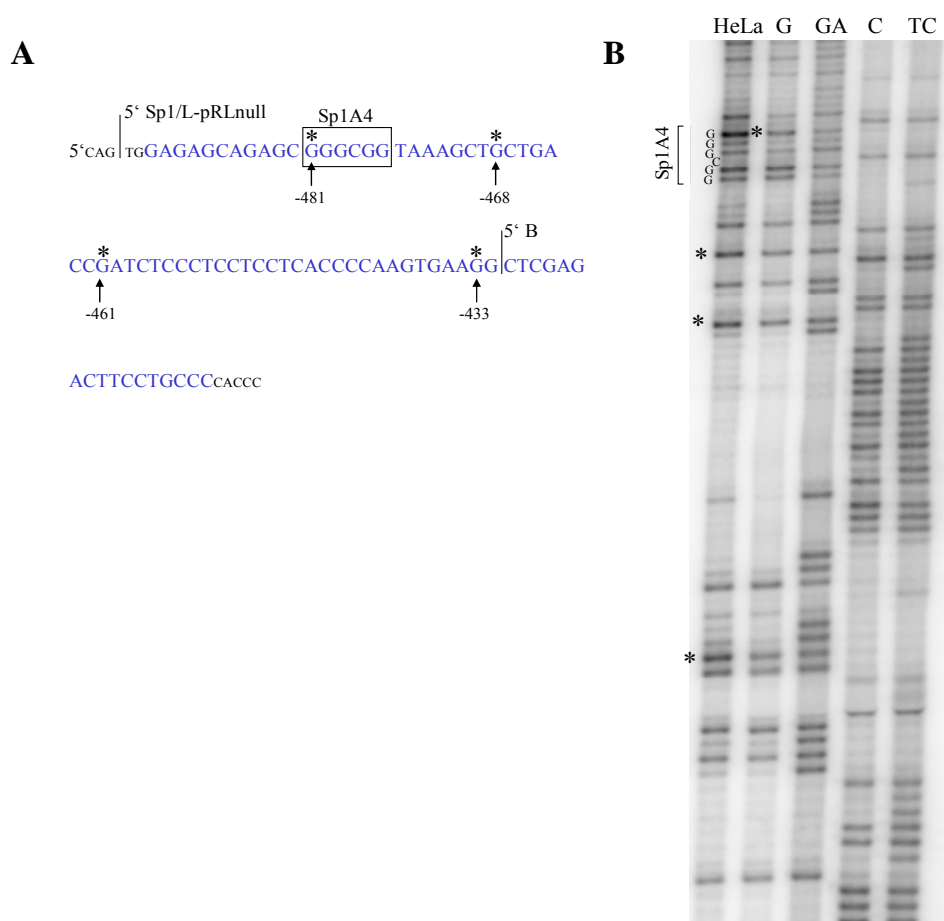
Figure 3-5. ***In vivo* footprinting of the *RASSF1A* promoter fragment. A.** Sequence of the *RASSF1A* promoter fragment. Capital blue letters present the promoter fragment, which was analyzed by LM-PCR. The *Sp1* site is indicated. Hyperreactive Gs in HeLa are marked by asterisks. 5' ends of the *RASSF1A* promoter fragments cloned in the Sp1/L-pRLnull and B vectors are shown. **B.** In *vivo* footprinting of the *RASSF1A* promoter fragment located between -490 and -417 was analyzed by LM-PCR. HeLa lane represents the DNA footprints of HeLa cells treated with DMS *in vivo*. G lane shows footprints of HeLa DNA treated with DMS *in vitro*. Hyperreactive Gs in HeLa and the *Sp1* site are marked. Maxam-Gilbert control sequences are shown (GA, C and TC).

3.5 Transcription patterns of the *RASSF1A* and *RASSF1C* genes in different human tissues.

To investigate the *RASSF1A* and *RASSF1C* expression patterns, expression levels of both genes were analyzed in different human tissues using the *Human MTC panel I* (Clontech). The *RASSF1A* and *RASSF1C* transcriptions were studied in the heart, brain, placenta, lung, liver, skeletal muscle (sk. muscle), kidney and pancreas by real time RT-PCR (Figure 3-6 B, for detail information see supplementary Table 7-1).
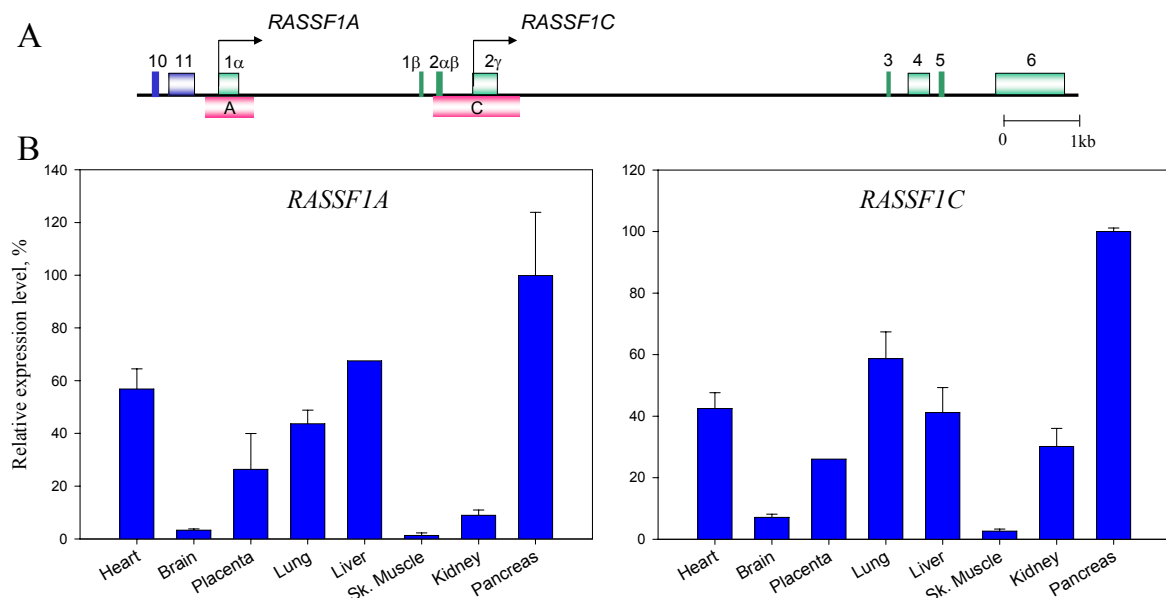
Figure 3-6. **Expression of *RASSF1A* and *RASSF1C* in different human tissues. A.** A map of the *RASSF1* locus. For further details see Figure 2-1. **B.** The expressions of *RASSF1A* and *RASSF1C* were analyzed in the indicated tissue samples by real time PCR using comparative method of Rotor Gene Software version 4.6. The *RASSF1A* and *RASSF1C* expression levels in different tissues were plotted relative to the transcription levels in the pancreas (=100%). The standard deviations are indicated.

Analysis of the *RASSF1A* and *RASSF1C* expression patterns identified the highest rate of the *RASSF1* transcripts in the pancreas compared to other analyzed tissues (Figure 3-6 B). The expressions of *RASSF1A* and *RASSF1C* in the brain and in the skeletal muscle were between 93% and 98% downregulated compared to the pancreas, respectively (Figure 3-6 B). In the placenta, the *RASSF1A* and *RASSF1C* expression levels were four times reduced compared to the pancreas (Figure 3-6 B). Expressions of *RASSF1* transcripts in the heart, lung and liver were between 42% - 67% of pancreas transcription (Figure 3-6 B). In kidney, *RASSF1A* and *RASSF1C* expressions were 91% and 70% decreased, respectively, compared to the transcription level in the

pancreas (Figure 3-6 B). Thus, similarities in the *RASSF1A* and *RASSF1C* transcription patterns were identified in tissues presented in the *Human MTC panel I*.

3.6 The transcription patterns of *RASSF1A* and *RASSF1C* in different cell lines

To investigate epigenetical inactivation mechanism of the *RASSF1A* promoter, human epithelial cells (HMECs) were analyzed. HMECs have two senescence barriers, which enforce a limited proliferative potential (reviewed by Stampfer and Yaswen, 2003). A first proliferation barrier is a <u>st</u>ress or <u>a</u>berrant <u>s</u>ignaling <u>i</u>nduced <u>s</u>enescence (stasis), which is mediated by *RB*. The second proliferation barrier is termed agonescence and is associated with chromosomal aberrations mediated by critically shortened telomeres.

To analyze the *RASSF1A* expression status, RNA was isolated at various growth phases of five HMEC lines grown for consecutive passages from primary tissue. HMEC-48R and HMEC-184 cell lines were obtained from reduction mammoplasty and provided by Martha Stampfer. HMEC-219 and HMEC-1001 cell lines were purchased from Clonetics and available only at post-stasis stadium. HMEC-219 and HMEC-1001 were sub-cultured until they reached agonescence. HMEC-141 cell line was isolated from normal mammary epithelium-141 (patient 141). HMEC-141 cell line was available at pre-stasis and stasis proliferation phases, since cultivated cells of HMEC-141 did not pass stasis.

The *RASSF1A* and *RASSF1C* expressions were analyzed in HMECs, HF, HeLa, peripheral blood mononuclear cells (PBMC), T47D, ZR75-1, MCF7 and mammary gland (Clontech) by real time RT-PCR (Figure 3-7, for detail information see supplementary Table 7-2 and Table 7-3). Analysis of the *RASSF1A* expression identified the highest transcription activity in PBMC (Figure 3-7 A). High *RASSF1A* expression levels were also observed in HeLa and HF. However, the *RASSF1A* expression in HeLa and HF was two times weaker compared to PBMC (Figure 3-7 A). In the breast cancer cell lines, the *RASSF1A* expression was dramatically reduced or absent and reactivated after four days treatment with 5-Aza-CdR (Figure 3-7 A). Analysis of the *RASSF1A* expression pattern in HMECs identified the *RASSF1A* inactivation during HMECs proliferation (Figure 3-7 A). In the pre-stasis HMECs, 84% reduction of the *RASSF1A* expression was identified compared to HF (Figure 3-7 A). The *RASSF1A* expression level of quiescent mammary gland was comparable to the cells at stasis (Figure 3-7 A).

Figure 3-7. Analysis of the *RASSF1A* and *RASSF1C* expressions in the different cell lines. A. The *RASSF1A* expression was analyzed in PBMC, HeLa, HF, mammary gland (Clontech), HMECs (pre-stasis, stasis and post-stasis) and in three breast cancer cell lines (T47D, MCF7 and ZR75-1) by real time RT-PCR using comparative method of the Rotor Gene Software version 4.6. The expression data of three pre-stasis and stasis HMEC isolates (184, 48R, 141) and four post-stasis HMEC (184, 48R, 219 and 1001) were combined. The breast cancer cells were treated for four days with 5-Aza-CdR. The expression levels were plotted relative to transcription level in HF (=100%). The standard deviations are indicated. **B.** The *RASSF1A* expression was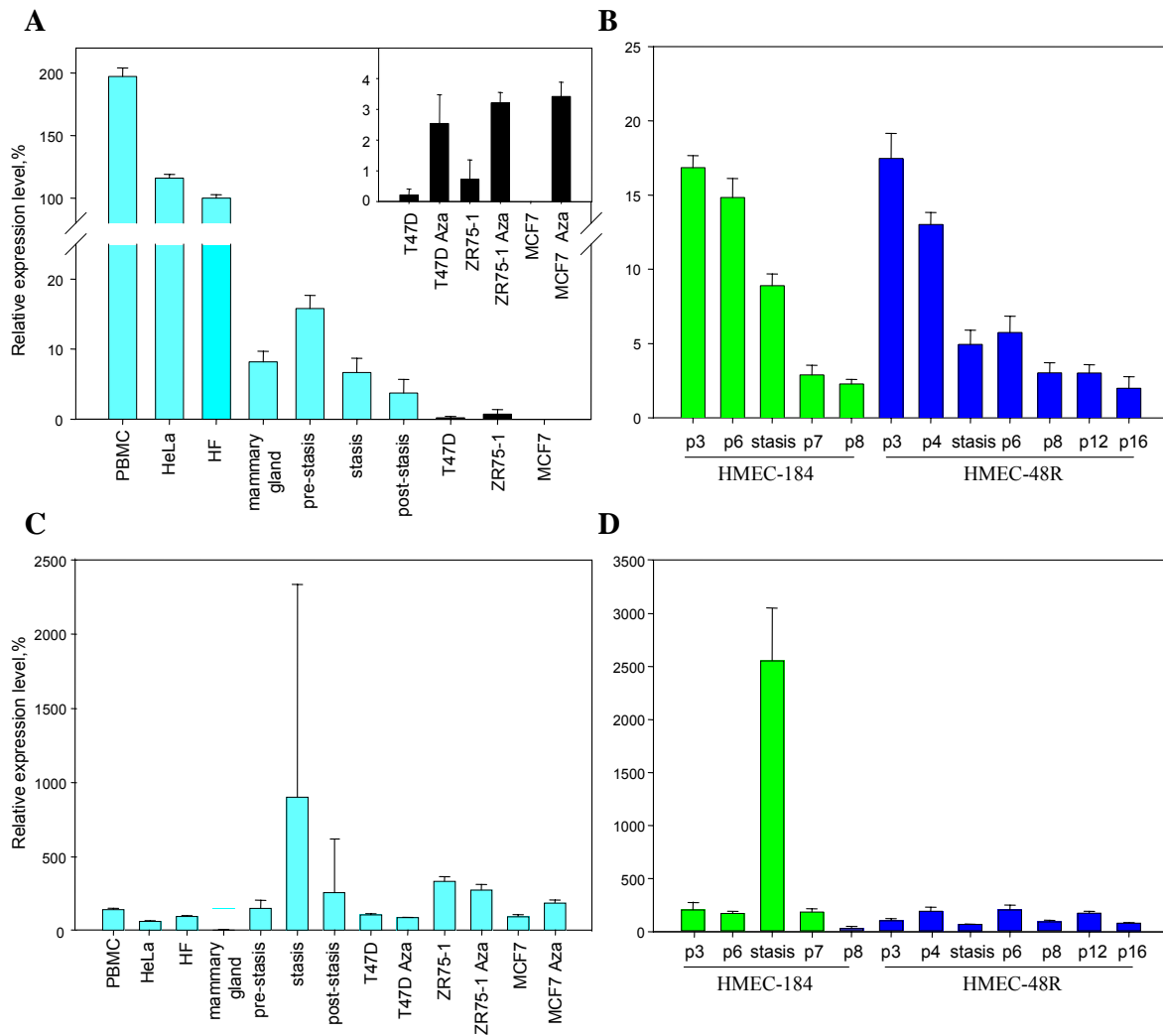 analyzed in consecutive passages of HMEC-184 and HMEC-48R. The expression levels were plotted relative to transcription level in HF (=100%). **C.** The *RASSF1C* expression was analyzed in PBMC, HeLa, HF, mammary gland, HMEC (pre-stasis, stasis and post-stasis) and in three breast cancer cell lines (T47D, MCF7 and ZR75-1). The expression data of three pre-stasis and stasis HMEC isolates (184, 48R, 141) and four post-stasis HMEC (184, 48R, 219 and 1001) were combined. The breast cancer cells were treated four days with 5-Aza-CdR. The expression levels were plotted relative to transcription level in HF (=100%). **D.** The *RASSF1C* expression was analyzed in consecutive passages of HMEC-184 and HMEC-48R. The expression levels were plotted relative to transcription level in HF (=100%).

In HMEC-48R cells, 70% and 90% reduction of the *RASSF1A* expression were observed in stasis and in post-stasis (p16) cells, respectively, compared to pre-stasis (p3) (Figure 3-7 B). *RASSF1A* inactivation tendency was identified in the HMEC-184 cells, since 50% and 90% inactivation of the *RASSF1A* transcription were detected in

stasis and post-stasis (p8) cells, respectively, compared to pre-stasis (p3) (Figure 3-7 B). In HMEC-141, HMEC-219 and HMEC-1001, downregulation of the *RASSF1A* expression was detected during proliferation (data are not shown). These data were used to determine the average of the *RASSF1A* expression in pre-stasis, stasis and post-stasis HMECs (Figure 3-7 A). The *RASSF1C* expression was unaffected in analyzed cell lines (Figure 3-7 C). After 5-Aza-CdR treatment of the breast cancer cell lines, no alteration in the *RASSF1C* expression was identified (Figure 3-7 C). Moreover, the *RASSF1C* transcription was not significantly changed in pre-stasis and post-stasis (Figure 3-7 B). However, an upregulation of the *RASSF1C* transcription was observed in HMEC-184 at stasis phase (Figure 3-7 B).
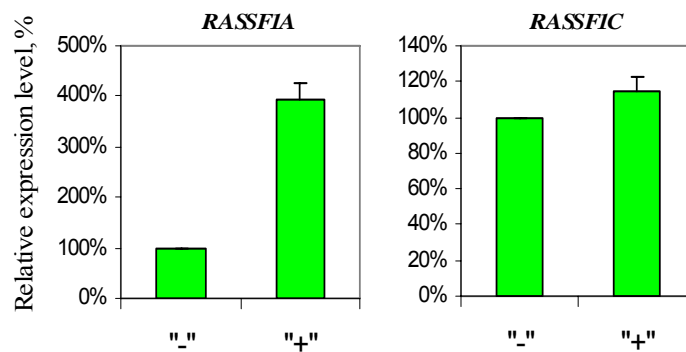
Figure 3-8. The *RASSF1A* and *RASSF1C* expressions in post-stasis HMECs after 5-Aza-CdR treatment. Using real time RT-PCR, the *RASSF1A* and *RASSF1C* expressions were analyzed in HMEC-184 passage 13 cells treated with 5-Aza-CdR for 4 days. The expression levels in the treated cells ("+") were plotted relative to transcription levels in untreated cells ("-") (=100%) using comparative method of the Rotor Gene Software version 4.6. The standard deviations are indicated.

Treatment of HMEC-184 passage 13 (post-stasis) with 5-Aza-CdR for 4 days was performed to investigate the mechanism of the *RASSF1A* inactivation in HMECs (Figure 3-8 and for detail information see Table 7-4). In treated cells, the *RASSF1A* transcription was four times increased compared to the untreated cells, whereas the *RASSF1C* expression was only 10% increased (Figure 3-8). Thus, the *RASSF1A* inactivation during HMEC senescence occurs by epigenetic modifications.

In summary, HMEC senescence is associated with inactivation of the *RASSF1A* transcription. According to Aza-CdR treatment experiments, this inactivation is mediated by DNA methylation.

3.7 Analysis of the epigenetical status of the $p16^{INK4}$ promoter in HMECs

Epigenetical inactivation of tumor suppressor gene, $p16^{INK4}$ was already observed in consecutive passages of HMEC-48R and HMEC-184 by Stampfer and colleagues (reviewed by Stampfer and Yaswen, 2003). To compare the *RASSF1A* silencing to $p16^{INK4}$ in HMECs, the $p16^{INK4}$ methylation pattern and transcription were analyzed in HMEC-141, HMEC-219 and in the breast cancer cell lines by real time RT-PCR and MSP (Figure 3-9, for detail information see supplementary Table 7-5).
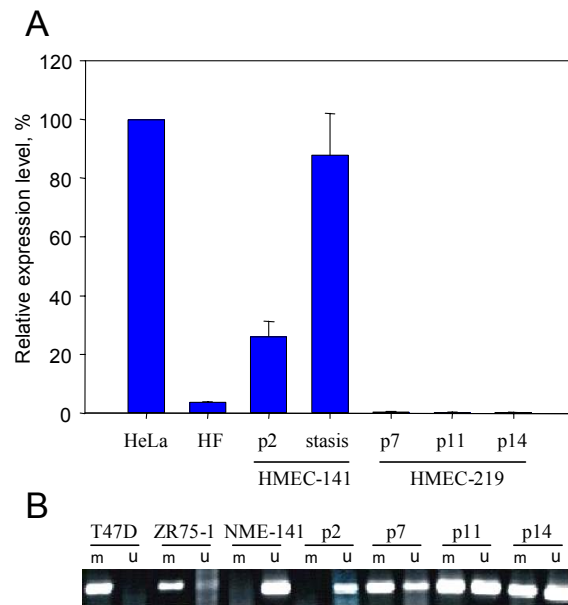
Figure 3-9. The inactivation of $p16^{INK4}$ in HMECs. A. The expression of $p16^{INK4}$ was analyzed in HeLa, HF, HMEC-141 (p2 and p4) and HMEC-219 (p7, p11 and p14) by real time RT-PCR and plotted relative to expression of HeLa (=100%) using comparative method of the Rotor Gene Software version 4.6. The standard deviations are indicated. **B.** The DNA methylation of the $p16^{INK4}$ CpG island was investigated by MSP in NME-141, HMEC-141 and HMEC-219 and in breast cancer cell lines (T47D and ZR75-1). PCR Products of specific primers to methylated (m) and unmethylated DNA (u) were separated on a 2% agarose gel.

In stasis cells (p4) of HMEC-141, three times upregulation of the $p16^{INK4}$ transcription was found compared to pre-stasis (p2) using real time RT-PCR (Figure 3-9). Furthermore, the considerably lower expression of $p16^{INK4}$ was identified in cells from post-stasis passages of HMEC-219 (Figure 3-9 A). The transcripts of $p16^{INK4}$ were completely not detectable in cancer cell lines: A549, T47D, ZR75-1, MCF7 and MDA-MB-231 (data are not shown).

Analysis of the $p16^{INK4}$ CpG island identified DNA methylation in post-stasis passages of HMEC-219, whereas in the breast tissue of patient-141 (NME-141) and in HMEC-

141 passage 2, DNA methylation was not detected (Figure 3-9 B). In breast cancer cell lines (T47D and ZR75-1), the $p16^{INK4}$ promoter was completely methylated in all cells, since PCR products of specific primers to the unmethylated $p16^{INK4}$ promoter were not detected (Figure 3-9 B). The upregulation of the $p16^{INK4}$ expression in stasis HMEC-141 and the epigenetical inactivation of $p16^{INK4}$ in post-stasis HMEC-291 confirms the data published by Stampfer and colleagues (Brenner *et al.*, 1998, Olsen *et al.*, 2002).

3.8   Methylation analysis of the *RASSF1* locus

The DNA methylation pattern of the *RASSF1A* locus was investigated by combined bisulfite restriction analysis (COBRA) (Figure 3-10). For COBRA, a 7 kb region flanking the *RASSF1A* CpG island was divided into 12 PCR fragments of 200 to 400 bp lengths containing restriction endonuclease sites for *TaqI*, *HpyCH4IV* or/and *BstUI* (Figure 3-10 A). The ratio of undigested PCR products between restriction (+) and mock (-) digested samples reflects the amount of unmethylated CpG at a specific cutting site (Figure 3-10 B). The *RASSF1A* (RA) and *RASSF1C* (RC) CpG island fragments revealed differences in DNA methylation pattern. In all analyzed cells, the RC fragment was unmethylated (Figure 3-10 B and C). In HF, blood and HeLa, the RA fragment was unmethylated (Figure 3-10 B and C). In contrast, completely DNA methylation of the RA fragment was observed in four breast cancer cell lines (T47D, MDA-MB-231, ZR75-1 and MCF7) and in lung cancer A549 cells (Figure 3-10 B and C). Further, the DNA methylation patterns of the sequences flanking the RA fragment were analyzed. All six segments (D1-D6) located downstream from the putative *RASSF1A* translation start codon were methylated in breast cancer cell lines and A549 cells (Figure 3-10 C). In HeLa and HF, D1 and D2 regions were unmethylated; and D3 and D5 fragments located in different *Alu* elements were methylated at 50% and 100%, respectively (Figure 3-10 C). However, a CpG site (D4) located in a *LINE2* element between the *Alus* was less frequently methylated (25 to 37%) in HeLa and HF (Figure 3-10 C). Three fragments (U2-U4) located upstream from the *RASSF1A* CpG island were frequently methylated in cancer and nonmalignant cells (Figure 3-10 C). In the T47D and MDA-MB-231 cells, DNA hypomethylation of the fragments U4 and U3 was observed (Figure 3-10 B and C). The U1 fragment containing the upstream putative *Sp1* site was less frequently methylated in the *RASSF1A* expressing cells (HeLa, HF, Blood) (0 to 33%) compared to breast cancer cells and A549 cells (>90%)

(Figure 3-10 B and C). Thus, in HF, HeLa and blood, the region containing RA, D1 and D2 fragments was unmethylated in contrast to the breast cancer cell lines and A549 cells, which were characterized by strong DNA methylation of this region. (Figure 3-10 B and C).
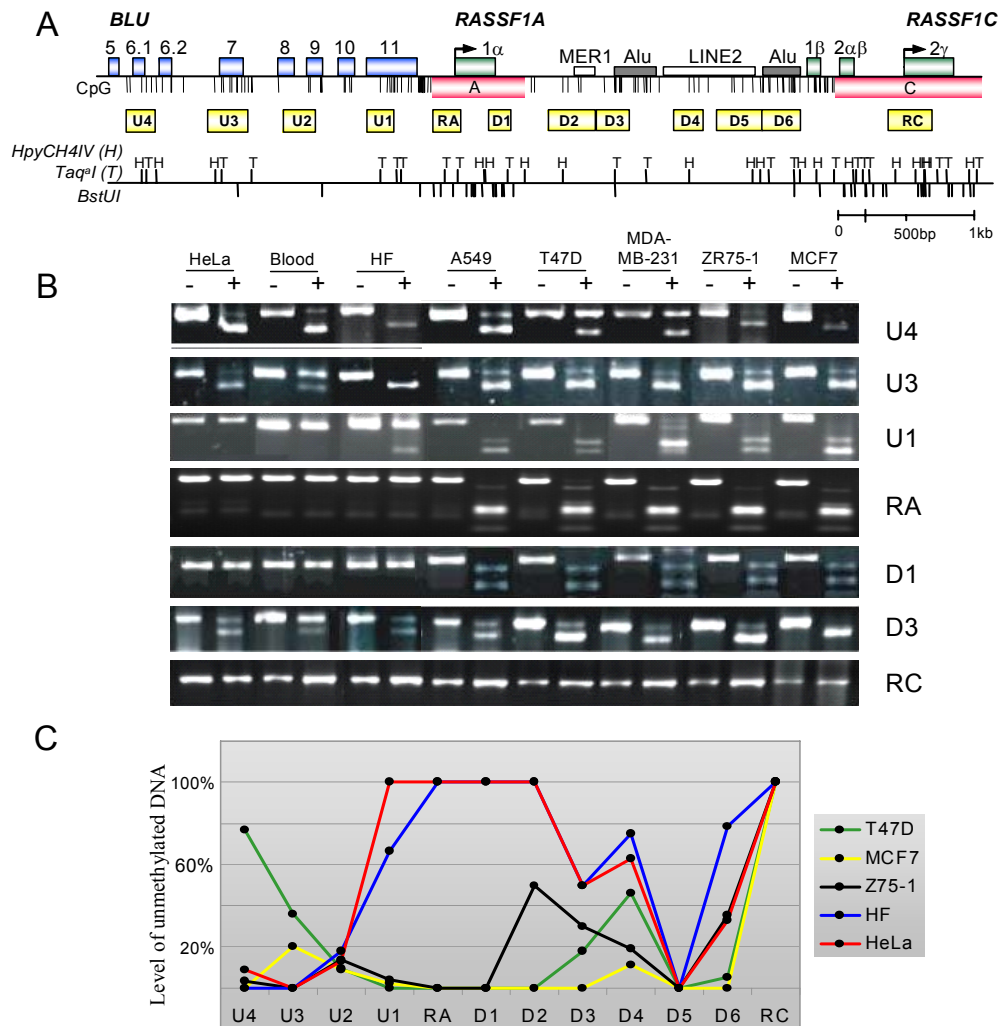
Figure 3-10. DNA methylation analysis of the *RASSF1* locus. A. Map of the *RASSF1* locus. The indicated 12 fragments of the 7 kb locus were analyzed by COBRA. For further details see Figure 2-1. **B.** Representative COBRA analysis of HeLa, blood, HF, A549 and of the breast cancer cell lines (T47D, MDA-MB-231, ZR75-1 and MCF7). PCR products of bisulfite-treated DNA were digested (+) or mock-digested (-) with the appropriate enzymes. **C.** The relative DNA methylation was plotted for the indicated breast cancer cell lines, HF and HeLa.

Furthermore, the DNA methylation patterns of U2, U1, RA, D1 and D2 fragments were investigated in consecutive passages of HMECs. The results of this analysis are presented in Figure 3-11. Using COBRA analysis in HMECs, the strong methylation of the D2 region was observed in contrast to HeLa, HF and blood (Figure 3-10 B and

C, Figure 3-11 B, C and D). In HMECs, DNA methylation was detected in the D1 fragment in contrast to HeLa, HF and blood (Figure 3-10 B and C, Figure 3-11 B, C and D). In HMEC-184, DNA methylation level of the D1 fragment was increasing with cell passages (Figure 3-11 B and D). However, in HMEC-48R, methylation level of the D1 segment was unaffected during cell senescence (Figure 3-11 B and D). In pre-stasis and stasis cells, the RA fragment was unmethylated (Figure 3-11 B, C and D). In this segment, DNA methylation was detected in all post-stasis passages (Figure 3-11 B, C and D). In the U1 region of HMEC-184 passage 8 (p8), level of unmethylated DNA was two times decreased compared to passage 3 (p3) (Figure 3-11 B and D). In HMEC-48R, 14% of unmethylated DNA in U1 region was almost unaffected during senescence (Figure 3-11 C and D). However, the DNA methylation frequency of the U1 fragment was increased and this is indicated by disappearance of partly methylated restriction products during senescence of HMEC-48R and HMEC-184 (Figure 3-11 B, C and D). In HMECs, the DNA methylation of U2 region had the same pattern as in other analyzed cell lines (Figure 3-10 C, Figure 3-11 B, C and D). Similar, COBRA analysis of NME-141, HMEC-141 and HMEC-219 identified spreading the DNA methylation from upstream and downstream into the RA region and *de novo* DNA methylation in the RA fragment (data are not shown).

In summary, the *RASSF1A* expressing cells (HF, HeLa and blood) were characterized by an unmethylated DNA region containing the *RASSF1A* CpG island in contrast to cancer cell lines, which do not express *RASSF1A*. The unmethylated DNA region in the *RASSF1A* CpG island decreased in pre-stasis HMEC compared to HF, HeLa and blood. During HMEC proliferation, spreading of DNA methylation from upstream and downstream into the *RASSF1A* promoter was detected. This was associated with inactivation of the *RASSF1A* expression in consecutive passages of HMECs.
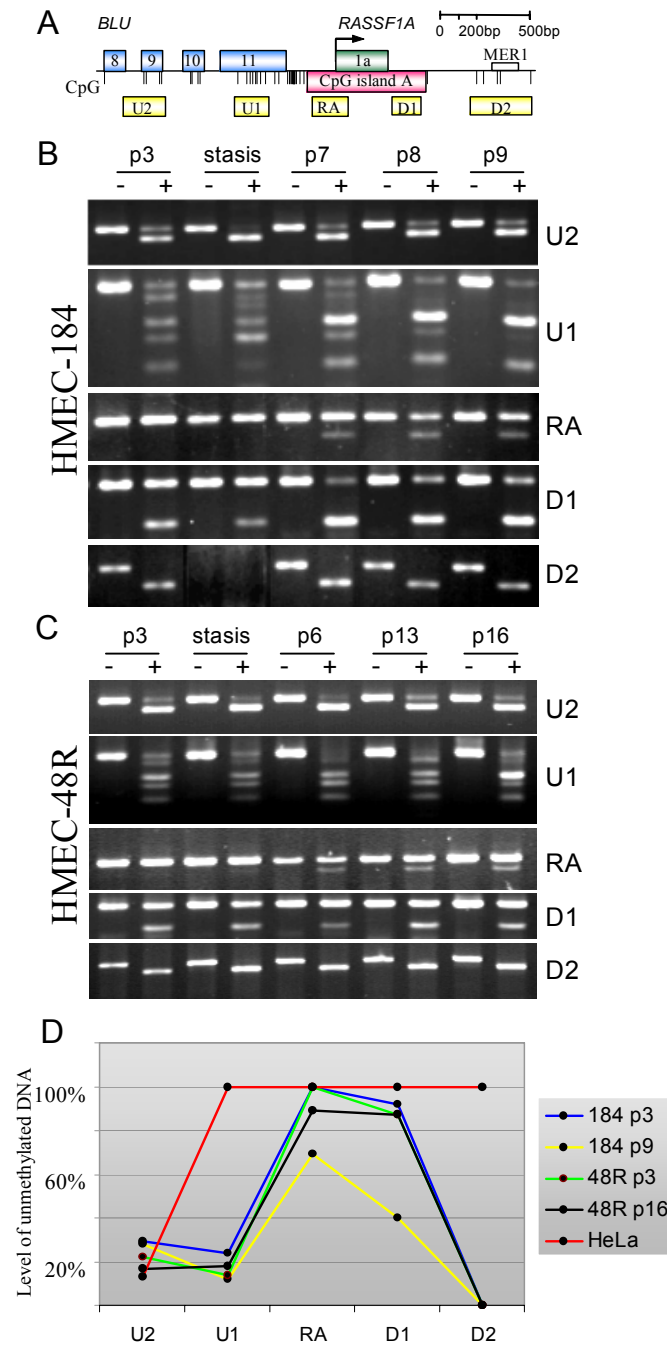
Figure 3-11. Methylation pattern of the *RASSF1A* CpG island and surrounded areas in HMECs.
A. A map of the *RASSF1* locus. The five indicated DNA fragments of the *RASSF1* locus were analyzed by COBRA. For further details see Figure 2-1. **B.** Representative COBRA analysis of consecutive cell passages of HMEC-184. PCR products of bisulfite-treated DNA were digested (+) or mock-digested (-) with the appropriate enzymes. **C.** Representative COBRA analysis of consecutive cell passages of HMEC-48R. PCR products of bisulfite-treated DNA were digested (+) or mock-digested (-) with the appropriate enzymes. **D.** The relative DNA methylation level was plotted for HMEC-184 passage p3 (p3) and passage 9 (p9), HMEC-48R passage 3 (p3) and passage p16 (p16) and HeLa.

3.9   Sequencing of bisulfite modified DNA of the *RASSF1A* promoter

To analyze DNA methylation pattern of single CpGs in the U1 and RA regions, PCR fragments of bisulfite modified DNA were subcloned and analyzed by sequencing (Figure 3-12). Sixteen and seven CpGs were examined in the RA and U1 fragments obtained from several independent clones, respectively (Figure 3-12). In HF and PBMC, the RA region was completely unmethylated and the U1 fragment was unmethylated in most of the clones. However, methylation of two CpGs located in the *Sp1* binding region at positions -482 and -478 were detected in few clones. In the breast cancer cell line MCF7, almost all analyzed CpGs were methylated in U1 and RA regions (Figure 3-12). Further, the DNA methylation patterns of the U1 and RA fragments were investigated in the consecutive passages of HMECs (Figure 3-12). The RA fragment located in the *RASSF1A* CpG island was unmethylated in NME-141, pre-stasis (p3) and stasis cells of HMEC-184 (Figure 3-12). In this region, methylated CpGs were identified in post-stasis cell (p8) of HMEC-184; however, the DNA methylation density was significantly lower compared to the breast cancer cells (Figure 3-12). The DNA methylation seeds were also identified in the *Sp1* sites located in the RA region. From the eight analyzed U1 sequences of NME-141, only two were unmethylated (Figure 3-12). Interestingly, the unmethylated U1 region was not identified in pre-stasis HMEC-141 cells, which were obtained from NME-141 (Figure 3-12). In HMEC-184, the U1 fragment was frequently methylated. In pre-stasis cells (p3) of HMEC-184, only one from the seven U1 fragments was unmethylated (Figure 3-12). Stasis and post-stasis cells (p8) of HMEC-184 contain only the methylated U1 region (Figure 3-12). Thus, in concordance with the COBRA data, *de novo* DNA methylation of the *RASSF1A* CpG island fragment (RA) located upstream from the *RASSF1A* translation start site was identified during proliferation of HMECs by sequencing of bisulfite modified DNA; and increasing of DNA methylation level in region (U1) containing the upstream *Sp1* site of the *RASSF1A* promoter was observed during senescence of HMECs.

In total, 65 clones containing the U1 fragments with partially methylated sequences from HF, PBMC, blood, MCF7, HMECs and of NME-141 were analyzed (Table 3-1 and data are not shown). In all these clones, DNA methylation of the at least one CpG at positions -482 or -478 was observed (Table 3-1). Both of these CpGs are located in the upstream *Sp1* binding region. Fifty five clones contained both methylated CpGs at these positions and 10 clones had only one methylated CpG at these positions (Table

3-1). Interestingly, DNA methylation occurred preferentially around these two CpGs in most analyzed clones (Table 3-1).

In summary, in pre-stasis cells, the upstream located *Sp1* site was frequently methylated. In the U1 region containing this site, increase of DNA methylation level was observed during senescence of HMECs. In post-stasis HMEC-184 cells, *de novo* DNA methylation occurred in the *RASSF1A* CpG island fragment located upstream from the putative *RASSF1A* translation start site. This methylation level was lower compared to cancer cell line, MCF7.

Table 3-1. Methylation of CpGs at -482 and -478 position in the sequenced clones

Number of clones[1]	CpG methylated at position -482 **OR** -478		CpGs methylated at positions -482 **AND** -478	
	Only one methylated CpG in *Sp1* site [2]	Additionally methylated CpGs [3]	Both methylated CpG in *Sp1* site[4]	Additionally methylated CpGs [5]
65	2/65 (3.08%)	8/65 (12.31%)	6/65 (9.23%)	49/65 (75.38%)
	10/65 (15.3%)		55/65 (84.6%)	

[1]Number of clones with the partially methylated U1 fragments. [2]Number of clones containing only one methylated CpG at positions -482 or -478. [3]Number of clones containing one methylated CpG at position -482 or -478 and methylated CpGs at other positions. [4]Number of clones containing only two methylated CpGs and they are at positions -482 and -478. [5]Number of clones containing methylated CpGs at positions -482 and -478 and methylated CpGs at other positions.
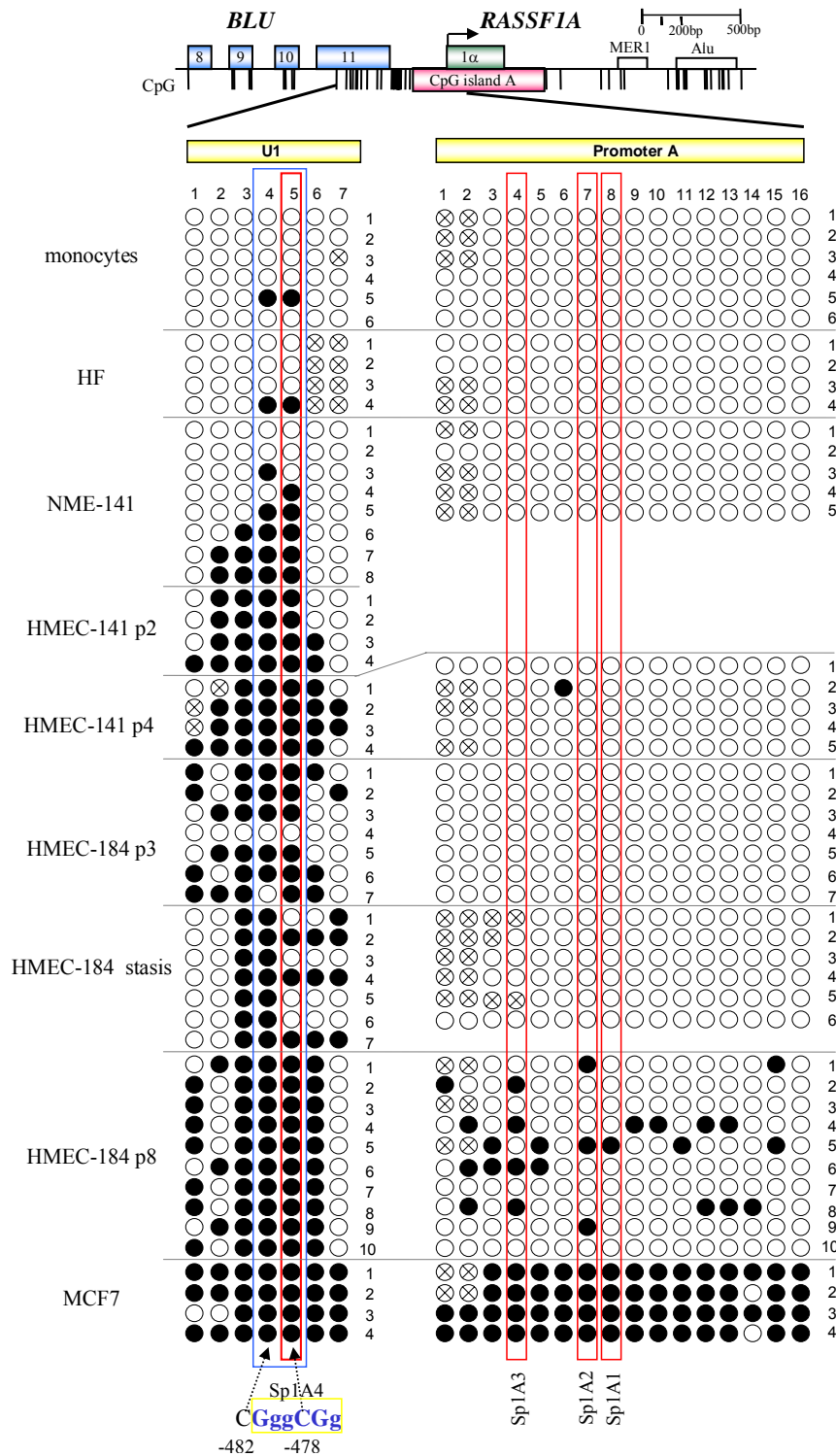
Figure 3-12. Sequencing of bisulfite modified DNA of the *RASSF1A* promoter. A map of the *RASSF1A* promoter region is shown. For further details see Figure 2-1. The two indicated PCR fragments were analyzed by sequencing. Seven and sixteen CpGs of the U1 and RA fragments, respectively, were analyzed in HF, PBMC, NME-141, HMEC-141, HMEC-184 and MCF7. Amplified PCR products were subcloned into the *pGEM-T* vector and several independent clones were sequenced. Black and white dots represent methylated and unmethylated CpGs, respectively. Dots marked with a cross were not analyzable by sequencing. Red and blue outlines indicate the *Sp1* sites and CpG located at positions -482 and -478 relative to the putative *RASSF1*A translation start codon, respectively.

3.10 Histone modifications in the *RASSF1A* and *RASSF1C* promoters

In addition to DNA methylation, distinct chromatin modifications are associated with gene activity (reviewed by Jenuwein and Allis, 2001). Trimethylated histone H3 lysine 9 is a histone modification, which is associated with condensed, inactive chromatin. In contrast, the acetylated histone H3 at lysine 9 and lysine 14 is a hallmark of active chromatin. To investigate histone modifications at the *RASSF1A* and *RASSF1C* promoters, chromatin immunoprecipitation (ChIp) experiments were performed. The A1 and A2 fragments were analyzed in the *RASSF1A* promoter. The A1 fragment contains the upstream *Sp1* binding site. The A2 region is the *RASSF1A* CpG island fragment with the three *Sp1* binding sites. In the *RASSF1C* promoter, the C region containing two *Sp1* sites at positions -187 and -273 was studied. In these three DNA regions, the level of acetylated histone H3 and trimethylated histone H3 lysine 9 were analyzed in HeLa, ZR75-1 and HMEC-184 (Figure 3-13, for detail information see supplementary Table 7-6 and Table 7-7). In HMEC-184, cells from pre-stasis and post-stasis proliferation phases were studied at passage 6 and passage 12, respectively.
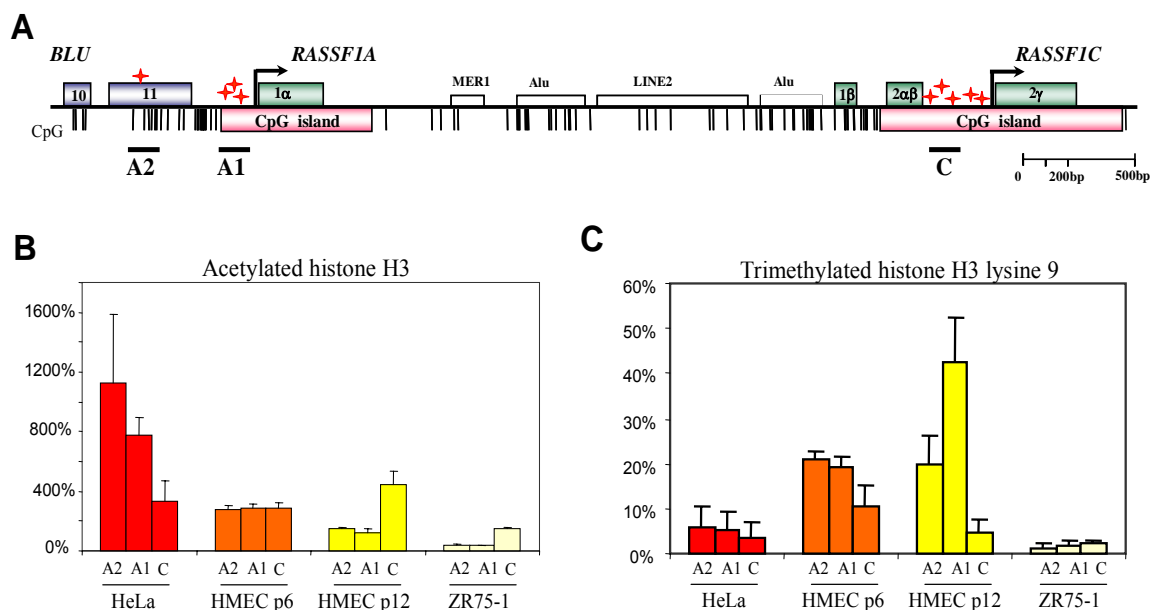
Figure 3-13. Histone modifications in the *RASSF1A* and *RASSF1C* promoters. A. A map of the *RASSF1* locus. For further details see Figure 2-1. Localizations of analyzed fragments are shown. Red stars indicate the *Sp1* sites. **B.** Pattern of acetylated histone H3 was analyzed in HeLa, ZR75-1, HMEC-184 passage 6 (p6) and 12 (p12) by ChIp using real time PCR. Data were verified by comparative method of Rotor Gene Software version 4.6. A "no antibody" probe (=0%) and "input" sample (=100%) were used as controls. The standard deviations are indicated **C.** ChIp assay was performed using antibodies to trimethylated histone H3 lysine 9 in HeLa, ZR75-1 and HMEC-184 passages 6 (p6) and 12 (p12).

Using ChIp, the highest frequency of acetylated histone H3 was detected in the *RASSF1A* promoter in HeLa (Figure 3-13 B). In these cells, level of acetylated histone H3 in the *RASSF1A* promoter was at least two times stronger compared to the *RASSF1C* promoter (Figure 3-13B). In HeLa, the A2 region was characterized by higher frequency of acetylated histone H3 compared to A1 region (Figure 3-13 B). In the *RASSF1C* promoter of pre-stasis HMECs and HeLa, levels of acetylated histone H3 were similar (Figure 3-13 B). The A1 and A2 regions of pre-stasis HMECs were characterized by 2.6 and 4 times decrease of acetylated histone H3 frequencies, respectively, compared to HeLa (Figure 3-13 B). The *RASSF1C* promoter in post-stasis HMECs contained more acetylated histone H3 in contrast to pre-stasis HMECs. In post-stasis HMECs, the *RASSF1A* promoter was associated with two times lower frequency of acetylated histone H3 compared to pre-stasis HMECs (Figure 3-13 B). Thus, level of acetylated histone H3 in the *RASSF1A* promoter decreased during senescence of HMEC-184. In ZR75-1 cells, level of acetylated histone H3 in the *RASSF1C* promoter was about four times higher compared to the *RASSF1A* promoter, which was characterized by the lowest level of acetylated histone H3.

Furthermore, the pattern of trimethylated histone H3 lysine 9 was analyzed (Figure 3-13 C). In ZR75-1 and HeLa, level of this histone modification was similar in the *RASSF1A* and *RASSF1C* promoters (Figure 3-13 C). In pre-stasis and post-stasis HMECs, the *RASSF1A* promoter was characterized by elevated frequency of trimethylated histone H3 lysine 9 compared to the *RASSF1C* promoter (Figure 3-13 C). In pre-stasis HMECs, levels of trimethylated histone H3 lysine 9 were similar in the regions A2 and A1 (Figure 3-13 C). In these cells, the *RASSF1A* promoter and the *RASSF1C* were characterized by elevated frequencies of trimethylated histone H3 lysine 9 compared to HeLa (Figure 3-13 C). During senescence of HMECs, level of trimethylated histone H3 lysine 9 was not changing in the region A2 (Figure 3-13 C). In the *de novo* methylated region A1 of post-stasis HMECs, the highest level of trimethylated histone H3 lysine 9 was identified compared to other analyzed cells (Figure 3-13 C). Thus, elevated frequency of trimethylated histone H3 lysine 9 is associated with *de novo* DNA methylation in the *RASSF1A* promoter in HMEC-184. In the *RASSF1C* promoter of post-stasis HMEC-184 and HeLa, levels of trimethylated histone H3 lysine 9 were similar. During senescence of HMEC, this promoter was associated with a decrease of frequency of trimethylated histone H3 lysine 9 (Figure 3-13 C). In summary, the active transcribing *RASSF1A* and *RASSF1C* promoters are

characterized by elevated frequency of acetylated histone H3. Decreasing of acetylated histone H3 level and increasing of trimethylated histone H3 lysine 9 frequencies were observed in the *RASSF1A* promoter during HMEC senescence. The highest level of trimethylated histone H3 lysine 9 frequency was detected in the *de novo* DNA methylated fragment of the *RASSF1A* CpG island in HMECs.

3.11 The *Sp1* binding to the *RASSF1A* and *RASSF1C* promoters in cell lines

ChIp experiments were performed to analyze *Sp1* binding *in vivo* and to verify EMSA, LM-PCR and luciferase assay data. The *Sp1* binding was studied in the *RASSF1A* (fragments A1 and A2) and *RASSF1C* (fragment C) promoters of HMEC-184 passage 6 and 12, HeLa and ZR75-1 (Figure 3-14).
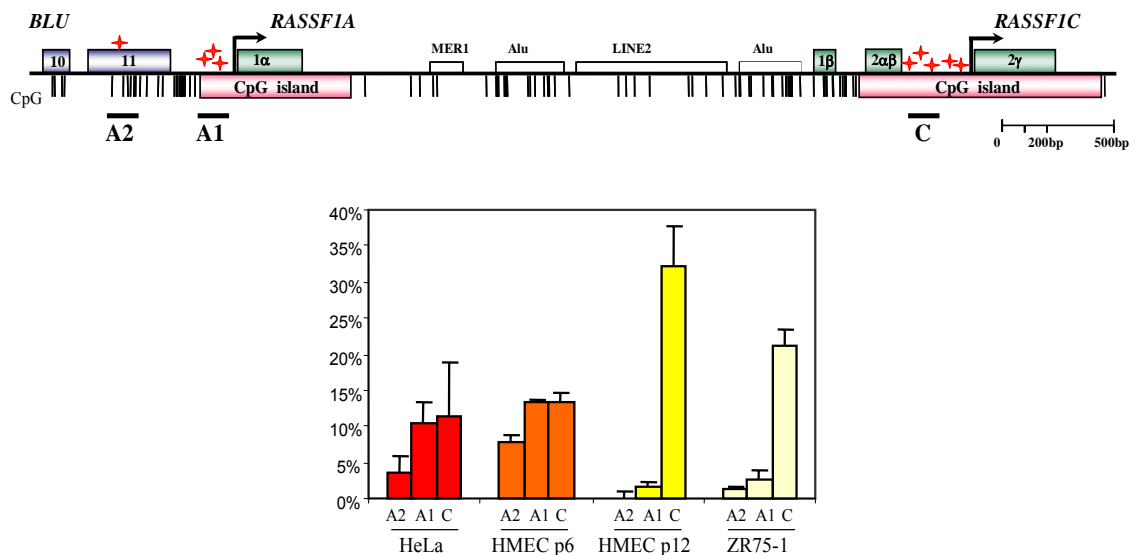
Figure 3-14. *Sp1* **binding of the** *RASSF1A* **and** *RASSF1C* **promoters.** A map of the *RASSF1* locus. For further details see Figure 2-1. Localizations of the analyzed fragments are shown. Red stars indicate the *Sp1* sites. The *Sp1* binding pattern was analyzed in HeLa, HMEC-184 passages 6 (p6) and 12 (p12), ZR75-1 cells using ChIp and real time PCR. Data were verified by comparative method of Rotor Gene Software version 4.6. "No antibody" probe (=0%) and "input" sample (=100%) were used as controls. The standard deviations are indicated.

Analysis of ChIp data indicated strong *Sp1* binding to the *RASSF1C* promoter in all analyzed cell lines (Figure 3-14, for detail information see supplementary Table 7-8). In HeLa and pre-stasis HMECs, the *Sp1* binding had the same pattern and *Sp1* bound with same efficiency both of analyzed CpG islands (A1 and C) (Figure 3-14). In these cells, the *Sp1* binding to the A2 region containing the one *Sp1* binding site was

decreased compared to the fragment A1 with the three *Sp1* sites (Figure 3-14). Interestingly, the methylated *Sp1* site in the A2 region in pre-stasis HMECs was bound by *Sp1* similar as the unmethylated region A2 in HeLa (Figure 3-14). Hence, the *Sp1* binding in the A2 region is not sensitive to DNA methylation. In post-stasis HMECs, repression of *Sp1* binding in the region A2 and strong decreasing of the *Sp1* binding in the region A1 were observed. In post-stasis HMECs, the *Sp1* binding to the *RASSF1C* CpG island (C) was 19 times increased compared to the *RASSF1A* CpG island (A1) and 2.4 times stronger compared to the *RASSF1C* promoter in pre-stasis HMECs (Figure 3-14). Analogously, in ZR75-1, unmethylated *RASSF1C* promoter was bound by *Sp1* at least nine times stronger compared to methylated *RASSF1A* promoter (A2 and A1) (Figure 3-14).

In summary, the *Sp1* binding to the *RASSF1C* promoter was identified in all analyzed cells using ChIp. HeLa cells were characterized by the *Sp1* binding to the *RASSF1A* promoter in contrast to ZR75-1 cells. During HMEC-184 proliferation, occlusion of the *Sp1* binding to the *RASSF1A* promoter was detected. The *Sp1* binding to the upstream located *Sp1* site in the *RASSF1A* promoter does not depend from DNA methylation.

4   Discussion

4.1   Regulation of *RASSF1A* transcription

RASSF1A is a tumor suppressor gene, which is frequently inactivated in human cancers (Dammann *et al.*, 2003). This silencing is associated with a DNA hypermethylation of the *RASSF1A* CpG island. However, the epigenetic mechanisms responsible for the *RASSF1A* inactivation are unknown. Since a protectional role of the *Sp1* sites from DNA methylation was demonstrated in several studies (Frank *et al.*, 1991; Brandeis *et al.*, 1994; Macleod *et al.*, 1994; Matsuo *et al.*, 1998; Qu and Ehrlich, 1999; Gazzoli and Kolodner, 2003); the four putative *Sp1* sites, which were identified in the *RASSF1A* promoter by *in silico* analysis, were intensively analyzed in present research. Three of these *Sp1* sites are located in the *RASSF1A* CpG island, whereas the fourth *Sp1* site is detected 478 bp upstream from the putative translation start site, in the last exon of the *BLU* gene. Luciferase assay analysis identified that mutation of the upstream *Sp1* site leads to a decrease of the *RASSF1A* promoter transcription activity. In this site, a hypersensitive G was detected in the *in vivo* footprinting experiments. Additionally, EMSA showed that proteins, which form complex with *Sp1* antibodies, bind to a 22 bp fragment of the *RASSF1A* promoter containing this *Sp1* site. Analogously, the binding of *Sp1* to this site was detected by ChIp. Thus, present data suggest that the upstream *Sp1* site in the *RASSF1A* promoter is functional. Surprisingly, the deletion of a 63 bp fragment containing this binding site leads to a three fold increase of the promoter activity. Analysis of footprinting *in vivo* identified additional hypersensitive Gs located in the 63 bp fragment. This indicates that this fragment is bound also by other regulatory elements, which may be involved in repression of the *RASSF1A* transcription.

Binding of *Sp1* at the *RASSF1A* CpG island was detected by EMSA *in vitro* and by ChIp *in vivo*. Luciferase assay of the *RASSF1A* promoter demonstrated that the *RASSF1A* CpG island fragment, which is located between -137 and +17 positions and containing the three *Sp1* sites, has 3% of promoter activity compared to the construct containing four *Sp1* sites. Deletion of this CpG island fragment resulted in a 45% decrease of transcription activity compared to the construct with all four *Sp1* sites. Thus, elements located in this CpG island fragment can mediate a very weak transcription activity (3%) by itself, but its presence supports the *RASSF1A* promoter

activity (45%). Hence, three *Sp1* sites located in the *RASSF1A* CpG island may be involved in induction of the *RASSF1A* promoter transcription. Further, promoter analysis by luciferase assay showed that the fragment located between -205 and +17 positions has 40% of promoter activity. Thus, adding of the 68 bp fragment located upstream from three *Sp1* sites leads to an increase of promoter activity from 3% up to 40%. Elements located in this 68 bp DNA region may be essential for expression of the *RASSF1A* promoter. Moreover, this region may be bound by the general transcription factor *TFIID*. Studies of *Sp1* from the last 25 years suggest that *Sp1* is involved in recruitment of the general transcription factor *TFIID* to the DNA through direct interaction with *TAFII130* (Pugh and Tjian, 1990; Tanese *et al.*, 1996). It is commonly believed, that *Sp1* can recruit *TFIID* to TATA-less promoter similar to the TATA box (Pugh and Tjian, 1990; Kaufmann and Smale, 1994; Tanese *et al.*, 1996). In the *RASSF1A* TATA-less promoter, three *Sp1* sites located in the *RASSF1A* CpG island flank a region, which may be bound by general transcription factor *TFIID*. Thus, the *TFIID* recruitment to the *RASSF1A* promoter may be supported by the *Sp1* binding to the CpG island.

In the *RASSF1A* promoter of pre-stasis HMECs, the *Sp1* binding pattern is similar to binding in HeLa cells. However, in pre-stasis HMECs, it is associated with the eight times decreased level of the *RASSF1A* transcription activity compared to HeLa. Chromatin state in the *RASSF1A* promoter in these cells is characterized by decrease of frequency of acetylated histone H3 and increase of level of trimethylated histone H3 lysine 9 compared to HeLa. Methylated histone H3 at lysine 9 is a histone modification, which is associated with inactive X chromosome and pericentric heterochromatin (Mermoud *et al.*, 2002; Peters *et al.*, 2002; Lehnertz *et al.*, 2003; Rougeulle *et al.*, 2004). Moreover, an elevated frequency of methylated histone H3 lysine 9 is an important characteristic of inactive genes (Litt *et al.*, 2001; Nielsen *et al.*, 2001; Fahrner *et al.*, 2002; Nguyen *et al.*, 2002; Kondo *et al.*, 2003; Mutskov and Felsenfeld, 2004; Su *et al.*, 2004). Thus, methylation at lysine 9 of histone H3 is a feature of repressed chromatin, which is not accessible for transcription factors. In contrast, absence or low level of acetylated histone H3 is correlated with inactive chromatin (Litt *et al.*, 2001; Fahrner *et al.*, 2002; Nguyen *et al.*, 2002; Kondo *et al.*, 2003; Mutskov and Felsenfeld, 2004; Su *et al.*, 2004). Thus, the reduced *RASSF1A* transcription in pre-stasis HMECs is associated with the active *Sp1* binding and repressed chromatin. Analogously, a number of studies demonstrated that

transcription, which is mediated by *Sp1*, can be repressed; and this is associated with inactivation of chromatin. Lagger and colleagues reported that the regulation of the $p21^{CIP1}$ expression is under control of *HDAC* and *p53* through interaction with C terminus of *Sp1* (Lagger *et al.*, 2003). In a suppressed state, *HDAC* binds *Sp1* and deacetylate histones; whereas active state of the $p21^{CIP1}$ promoter is characterized by the interaction of *Sp1* with *p53*, which recruits *HAT* and *p300* and this interaction is crucial for transcription activation. Analogous to the $p21^{CIP1}$ promoter, repression of transcription activity by *Sp1-HDAC* complex was demonstrated for *S-phase specific mouse thymidine kinase*, *human telomerase reverse transcriptase*, *manganese superoxide dismutase*, *ORF50* core promoter of Kaposi's sarcoma-associated herpes virus, $p19^{INKd}$, *transforming growth factor-β receptor type I*, *human luteinizing hormone receptor*, *dihydrofolate reductase* and *reversion-inducing-cysteine-rich protein* (*RECK*) (Doetzlhofer *et al.*, 1999; Chang *et al.*, 2001; Hou *et al.*, 2002; Maehara *et al.*, 2002; Won *et al.*, 2002; Zhang and Dufau, 2002; Ammanamanchi and Brattain, 2004; Chang *et al.*, 2004; Yokota *et al.*, 2004). Thus, changing of chromatin state around the *Sp1* binding site may result in changing of transcription activity, which is regulated by *Sp1*. Therefore, in pre-stasis HMECs, the inactivation of chromatin in the *RASSF1A* promoter may result in repression of transcription.

From the other side, *Sp1* interacts with *HAT* and this results in acetylation of the *Sp1* zinc fingers (Suzuki *et al.*, 2000; Torigoe *et al.*, 2004). Torigoe and colleagues demonstrated that the *Sp1* acetylation is associated with reactivation of the *SV40* promoter (Torigoe *et al.*, 2004). Thus, additionally to the chromatin state, acetylation and deacetylation of *Sp1* can regulate changes in transcription. The *RASSF1A* promoter in pre-stasis HMECs is characterized by decreased level of acetylated histone H3 compared to HeLa. This indicates a decrease of level of *HATs* and an increase of level of *HDAC*. These changes may result in deacetylation of the *Sp1* in the *RASSF1A* promoter with a following repression of the *RASSF1A* promoter activity in pre-stasis HMECs.

Additionally, transcription regulated by *Sp1* can be repressed by *MBD*. In 1998, Kudo demonstrated that the human leukosialin transcription activated by *Sp1* is repressed by DNA methylation through methyl-CpG binding protein *MeCP2* (Kudo, 1998). Moreover, an other methyl-CpG binding protein, *MBD1* in a complex with MBD1-containing chromatin-associated factor (*MCAF*) can interact with *Sp1* through *MCAF* and repress transcription of the methylated *p16* and *small nuclear ribonucleoprotein*

polypeptide N (*SPRPN*) promoters (Fujita *et al.*, 2003). In unmethylated promoters, *MCAF* facilitates the *Sp1*–mediated transcription. In pre-stasis HMECs, the *RASSF1A* promoter is characterized by heavy methylation of the upstream *Sp1* site. Thus, presence of *MBD* in the upstream *Sp1* site of the *RASSF1A* promoter in pre-stasis HMECs may result in a repression of the *RASSF1A* transcription. Hence, repression of the *RASSF1A* transcription in pre-stasis HMECs may be regulated by deacetylation of *Sp1*, repression of chromatin and by *MBD*, which are directed by elevated level of DNA methylation in the *RASSF1A* promoter.

4.2   DNA methylation and the *RASSF1A* promoter inactivation

The role of DNA methylation in the inactivation of the *RASSF1A* transcription was revealed by treatment of post-stasis HMECs and no expressing *RASSF1A* cancer cells with 5-Aza-CdR, since after this treatment, transcriptional reactivation of the *RASSF1A* promoter was observed. Recent studies of the hypermethylated *p16^{INKa}*, *mutL homologue 1* (*MLH1*) and *O^6-methylguanine-DNA methyltransferase* promoters showed that the inhibition of *DNMT* with 5-Aza-CdR results in transcriptional reactivation, decrease of DNA methylation and reactivation of chromatin in these promoters (Nguyen *et al.*, 2002; Kondo *et al.*, 2003). Moreover, open chromatin structure occurs in whole genome of cancer cells after 5-Aza-CdR treatment (Espada *et al.*, 2004). Thus, in cancer cells, inactivation of *DNA* methyltransferases leads to opening of chromatin and transcriptional reactivation of silenced genes. Interaction partners of *MBD* are *HDAC* and histone H3 lysine 9 methyltransferase (Jones *et al.*, 1998; Ng *et al.*, 1999; Fuks *et al.*, 2000; Tatematsu *et al.*, 2000). Moreover, *MBDs* have the ability to repress transcription by itself (reviewed by Herman and Baylin, 2003). Thus, the *RASSF1A* transcription may be repressed by *MBD* directly and by *HDAC* and histone H3 lysine 9 methyltransferase through compactization of chromatin. Therefore, decrease of the *MBD* level in the *RASSF1A* promoter after 5-Aza-CdR treatment may result in a reactivation of the transcription through decrease of the *MBDs* negative control of transcription and through opening of chromatin structure for transcriptional factors. This suggestion is supported by observation of Sarraf and Stancheva. They demonstrated that the absence of *MBD1* resulted in loss of methylated histone H3 lysine 9 at multiple genomic loci and the *p53BP2* transcriptional reactivation (Sarraf and Stancheva, 2004).

Analysis of the DNA methylation pattern in the *RASSF1A* promoter identified an methylation free region around the unmethylated CpG island in the *RASSF1A* transcribing cells such as HeLa, HF and blood, whereas this DNA area is frequently methylated in the no expressing *RASSF1A* cancer cells. The 3'-end of this unmethylated DNA fragment in the *RASSF1A* expressing cells flanks a partly methylated (50%) *Alu* repeats; whereas the 5'-end of this region flanks a lightly methylated or completely unmethylated DNA region containing the upstream *Sp1* site. The region containing the upstream *Sp1* site is close to a DNA area, which is strongly methylated in the *RASSF1A* expressing and not expressing cells. Thus, in the *RASSF1A* expressing cells, the DNA methylation level is gradually increased outside from the methylation free area of the *RASSF1A* promoter. In pre-stasis HMECs, the DNA methylation free region in the *RASSF1A* promoter is smaller compared to the *RASSF1A* expressing cells as HeLa, HF and blood. Pre-stasis HMECs are characterized by methylation of the *RASSF1A* exon 1α and region containing the upstream *Sp1* site; whereas the methylation free area was detected only in the *RASSF1A* CpG island fragment located upstream from translation start site. In post-stasis HMECs, this CpG island fragment was partially methylated and an increase of DNA methylation was observed in the *RASSF1A* exon 1α and the region containing the upstream *Sp1* site. Thus, DNA methylation spreads from upstream and downstream into the *RASSF1A* promoter during senescence of HMECs. Similar results were reported by Yan and colleagues (Yan *et al.*, 2003). They identified DNA methylation in the *RASSF1A* exon 1α in all normal breast tissues, primary tumors and cancer cell lines. They detected DNA methylation in the *RASSF1A* CpG island fragment located upstream from translation start site in 90% of normal breast tissue and 90% of primary breast tumors. However, the methylation level in this CpG island fragment in normal breast tissue and primary breast tumors was lower compared to breast cancer cell lines. Thus, DNA methylation pattern of the *RASSF1A* CpG island, which was observed by Yan and colleagues in normal breast tissues and primary breast tumors, is similar as we observed in pre-stasis and post-stasis HMECs. Further, Yan and colleagues showed that level of DNA methylation is strongly enhanced in the exon 1α in normal breast tissues and primary breast tumors compared to the CpG island fragment located upstream from translation start site. Moreover, they detected the methylation pattern of the *RASSF1A* promoter in breast tissues where exon 1α was methylated and the CpG island fragment located upstream from translation start site was unmethylated. Thus,

the observed spreading of DNA methylation from downstream into the *RASSF1A* promoter in our study is also supported by methylation profiling detected by Yan and colleagues (Yan *et al.*, 2003). Analogously, Millar and colleagues identified a spreading of the DNA methylation from upstream and downstream into the *GSTP1* promoter in prostate cancer cells (Millar *et al.*, 2000). Inactivation of the *E-cadherin* gene promoter in human fibroblasts, which overexpress *DNMT1*, is associated with a spreading of DNA methylation from upstream and downstream into promoter (Graff *et al.*, 1997). Thus, spreading of DNA methylation from upstream and downstream into CpG islands can be a common mechanism of epigenetical inactivation of genes.

Further, analysis of the DNA methylation pattern of the region containing upstream *Sp1* site of the *RASSF1A* promoter by bisulfite sequencing revealed only two methylated CpGs in the *RASSF1A* expressing cells, HeLa and PBMC. One methylated cytosine belongs to the 5'GGG**C**GG sequence of the upstream *Sp1* site in the *RASSF1A* promoter, whereas the second methylated cytosine is an upstream nucleotide (5'**C**GGGCGG). An *in vivo* footprinting analysis of the upstream *Sp1* site detected hypersensitive G next to this cytosine (5'C**G**GGCGG). Moreover, two research groups defined the *Sp1* consensus sequence as 5'**C**GGGCGG (Seguin and Hamer, 1987; Boyer and Maquat, 1990). Thus, this cytosine can be involved in the *Sp1* binding. Additionally, the DNA methylation pattern of this region was analyzed in cell lines and human mammary epithelium. Analysis of clones containing this fragment of the *RASSF1*A promoter from different cell types identified similarity in the methylation pattern of partly methylated sequences. All partly methylated sequences contained at least one methylated CpG in the upstream *Sp1* site. In these clones, the frequency of methylation of both CpGs in the upstream *Sp1* site was 5.5 times higher compared to the event, when only one from these CpGs was methylated. This indicates that DNA methylation occurs preferently in the upstream *Sp1* site of the *RASSF1A* promoter compared to flanking CpGs (Figure 4-1).

Since the upstream *Sp1* site is frequently methylated, *Sp1* at this site can be associated with *DNMT1*. *DNMT1* in complex with *DNMT3* controls about 95% DNA methylation in cells and is involved in aberrant DNA methylation in cancer cells (Rhee *et al.*, 2002). Overexpression of *DNMT1* in cells leads to an increase of DNA methylation, which is accompanied by malignant transformation (Wu *et al.*, 1993; Graff *et al.*, 1997). *In vitro* experiments showed that *DNMT1* methylates unmethylated CpGs with very low efficiency *de novo* (Fatemi *et al.*, 2002; Hermann *et al.*, 2004). The

association of *Sp1* with *DNMT1* was demonstrated by Milutinovic and colleagues (Milutinovic *et al.*, 2004). In the *DNMT1* antisense knock down cells, they identified expressional induction of the unmethylated *p21* promoter in a *Sp1*-dependent manner. Moreover, it is well known that aberrant DNA methylation occurs during aging of cells (reviewed by Issa, 1999). Thus, *DNMT1* may be associated with the upstream *Sp1* site of the *RASSF1A* promoter; and this may result in preferential aberrant DNA methylation of this site during aging (Figure 4-1). Additionally, the association of *Sp1* with *DNMT1* may be performed through *HDAC* in the *RASSF1A* promoter. Since, *HDAC* is a interaction partner of *Sp1* and *DNMT1* (Doetzlhofer *et al.*, 1999; Fuks *et al.*, 2000; Robertson *et al.*, 2000; Rountree *et al.*, 2000; Chang *et al.*, 2001; Hou *et al.*, 2002; Won *et al.*, 2002; Zhang and Dufau, 2002; Lagger *et al.*, 2003; Ammanamanchi and Brattain, 2004). *In vitro* studies of the activity of *DNMT1* showed that *de novo* DNA methylation is stimulated by the presence of methylated DNA in solution (Hermann *et al.*, 2004; Fatemi *et al.*, 2002; Fatemi *et al.*, 2001). Therefore, DNA methylation at the upstream *Sp1* site in the *RASSF1A* promoter may initiate the methylation of the surrounding CpGs (Figure 4-1). This is supported by methylation profiling of the fragment containing the upstream *Sp1* site. Analysis of this region in mammary epithelium demonstrated all steps of possible progression of the DNA methylation from unmethylated state and gradual increase of the DNA methylation around the *Sp1* site. Thus, the DNA methylation may spread from the upstream *Sp1* site (Figure 4-1). Moreover, *de novo* DNA methylation of this region may be initiated by the heavy methylated DNA fragment located upstream from this region (Figure 4-1).

Methylated DNA is a target for *MBDs*, which interact with *DNMT1*, *HDAC* and histone H3 lysine 9 methyltransferase (Jones *et al.*, 1998; Ng *et al.*, 1999; Tatematsu *et al.*, 2000; Fuks *et al.*, 2003; Kimura and Shiota, 2003; Sarraf and Stancheva, 2004). Recruitment of *HDAC* and histone H3 lysine 9 methyltransferase by *MBD* can lead to chromatin inactivation, which can directs DNA methylation (Tamaru and Selker, 2001; Johnson *et al.*, 2002; Lehnertz *et al.*, 2003; Jackson *et al.*, 2004). Thus, the *RASSF1A* transcription can be inactivated using the following mechanism. The association of *Sp1* with *DNMT1* at upstream *Sp1* site of the *RASSF1A* promoter may result in aberrant DNA methylation at this site during aging and in the subsequent *MBDs* binding (Figure 4-1, Figure 4-3). *MBDs* repress the *RASSF1A* transcription through *Sp1* and recruit the *HDAC* and histone H3 lysine 9 methyltransferase to the *RASSF1A* promoter

(Figure 4-3). These enzymes inactivate chromatin and recruit *DNMT1*, which actively methylate *de novo* the *RASSF1A* promoter (Figure 4-3). Thus, epigenetical inactivation of the *RASSF1A* promoter may be mediated by DNA methylation at the upstream *Sp1* site (Figure 4-3).
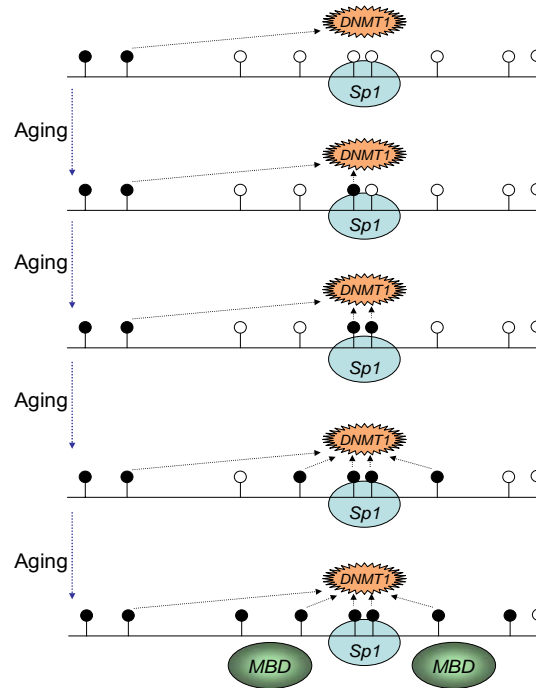
Figure 4-1. Model of mechanism of aberrant DNA methylation of the upstream *Sp1* site in the *RASSF1A* promoter during aging. The association of *Sp1* with *DNMT* at the upstream *Sp1* site results in *de novo* aberrant DNA methylation of this site during aging. Presence of the methylated CpGs stimulates *de novo* methylation of the other CpGs by *DNMT*. Subsequently, aberrant DNA methylation is resulted in the recruitment of *MBDs* to promoter. Black and white lollipops represent methylated and unmethylated CpGs, respectively. Arrows indicate an effect of the methylated CpGs to *DNMT1*.

In pre-stasis HMECs, the *RASSF1A* promoter is characterized by the active binding of *Sp1* and elevated frequency of methylated CpGs compared to HeLa. This indicates that the binding of *Sp1* does not prevent the epigenetical inactivation of *RASSF1A* in HMECs. This observation contradicts a number of studies. In 1994, two independent groups reported that mutation of the *Sp1* site located in the *adenine phosphoribosyltransferase* (*Aprt*) promoter results in spreading of *de novo* DNA methylation in transgenic mice and transfected embryonic cells (Brandeis *et al.*, 1994; Macleod *et al.*, 1994). Moreover, in mouse embryonic stem cells, the presence of *Sp1* site in an *in vitro* methylated construct leads to demethylation of a CpG island upstream from the hamster *Aprt* gene (Brandeis *et al.*, 1994). Matsuo and colleagues

demonstrated, that the binding of *Sp1* induces demethylation of the *in vitro* methylated *β-globin* promoter in *Xenopus* fertilized eggs after midblastula transduction (Matsuo *et al.*, 1998). Qu and Ehrlich identified demethylation of DNA induced by *Sp1* in non-embryonic cells (Qu and Ehrlich, 1999). Thus, *Sp1* is involved in demethylation of promoters in embryonic and non-embryonic cells. Recently, this hypothesis was supported by observation of Gazzoli and Kolodner. They identified that polymorphisms at the *Sp1* site in the *MSH6* promoter are associated with the epigenetical inactivation of *MSH6* (Gazzoli and Kolodner, 2003). Moreover, the localizations of the *Sp1* sites between methylated flanking DNA and unmethylated promoter regions in *E-cadherin* (E-cad) gene, von *Hippel-Lindau* gene (*VHL*), *BRCA1* and *iduronate-2-sulfatase* gene (*IDS*) may be additional proofs of the protectional role of *Sp1* from spreading *de novo* DNA methylation into promoter (Graff *et al.*, 1997; Butcher *et al.*, 2004; Tomatsu *et al.*, 2004). In contrast to this, epigenetical inactivation of the *RASSF1A* promoter is not sensitive to the binding of *Sp1*, since the *Sp1* binding to the *RASSF1A* promoter in pre-stasis HMEC is associated with repressed chromatin and an increase of DNA methylation level in promoter. There are several explanations for these observations. First, the control of the DNA methylation free promoter can be performed by other mechanism as *Sp1*. The presence of such mechanism is supported by a study of Marin and colleagues, which identified DNA methylation free CpG islands in the genome of *Sp1-null* mice (Marin *et al.*, 1997). Moreover, Mummaneni and colleagues demonstrated that only one from four functional *Sp1* sites in the *Aprt* promoter has the ability to inhibit the epigenetical inactivation of *Aprt* and is not required for transcriptional activity in contrast to the other three *Sp1* sites (Mummaneni *et al.*, 1998). Analysis of the *glutathione-S-transferase* gene (*GSTP1*) showed that a *Sp1* site located in the promoter is not involved in its epigenetical protection, since mutation and deletion of this site does not lead to DNA methylation (Song *et al.*, 2002). Thus, different *Sp1* sites may realize different functions. One of several *Sp1* sites regulates transcriptions, whereas others are involved in the protection from epigenetical inactivation of the promoters. Hence, the *Sp1* sites in the *RASSF1A* promoter may be only involved in transcriptional regulation and do not mediate protection from epigenetical inactivation. Second explanation is that the *Sp1* binding may protect the *RASSF1A* promoter from *de novo* DNA methylation only during embryonic reprogramming; and the control of the methylation free *RASSF1A* promoter may be mediated by mechanisms other as *Sp1* in non-embryonic cells.

4.3 Mechanism of epigenetical inactivation of the *RASSF1A* promoter

In pre-stasis HMECs, the chromatin state in the *RASSF1A* promoter is repressed compared to HeLa cells, which actively transcribe *RASSF1A*. The chromatin state of the methylated region containing the upstream *Sp1* sites is similar to the unmethylated CpG island fragment containing three *Sp1* sites. Thus, a repressed state of chromatin is detected in the unmethylated and methylated *RASSF1A* promoter fragments. Further, analysis of post-stasis HMECs identified a *de novo* DNA methylation in the *RASSF1A* CpG island fragment and enhanced repression of chromatin compared to pre-stasis HMECs. Thus, an inactive chromatin state observed in the *RASSF1A* CpG island fragment at pre-stasis proliferation state precedes the *de novo* DNA methylation of this region detected in post-stasis HMECs. This observation is supported by several studies, which demonstrated that repression of chromatin occurs before DNA methylation during epigenetical inactivation. The best example of epigenetical inactivation is methylation of X chromosome. During X chromosome inactivation, repression of chromatin and following inactivation of *X* linked genes occur before DNA methylation (Heard *et al.*, 2001). Similar data were obtained by Bachman and colleagues when they analyzed the promoter silencing of $p16^{INK4a}$ in colorectal cancer cells with inactivated *DNMT1* and *DNMT3* (Bachman *et al.*, 2003). They observed that changing of chromatin precedes inactivation of the $p16^{INK4}$ transcription and DNA methylation of the promoter is the last step of this inactivation process. Furthermore, study of thymocytes maturation showed that chromatin repression in the *terminal deoxynucleotidyltransferase* (*Dntt*) promoter occurs before transcription inactivation and an increase of DNA methylation is only observed in mature T-lymphocytes (Su *et al.*, 2004). Analogously, repression of chromatin takes place before DNA methylation during inactivation of transgene (Mutskov and Felsenfeld, 2004). However, Stirzaker and colleagues identified that chromatin inactivation is directed by DNA methylation when prostate cancer cells were transfected with a plasmid containing the *GSTP1* promoter and exon 1 (Stirzaker *et al.*, 2004). Histone deacetylation of this construct was directed by seeds of introduced DNA methylation and occurs before histone methylation. However, this study was performed in an artificial situation. Whereas inactivation of the X chromosome during embryonic development, inactivation of *Dntt* during thymocytes maturation and the *RASSF1A* inactivation in HMECs take place *in vivo*. Moreover, the inactivation of $p16^{INKa}$ in DKO cells and transgene inactivation are models, which represent *in vivo* situation.

In pre-stasis HMECs, the *RASSF1A* transcription was reduced compared to the strongly *RASSF1A* expressing cells. As discussed above, chromatin modifications and DNA methylation may be responsible for the decreased level of the *Sp1*-mediated *RASSF1A* transcription in pre-stasis HMECs. Moreover, transcription, which is not mediated by *Sp1*, can be also repressed by chromatin, since during epigenetical inactivation of the $p16^{INK4}$ promoter, X chromosome, *Dntt* and transgene, changing of chromatin was associated with repression of transcription and DNA methylation was observed after this repression (Heard *et al.*, 2001; Bachman *et al.*, 2003; Su *et al.*, 2004; Mutskov and Felsenfeld, 2004). Moreover, *Caenorhabdidtis elegans* and *Saccharomyces cerevisiae* lack DNA methylation (Reuben and Lin, 2002; Osley, 2004; reviewed by Rountree *et al.*, 2001; Martin *et al.*, 2004). Thus, repression of gene activity can be performed by chromatin in absence of DNA methylation. A similar mechanism was observed in mammals by Lewis and colleagues. They found in placenta that imprinted genes flanking the imprinting center 2 (*IC2*) on mouse distal chromosome 7, are inactivated by repressive chromatin modifications in the absence of DNA methylation (Lewis *et al.*, 2004). Thus, repression of transcription by chromatin is a common mechanism, and the *RASSF1A* expression may be repressed by chromatin state independent from *Sp1* in pre-stasis HMECs. In post-stasis HMECs, the DNA methylation pattern of the *RASSF1A* CpG island is completely different from breast cancer cell lines; however, the transcriptional rate is only slightly higher. Thus, in the proliferating post-stasis HMECs a new transcriptional pattern is established by a repressed chromatin state and then this aberrant expression profile is maintained by DNA hypermethylation in tumor cells.

In post-stasis HMECs, *de novo* DNA methylation in the *RASSF1A* promoter is associated with elevated frequency of trimethylated histone H3 lysine 9. This observation supported by interaction of *DNMT1* with *SUV39H1* histone H3 lysine 9 methyltransferase (Fuks *et al.*, 2003). Moreover, recent studies showed that DNA methylation can be directed by methylation of histone H3 at lysine 9 position (Tamaru and Selker, 2001; Johnson *et al.*, 2002, Lehnertz *et al.*, 2003). In experiments with fungus *Neurospora crassa,* the control of DNA methylation by histone methylation was demonstrated, since absences of histone methyltransferase or DNA methyltransferase result in the loss of DNA methylation (Tamaru and Selker, 2001). Analogously, in *Arabidopsis thaliana*, mutation of the methyltransferase gene, which is specific for histone H3 lysine 9 (homolog of *SU(VAR)3-9*), and mutation of the

DNA methyltransferase lead to loss of cytosine methylation at CpNpG trinucleotides (where N is A, C, G or T) (Johnson *et al.*, 2002; Jackson *et al.*, 2004). Moreover, Lehnertz and colleagues identified that presence of trimethylated histone H3 lysine 9 is necessary for DNA methylation of major satellite repeats at pericentric heterochromatin in mice (Lehnertz *et al.*, 2003). However, absence of *DNMT1* or *DNMT3a/DNMT3b* does not result in changing of chromatin state at these sites (Lehnertz *et al.*, 2003). Thus, histone methylation can direct DNA methylation in different organisms. Additional proof of the control of DNA methylation by chromatin is a *de novo* DNA methylation in early development, since DNA should be marked for this process to direct the work of *DNMT*. Proteins like *Sp1*, which interact with DNA, may play the role of these marks. There is no evidence, that every unmethylated DNA area is marked by *Sp1*. Histones are the best candidates to direct *de novo* DNA methylation in development. Thus, DNA methylation can be directed by chromatin. Hence, d*e novo* DNA methylation in the *RASSF1A* CpG island may be mediated by elevated level of trimethylated histone H3 lysine 9. Similar explanation may be used for observations, which were done by two research groups. Mutskov and Felsenfeld, 2004 showed that *de novo* DNA methylation of transgene occurs in the same window of time as histone H3 lysine 9 methylation (Mutskov and Felsenfeld, 2004). Moreover, analysis of prostate cancer cells transfected with a partly methylated plasmid containing the *GSTP1* promoter and exon 1 showed that extensive DNA methylation of the *GSTP1* CpG island is associated with histone H3 lysine 9 methylation (Stirzaker *et al.*, 2004). Thus, direction of *de novo* DNA methylation in the *RASSF1A* CpG island by chromatin may be a common mechanism during epigenetical inactivation.

4.4   The modulation of the binding of *Sp1* to the *RASSF1A* promoter

Using ChIp, the *Sp1* binding to the upstream *Sp1* site of the *RASSF1A* promoter was observed, when this site is unmethylated in HeLa and methylated in pre-stasis HMECs. Similar results were obtained by EMSA, which indicated binding of *Sp1* to the methylated and unmethylated oligos containing *Sp1* sites. Thus, the binding of *Sp1* to the upstream consensus of *RASSF1A* is unaffected by DNA methylation. Concordantly, Holler and colleagues showed that DNA methylation of the *Sp1* site does not influence the binding of *Sp1 in vitro* (Holler *et al.*, 1988). Moreover, an *in vitro* analysis by EMSA identified that *Sp1* binds with same efficiency methylated and

unmethylated oligos containing the *human metallothionein IIA* promoter fragment and *neurofibromatosis* gene (*NF1*) promoter fragment (Harrington *et al.*, 1988; Mancini *et al.*, 1999). Interestingly, analysis of the *Sp1* binding to the *p21^{Cip1}* promoter by EMSA showed that *Sp1* is insensitive to DNA methylation at binding consensus, however sensitive to DNA methylation of the CpGs in the surrounding sequences (Zhu *et al.*, 2003). Analysis of *Sp1* sites in the *MSH6* (mismatch repair protein) and *insulin-like growth factor-binding protein-3* (*IGFBP-3*) promoters by EMSA showed, that *Sp1* binds more effectively to unmethylated oligos compared to methylated (Gazzoli and Kolodner, 2003; Chang *et al.*, 2004). Furthermore, an increase of the DNA methylation around the methylated *Sp1* site of the *IGFBP-3* promoter resulted in completely inactivation of the *Sp1* binding in EMSA experiments (Chang *et al.*, 2004). In our experiments, the binding of *Sp1* to the methylated and unmethylated upstream *Sp1* site of the *RASSF1A* promoter was analyzed *in vitro* and *in vivo*, however the binding of *Sp1* was investigated in the discussed studies *in vitro* (Harrington *et al.*, 1988; Zhu *et al.*, 2003; Gazzoli and Kolodner, 2003; Chang *et al.*, 2004). Butcher and colleagues studied the *Sp1* binding to the *BRCA1* promoter by *in vitro* and *in vivo*. They showed that the binding of *Sp1* to the methylated *BRCA1* promoter fragment is inhibited in EMSA experiments; however, active binding of *Sp1* to the methylated site in transcribing promoter was observed by ChIp (Butcher *et al.*, 2004). Thus, *Sp1* may bind methylated DNA *in vivo* even if *in vitro* experiments demonstrated inhibition of the *Sp1* binding by DNA methylation. Additionally, the differences in the *Sp1* binding to methylated DNA *in vitro* may be attributed to differences in DNA sequences surrounding the *Sp1* sites. Thus, present data suggest, that the *Sp1* binding to the upstream *Sp1* site is insensitive to DNA methylation in the *RASSF1A* promoter.

Since the binding of *Sp1* to the upstream site of *RASSF1A* is independent from the DNA methylation, this binding may be mediated by chromatin state. In accordance, a decrease of acetylated histone H3 level at this site in post-stasis HMECs compared to pre-stasis HMECs was associated with occlusion of the *Sp1* binding. It is important to note that chromatin at the upstream *Sp1* site of the *RASSF1A* promoter was repressed in pre-stasis HMECs compared to HeLa; however, this chromatin changing does not inhibit the binding of *Sp1* to this site. Recently, a factor was revealed, which interacts with *Sp1* and may mediate the binding of *Sp1*. Suzuki and colleagues reported that the DNA binding domain of *Sp1* interacts with acetyltransferase region of *p300* and the *Sp1-p300* interaction stimulates the binding of *Sp1* to DNA (Suzuki *et al.*, 2000). Thus,

a decrease of *p300* at the upstream *Sp1* site of *RASSF1A* may be associated with reduction of the *Sp1* binding to DNA. Additionally, deacetylation of histone H3 could be involved in the formation of inaccessible chromatin for transcription factors in post-stasis HMECs. For instance, inactive chromatin is detected in the *RASSF1A* promoter of ZR75-1 cells and associated with inhibition of the *Sp1* binding. Moreover, the *RASSF1C* promoter in post-stasis HMECs is characterized by an increased level of acetylated histone H3 and an decreased frequency of trimethylated histone H3 lysine 9 and this is associated with increasing of *Sp1* binding. Thus, two factors may be involved in inhibition of *Sp1* binding to the upstream *Sp1* site of the *RASSF1A* promoter in post-stasis HMECs: a repressive chromatin state and the absence of *p300*.

Analogous to the upstream *Sp1* site region of the *RASSF1A* promoter, the *Sp1* binding in the *RASSF1A* CpG island may be inhibited by additional chromatin modifications and a decrease of the *p300* level in post-stasis HMECs. Additionally, *de novo* DNA methylation may be reason for the *Sp1* binding inactivation in the *RASSF1A* CpG island of post-stasis HMECs. As was shown previously, *Sp1* binding is sensitive to DNA methylation (Zhu *et al.*, 2003; Butcher *et al.*, 2004; Gazzoli and Kolodner, 2003; Chang *et al.*, 2004). In the *RASSF1A* CpG island of post-stasis HMECs, seeds of DNA methylation were detected in *Sp1* sites. However, *Sp1 in vitro* binds oligos containing the *Sp1* sites of the *RASSF1A* promoter in unmethylated as completely methylated state. There are no evidences that the *Sp1* binding is dependent from the DNA methylation in the *RASSF1A* CpG island. Thus, the binding of *Sp1* to the *RASSF1A* promoter may be mediated by chromatin state.

4.5 Comparing the *RASSF1A* promoter to the *RASSF1C* promoter

RASSF1A and *RASSF1C* are the two major transcripts of *RASSF1*, which are transcribed from two different CpG islands located approximately 3.5 kb apart and expressed in normal cells (Dammann *et al.*, 2000). *RASSF1A* is frequently epigenetically inactivated in cancer cells in contrast to the unaffected *RASSF1C* transcript. Here, the epigenetic states of *RASSF1C* and *RASSF1A* promoter were analyzed and compared between each other.

DNA methylation analysis identified that the *RASSF1C* promoter is completely unmethylated in all analyzed cells. The transcription analysis of *RASSF1C* revealed no inactivation in HMECs, cancer cells and non malignant cells. Thus, the transcription

and DNA methylation status of *RASSF1C* are not associated with the *RASSF1A* epigenetical inactivation. Analysis of chromatin state in the *RASSF1C* promoter identified the increased level of trimethylated histone H3 lysine 9 in pre-stasis HMECs compared to HeLa, whereas the frequency of trimethylated histone H3 lysine 9 in post-stasis HMECs was similar to HeLa. Thus, establishment of inactive chromatin in the *RASSF1A* promoter in pre-stasis HMECs may influence to chromatin state in the *RASSF1C* promoter. However, these chromatin changes do not result in an inhibition of *Sp1* binding to the *RASSF1C* promoter and inactivation of the *RASSF1C* transcription. In post-stasis HMECs, chromatin is repressed in the *RASSF1A* promoter, whereas the *RASSF1C* promoter is characterized by increase of level of active chromatin compared to HeLa. Moreover, this chromatin remodeling of the *RASSF1* locus in post-stasis cells is associated with loss of *Sp1* in the *RASSF1A* promoter and an increase of the *Sp1* binding in the *RASSF1C* promoter. Analogously, the elevated level of the *Sp1* binding to the *RASSF1C* promoter was observed in ZR75-1 compared to HeLa and pre-stasis HMECs. Thus, chromatin inactivation in the *RASSF1A* promoter may result in an increase of active chromatin state in the *RASSF1C* promoter.

These observations suggest that there is a mechanism, which prevents spreading of inactive chromatin and DNA methylation into the *RASSF1C* promoter. *RASSF1C* promoter contains five *Sp1* sites upstream from translation start site, whereas in the *RASSF1A* promoter, only four *Sp1* sites are found. Mutations in two *Sp1* sites in the *RASSF1C* promoter result in abolishment of promoter activity. Thus, *Sp1* may play a critical role in transcription regulation of the *RASSF1C* promoter. As discussed above, *Sp1* is involved in promoter protection from epigenetical inactivation (Brandeis *et al.*, 1994; Matsuo *et al.*, 1998; Qu and Ehrlich, 1999; Gazzoli and Kolodner, 2003). Thus, DNA methylation free state of the *RASSF1C* promoter may be promoted by one from five *Sp1* sites in the promoter. From other side, the *RASSF1C* promoter is more transcriptional active compared to the *RASSF1A* promoter. Thus, active transcription of the *RASSF1C* may be involved in the protection of the promoter from its inactivation. Interestingly, that *RASSF1A* and *RASSF1C* are expressed in similar pattern in different human tissues. This suggests that both proteins are involved in the same pathways. This hypothesis may be supported by recent studies of the *RASSF1A* and *RASSF1C* functions. As was found, both proteins have the following common characteristics: an association with microtubules, induction of cell cycle arrest, binding of proapoptotic kinase *MST1*, repression of *Ras*-genomic instability and growth

inhibition of the cancer cells *in vivo* and *in vitro* (Dammann *et al.*, 2000; Khokhlatchev *et al.*, 2002; Ortiz-Vega *et al.*, 2002; Liu *et al.*, 2003; Li *et al.*, 2004; Rong *et al.*, 2004; Song *et al.*, 2004; Vos *et al.*, 2004). However, the *RASSF1A* promoter is frequently inactivated in cancer cells in contrast to *RASSF1C*.

4.6   The role of the *RASSF1A* transcription in HMECs

The *RASSF1A* promoter is methylated in 49% up to 65% of primary breast carcinomas (reviewed by Dammann *et al.*, 2003). Its methylation in serum of breast cancer patients is associated with poor prognosis (Muller *et al.*, 2003). Moreover, a new study of Lewis and colleagues showed that methylation of the *RASSF1A* promoter is associated with an increase of breast cancer risk (Lewis *et al.*, 2005). Thus, analysis of methylation of the *RASSF1A* promoter in HMECs may elucidate the mechanism of malignant reprogramming of the mammary epithelium. This is the first study, which analyzes the inactivation of *RASSF1A* in the proliferation of HMECs before and after overcoming stasis. Our results show that *RASSF1A* is epigenetically inactivated during senescence of HMECs. Transcriptional inactivation of *RASSF1A* during proliferation of HMECs is associated with spreading of DNA methylation into promoter and repression of chromatin. As discussed above, healthy breast tissues have the methylation pattern of the *RASSF1A* promoter similar as pre-stasis and post-stasis HMECs (Yan *et al.*, 2003). Thus, initiation of the epigenetical inactivation of *RASSF1A* already occurs in normal breast tissues and continues in dividing HMECs. Moreover, this demonstrates that epigenetical inactivation, which we observed in HMECs, takes place in tissues during aging. This is also supported by observation of Meeker and colleagues. They identified that cells from histological-normal terminal duct lobular units are characterized by a high level of the chromosome shortenings, which were detected in post-stasis HMECs (Meeker *et al.*, 2004). Thus, analogous to *de novo* DNA methylation of the *RASSF1A* promoter, shortenings of chromosomes take place in HMECs in culture and in healthy breast tissues. These data suggest that the processes, which are observed during proliferation of HMECs in culture, may be equal to processes in HMECs in tissue.

Bisulfite sequencing identified that the level of DNA methylation in the region containing the upstream *Sp1* site is increased in pre-stasis HMECs compared to normal mammary epithelium. Thus, cells proliferating in culture have a higher level of DNA

methylation compared to breast tissue. Increased level of DNA methylation may be associated with repression of the *RASSF1A* transcription activity. In concordance, in pre-stasis HMECs, the *RASSF1A* transcription level was decreased compared to HeLa, HF and PBMC. Repression of this transcription may be associated with selection, which may occur during cultivation of HMECs. This transcriptional inactivation may be necessary for further proliferation of HMECs in culture. From other side, normal mammary epithelium has a low level of the *RASSF1A* transcription. However, breast tissue contains various types of cells, which may have differences in transcription patterns. Thus, the *RASSF1A* transcription in normal breast tissue may be distinct from isolates of mammary epithelium. This is supported by the *RASSF1C* transcription, which is strongly decreased in normal mammary epithelium compared to proliferating HMECs. Thus, repression of the *RASSF1A* transcription may be associated with selection of HMECs in culture.

Additionally to the *de novo* methylation of the *RASSF1A* CpG island fragment, the post-stasis HMECs are characterized by DNA hypermethylation of the *p16^{INK4}* promoter and absence of the *p16^{INK4}* transcription (Brenner *et al.*, 1998; Foster *et al.*, 1998). In contrast to *RASSF1A*, *p16^{INK4}* is induced in pre-stasis and highest transcription activity of *p16^{INK4}* is observed in stasis proliferation phase Brenner *et al.*, 1998, Foster *et al.*, 1998). In stasis, HMECs with the elevated *p16^{INK}* transcription went under G1 arrest; whereas the *p16^{INK}* negative cells overcome this proliferation barrier. The *RASSF1A* inactivation is not associated with stasis of HMECs, since its epigenetical inactivation occurs during pre-stasis and post-stasis proliferation phases. Thus, epigenetical inactivation of the two tumor suppressor genes, *RASSF1A* and *p16^{INK}* during senescence of HMECs may be associated with different processes in cells. Aberrant methylation was observed in the *RASSF1A* and *p16^{INK}* promoters in normal breast tissues (Dammann *et al.*, 2001; Holst *et al.*, 2003; Yan *et al.*, 2003; Crawford *et al.*, 2004). However, pre-stasis cells are characterized by active *p16^{INK}* and repressed *RASSF1A* transcriptions. This indicates that transcription of *p16^{INK}* does not inhibit proliferation of HMECs and all cells with active and the not active *p16^{INK}* promoter dividing in culture, whereas the repressed transcription of *RASSF1A* may be a necessary condition for proliferation of HMECs. This may be an additional proof of selection, which can take place during cultivation of HMECs. Moreover, this indicates a function of *RASSF1A* as tumor suppressor gene.

The inactivation of *RASSF1A* plays an important role in the breast cancer. This was demonstrated by a study of Lewis and colleagues, who observed DNA methylation of the *RASSF1A* promoter in 70% of healthy women with high risk of breast cancer (Lewis *et al.*, 2005). In concordance, epigenetical inactivation of the *RASSF1A* promoter is frequently detected in primary breast tumors (reviewed by Dammann *et al.*, 2003). Recent study of Shivakumar and colleagues demonstrated the possible function of *RASSF1A*. They identified that the accumulation of cyclin *D1* in cells is negatively regulated by *RASSF1A* (Shivakumar *et al.*, 2002). Cyclin *D1* plays a critical and uncompensated role in the breast tissue development (reviewed by Sherr, 1996). Overexpression of cyclin D1 in transgenic mice results in abnormal mammary cell proliferation including the development of mammary adenocarcinomas (Wang *et al.*, 1994). Moreover, cyclin *D1* gene is amplified in 15% and overexpressed in 30–50% of primary human breast tumors (reviewed by Fu *et al.*, 2004). Thus, inactivation of the *RASSF1A* may be necessary for hyperproliferation of mammary epithelial cells, which can be mediated by an increased level of cyclin *D1*. Moreover, the repression of *RASSF1A* transcription in HMEC and not in other nonmalignant cells can be explained by role of cyclin D1 in HMEC.

p16^{INK4} negatively mediates cyclin *D1* dependent kinase activity (reviewed by Sherr, 1996). Analogous to *p16^{INK4}*, *RASSF1A* may negatively regulate cyclin *D1* dependent kinase activity, since control of this activity can be performed by different mechanism. The mechanism used by *p16^{INK4}* is direct blocking of cyclin *D1* dependent kinase activity (reviewed by Sherr, 1996). Analogously, cyclin *D1* dependent kinase activity is decreased when level of cyclin *D1*, which is controlled by *RASSF1A*, is reduced. Thus, post-stasis HMECs are characterized by repression of two negative regulators of cyclin *D1* dependent kinase activity and this may be involved in the premalignant program of HMECs. Sandhu and colleagues identified reduction of cyclin *D1* dependent kinase activity during proliferation of post-stasis HMECs; and HMECs at agonescence are characterized by the lowest level of this activity (Sandhu *et al.*, 2000). This indicates that activation of other such as *p16^{INK4}* and *RASSF1A* negative regulators of cyclin *D1* dependent kinase activity takes place in post-stasis HMECs.

In post-stasis proliferation phase, HMECs are characterized by chromosome abnormalities associated with critically shortened telomeres (Romanov *et al.*, 2001; Tlsty *et al.*, 2001). Vos and colleagues demonstrated that the *RASSF1A* inactivation results in genomic instability (Vos *et al.*, 2004). Thus, inactivation of the *RASSF1A*

promoter may promote the dividing of HMECs with chromosome abnormalities. Moreover, recent studies demonstrated that *RASSF1A* is associated with the control cell of cycle and apoptosis. Since chromosome abnormalities can mediate malignant transformation of the cells and the *RASSF1A* negatively regulates this process, silencing of *RASSF1A* may result in malignant transformation of HMECs.
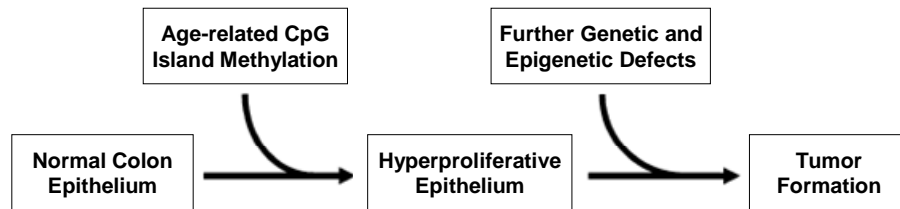
Figure 4-2. A model of the interactions between aging, CpG island methylation and cancer (Adopted from Issa, 1999).

In 1999, Issa suggested a model of neoplastic transformation of normal colon epithelium to tumor (Figure 4-2) (Issa, 1999). A similar mechanism may be involved in the malignant transformation of mammary epithelium (Figure 4-3). The epigenetical inactivation of *RASSF1A* during malignant transformation of mammary epithelium may have following steps. During aging, aberrant DNA methylation in the *RASSF1A* promoter accumulates in normal mammary epithelium and may induce the epigenetical inactivation of the *RASSF1A* promoter (Figure 4-3). This inactivation may mediate repression of the *RASSF1A* transcription and subsequent increase of cyclin *D1* level, which may allow a hyperproliferation of HMECs. Further, the repressed *RASSF1A* transcription permits a proliferation of cells with chromosome abnormalities, as was detected in post-stasis HMECs and histological-normal terminal duct lobular units. Accumulation of chromosome abnormalities may result in new mutations, which may support malignant transformation of HMECs. The epigenetical inactivation of *RASSF1A* started in normal mammary cells leads to completely inactivation of the *RASSF1A* transcription and to hypermethylation of the *RASSF1A* promoter in cancer breast cells (Figure 4-3). Thus, aberrant methylation of the *RASSF1A* promoter may mediate malignant transformation of HMECs.

The *RASSF1A* promoter	The expression of *RASSF1A*	Human mammary epithelium

Unmethylated promoter with open chromatin structure   Active transcription   Normal mammary epithelium

Aging   Aging   Aging

Aberrant DNA methylation

Binding of *MBDs*

Recruitment of *H3K9 MT*   Recruitment of *HDAC*   →   Repression of transcription   →   Increase of cyclin *D1* level

Spreading of repressed chromatin

Recruitment of *DNMT*   Hyperproliferation of HMEC

Spreading of DNA methylation   Chromosome aberrations mediated by short telomers

Increasing of pool of mutations

Malignant transformation

Epigenetical inactivation   Absence of transcription   Cancer cells

Figure 4-3. Epigenetical inactivation of the *RASSF1A* promoter during malignant transformation of human mammary epithelium. In normal mammary epithelium, the *RASSF1A* promoter may be characterized by active expression, unmethylated promoter area and open chromatin structure. During aging, the *SP1-DNMT* association at the upstream *Sp1* site may result in aberrant DNA methylation with following binding of *MBDs*. *MBDs* may repress the *RASSF1A* transcription through *Sp1* and recruit histone H3 lysine 9 methyltransferase (*H3K9 MT*) and *HDAC*. Both of these enzymes repress chromatin. This repression may result in additional inactivation of *RASSF1A* expression. Moreover, an increased level of *HDAC* may mediate deacetylation of *Sp1* in the *RASSF1A* promoter and following repression of transcription. The increase of histone H3 lysine 9 methyltransferase level may direct a *de novo* DNA methylation in the *RASSF1A* promoter. Repressed *RASSF1A* transcription may result in increase of level of cyclin *D1* and subsequent hyperproliferation of mammary epithelium. This proliferation and the extremely low expression level of *RASSF1A* may lead to occurrence of the cells with chromosome abnormalities. Accumulation of the mutations may mediate malignant transformation of mammary epithelium, which is characterized by epigenetically inactivated *RASSF1A* promoter. Arrows indicate directed processes. Dot arrows represent processes, which are directed by other mechanisms.

4.7   Outlook of project

To understand the mechanism of epigenetical inactivation of the *RASSF1A* promoter in HMECs, it is very important to analyze the chromatin state in the *RASSF1A* promoter by ChIp using antibodies to *MBD*, monomethylated and dimethylated histone H3 lysine 9 and other chromatin modifications during HMEC senescence. *In vivo* footprinting of the *RASSF1A* promoter fragments located from -429 up to -315 and from -205 up to -137 should be performed to identify transcriptional regulators in these regions. The *Sp1* interaction with putative partners and modifications of *Sp1* should be analyzed in the *RASSF1A* promoter. Analysis of nucleosome positions in the *RASSF1A* promoter during HMEC proliferation could help to reveal the mechanism of the transcriptional inactivation of *RASSF1A*. It would be very interesting to study the *RASSF1A* expression in HMECs grown on feed layers; this could help to understand the role of *RASSF1A* in HMECs. The inactivation of *Sp1* by siRNA in embryonal cells can elucidate the involvement of *Sp1* in the epigenetical protection of *RASSF1A* from *de novo* DNA methylation. Taken together, analysis of *RASSF1A* promoter in HMECs and in embryonal cells could help to understand mechanism of epigenetical control of genes.

5 Summary

Epigenetical inactivation of the *RASSF1A* tumor suppressor gene was frequently detected in cancer. However, the mechanisms of aberrant DNA methylation in the *RASSF1A* CpG island are unknown. In the present study, four *Sp1* sites in the *RASSF1A* promoter were characterized; and the functional relationship between DNA methylation, histone modification, *Sp1* binding and *RASSF1A* expression was examined in proliferating human mammary epithelial cells. With increasing passages of HMECs, the transcription of *RASSF1A* was dramatically silenced and this was associated with deacetylation and lysine 9 trimethylation of histone H3 and spreading DNA methylation from upstream and downstream into promoter. The *RASSF1A* CpG island in HMECs, which had overcome a stress-associated senescence barrier, was characterized by *de novo* DNA methylation and an elevated level of trimethylated histone H3 lysine 9. The binding of *Sp1* to the *RASSF1A* promoter was impaired in these cells. The present data suggest that the chromatin inactivation occurs in the same time window as gene inactivation and may precede the *de novo* DNA methylation. Moreover, present results indicate that the *Sp1* binding is mediated by chromatin state and not by DNA methylation. In summary, progressive histone inactivation, spreading of DNA methylation and inactivation of the *Sp1* binding were observed in the *RASSF1A* promoter during senescence of HMECs and this system may serve as a model for the epigenetical inactivation of the tumor suppressor gene in carcinogenesis.

6   Literature

Alcorta, D. A., Xiong, Y., Phelps, D., Hannon, G., Beach, D. and Barrett, J. C. (1996). "Involvement of the cyclin-dependent kinase inhibitor p16 (INK4a) in replicative senescence of normal human fibroblasts." Proc Natl Acad Sci U S A 93(24): 13742-7.

Ammanamanchi, S. and Brattain, M. G. (2004). "Restoration of transforming growth factor-beta signaling through receptor RI induction by histone deacetylase activity inhibition in breast cancer cells." J Biol Chem 279(31): 32620-5.

Bachman, K. E., Park, B. H., Rhee, I., Rajagopalan, H., Herman, J. G., Baylin, S. B., Kinzler, K. W. and Vogelstein, B. (2003). "Histone modifications and silencing prior to DNA methylation of a tumor suppressor gene." Cancer Cell 3(1): 89-95.

Boyer, T. G. and Maquat, L. E. (1990). "Minimal sequence and factor requirements for the initiation of transcription from an atypical, TATATAA box-containing housekeeping promoter." J Biol Chem 265(33): 20524-32.

Bradford, M. M. (1976). "A rapid and sensitive method for the quantitation of microgram quantities of protein utilizing the principle of protein-dye binding." Anal Biochem 72: 248-54.

Brandeis, M., Frank, D., Keshet, I., Siegfried, Z., Mendelsohn, M., Nemes, A., Temper, V., Razin, A. and Cedar, H. (1994). "Sp1 elements protect a CpG island from de novo methylation." Nature 371(6496): 435-8.

Brenner, A. J., Stampfer, M. R. and Aldaz, C. M. (1998). "Increased p16 expression with first senescence arrest in human mammary epithelial cells and extended growth capacity with p16 inactivation." Oncogene 17(2): 199-205.

Butcher, D. T., Mancini-DiNardo, D. N., Archer, T. K. and Rodenhiser, D. I. (2004). "DNA binding sites for putative methylation boundaries in the unmethylated region of the BRCA1 promoter." Int J Cancer 111(5): 669-78.

Chang, H. C., Liu, L. T. and Hung, W. C. (2004). "Involvement of histone deacetylation in ras-induced down-regulation of the metastasis suppressor RECK." Cell Signal 16(6): 675-9.

Chang, Y. C., Illenye, S. and Heintz, N. H. (2001). "Cooperation of E2F-p130 and Sp1-pRb complexes in repression of the Chinese hamster dhfr gene." Mol Cell Biol 21(4): 1121-31.

Chang, Y. S., Wang, L., Suh, Y. A., Mao, L., Karpen, S. J., Khuri, F. R., Hong, W. K. and Lee, H. Y. (2004). "Mechanisms underlying lack of insulin-like growth factor-binding protein-3 expression in non-small-cell lung cancer." Oncogene 23(39): 6569-80.

Clark, S. J., Harrison, J., Paul, C. L. and Frommer, M. (1994). "High sensitivity mapping of methylated cytosines." Nucleic Acids Res 22(15): 2990-7.

Crawford, Y. G., Gauthier, M. L., Joubel, A., Mantei, K., Kozakiewicz, K., Afshari, C. A. and Tlsty, T. D. (2004). "Histologically normal human mammary epithelia with silenced p16(INK4a) overexpress COX-2, promoting a premalignant program." Cancer Cell 5(3): 263-73.

Czermin, B., Schotta, G., Hulsmann, B. B., Brehm, A., Becker, P. B., Reuter, G. and Imhof, A. (2001). "Physical and functional association of SU(VAR)3-9 and HDAC1 in Drosophila." EMBO Rep 2(10): 915-9.

Dai, S. M., Chen, H. H., Chang, C., Riggs, A. D. and Flanagan, S. D. (2000). "Ligation-mediated PCR for quantitative in vivo footprinting." Nat Biotechnol 18(10): 1108-11.

Dallol, A., Agathanggelou, A., Fenton, S. L., Ahmed-Choudhury, J., Hesson, L., Vos, M. D., Clark, G. J., Downward, J., Maher, E. R. and Latif, F. (2004). "RASSF1A interacts with microtubule-associated proteins and modulates microtubule dynamics." Cancer Res 64(12): 4112-6.

Dammann, R., Li, C., Yoon, J. H., Chin, P. L., Bates, S. and Pfeifer, G. P. (2000). "Epigenetic inactivation of a RAS association domain family protein from the lung tumour suppressor locus 3p21.3." Nat Genet 25(3): 315-9.

Dammann, R. and Pfeifer, G. P. (1997). "Lack of gene- and strand-specific DNA repair in RNA polymerase III-transcribed human tRNA genes." Mol Cell Biol 17(1): 219-29.

Dammann, R., Schagdarsurengin, U., Strunnikova, M., Rastetter, M., Seidel, C., Liu, L., Tommasi, S. and Pfeifer, G. P. (2003). "Epigenetic inactivation of the Ras-association domain family 1 (RASSF1A) gene and its function in human carcinogenesis." Histol Histopathol 18(2): 665-77.

Dammann, R., Yang, G. and Pfeifer, G. P. (2001). "Hypermethylation of the cpG island of Ras association domain family 1A (RASSF1A), a putative tumor suppressor gene from the 3p21.3 locus, occurs in a large percentage of human breast cancers." Cancer Res 61(7): 3105-9.

Doetzlhofer, A., Rotheneder, H., Lagger, G., Koranda, M., Kurtev, V., Brosch, G., Wintersberger, E. and Seiser, C. (1999). "Histone deacetylase 1 can repress transcription by binding to Sp1." Mol Cell Biol 19(8): 5504-11.

Dominguez, G., Silva, J., Garcia, J. M., Silva, J. M., Rodriguez, R., Munoz, C., Chacon, I., Sanchez, R., Carballido, J., Colas, A., Espana, P. and Bonilla, F. (2003). "Prevalence of aberrant methylation of p14ARF over p16INK4a in some human primary tumors." Mutat Res 530(1-2): 9-17.

Drayton, S. and Peters, G. (2002). "Immortalisation and transformation revisited." Curr Opin Genet Dev 12(1): 98-104.

Dulaimi, E., Hillinck, J., Ibanez de Caceres, I., Al-Saleem, T. and Cairns, P. (2004). "Tumor suppressor gene promoter hypermethylation in serum of breast cancer patients." Clin Cancer Res 10(18 Pt 1): 6189-93.

Dynan, W. S. and Tjian, R. (1983). "Isolation of transcription factors that discriminate between different promoters recognized by RNA polymerase II." Cell 32(3): 669-80.

Ehrenhofer-Murray, A. E. (2004). "Chromatin dynamics at DNA replication, transcription and repair." Eur J Biochem 271(12): 2335-49.

Espada, J., Ballestar, E., Fraga, M. F., Villar-Garea, A., Juarranz, A., Stockert, J. C., Robertson, K. D., Fuks, F. and Esteller, M. (2004). "Human DNA methyltransferase 1 is required for maintenance of the histone H3 modification pattern." J Biol Chem 279(35): 37175-84.

Esteller, M., Corn, P. G., Baylin, S. B. and Herman, J. G. (2001). "A gene hypermethylation profile of human cancer." Cancer Res 61(8): 3225-9.

Esteller, M. and Herman, J. G. (2002). "Cancer as an epigenetic disease: DNA methylation and chromatin alterations in human tumours." J Pathol 196(1): 1-7.

Fahrner, J. A., Eguchi, S., Herman, J. G. and Baylin, S. B. (2002). "Dependence of histone modifications and gene expression on DNA hypermethylation in cancer." Cancer Res 62(24): 7213-8.

Fatemi, M., Hermann, A., Gowher, H. and Jeltsch, A. (2002). "Dnmt3a and Dnmt1 functionally cooperate during de novo methylation of DNA." Eur J Biochem 269(20): 4981-4.

Fatemi, M., Hermann, A., Pradhan, S. and Jeltsch, A. (2001). "The activity of the murine DNA methyltransferase Dnmt1 is controlled by interaction of the catalytic domain with the N-terminal part of the enzyme leading to an allosteric activation of the enzyme after binding to methylated DNA." J Mol Biol 309(5): 1189-99.

Fenton, S. L., Dallol, A., Agathanggelou, A., Hesson, L., Ahmed-Choudhury, J., Baksh, S., Sardet, C., Dammann, R., Minna, J. D., Downward, J., Maher, E. R. and Latif, F. (2004). "Identification of the E1A-regulated transcription factor p120 E4F as an interacting partner of the RASSF1A candidate tumor suppressor gene." Cancer Res 64(1): 102-7.

Figueroa, R., Lindenmaier, H., Hergenhahn, M., Nielsen, K. V. and Boukamp, P. (2000). "Telomere erosion varies during in vitro aging of normal human fibroblasts from young and adult donors." Cancer Res 60(11): 2770-4.

Foster, S. A., Wong, D. J., Barrett, M. T. and Galloway, D. A. (1998). "Inactivation of p16 in human mammary epithelial cells by CpG island methylation." Mol Cell Biol 18(4): 1793-801.

Frank, D., Keshet, I., Shani, M., Levine, A., Razin, A. and Cedar, H. (1991). "Demethylation of CpG islands in embryonic cells." Nature 351(6323): 239-41.

Fu, M., Wang, C., Li, Z., Sakamaki, T. and Pestell, R. G. (2004). "Minireview: Cyclin D1: normal and abnormal functions." Endocrinology 145(12): 5439-47.

Fujita, N., Watanabe, S., Ichimura, T., Ohkuma, Y., Chiba, T., Saya, H. and Nakao, M. (2003). "MCAF mediates MBD1-dependent transcriptional repression." Mol Cell Biol 23(8): 2834-43.

Fuks, F., Burgers, W. A., Brehm, A., Hughes-Davies, L. and Kouzarides, T. (2000). "DNA methyltransferase Dnmt1 associates with histone deacetylase activity." Nat Genet 24(1): 88-91.

Fuks, F., Hurd, P. J., Deplus, R. and Kouzarides, T. (2003). "The DNA methyltransferases associate with HP1 and the SUV39H1 histone methyltransferase." Nucleic Acids Res 31(9): 2305-12.

Fuks, F., Hurd, P. J., Wolf, D., Nan, X., Bird, A. P. and Kouzarides, T. (2003). "The methyl-CpG-binding protein MeCP2 links DNA methylation to histone methylation." J Biol Chem 278(6): 4035-40.

Gartel, A. L., Ye, X., Goufman, E., Shianov, P., Hay, N., Najmabadi, F. and Tyner, A. L. (2001). "Myc represses the p21(WAF1/CIP1) promoter and interacts with Sp1/Sp3." Proc Natl Acad Sci U S A 98(8): 4510-5.

Gazzoli, I. and Kolodner, R. D. (2003). "Regulation of the human MSH6 gene by the Sp1 transcription factor and alteration of promoter activity and expression by polymorphisms." Mol Cell Biol 23(22): 7992-8007.

Graff, J. R., Herman, J. G., Myohanen, S., Baylin, S. B. and Vertino, P. M. (1997). "Mapping patterns of CpG island methylation in normal and neoplastic cells implicates both upstream and downstream regions in de novo methylation." J Biol Chem 272(35): 22322-9.

Hagen, G., Muller, S., Beato, M. and Suske, G. (1992). "Cloning by recognition site screening of two novel GT box binding proteins: a family of Sp1 related genes." Nucleic Acids Res 20(21): 5519-25.

Hagen, G., Muller, S., Beato, M. and Suske, G. (1994). "Sp1-mediated transcriptional activation is repressed by Sp3." Embo J 13(16): 3843-51.

Harrington, M. A., Jones, P. A., Imagawa, M. and Karin, M. (1988). "Cytosine methylation does not affect binding of transcription factor Sp1." Proc Natl Acad Sci U S A 85(7): 2066-70.

Heard, E., Rougeulle, C., Arnaud, D., Avner, P., Allis, C. D. and Spector, D. L. (2001). "Methylation of histone H3 at Lys-9 is an early mark on the X chromosome during X inactivation." Cell 107(6): 727-38.

Herbert, B. S., Wright, W. E. and Shay, J. W. (2002). "p16(INK4a) inactivation is not required to immortalize human mammary epithelial cells." Oncogene 21(51): 7897-900.

Herman, J. G. and Baylin, S. B. (2003). "Gene silencing in cancer in association with promoter hypermethylation." N Engl J Med 349(21): 2042-54.

Herman, J. G., Graff, J. R., Myohanen, S., Nelkin, B. D. and Baylin, S. B. (1996). "Methylation-specific PCR: a novel PCR assay for methylation status of CpG islands." Proc Natl Acad Sci U S A 93(18): 9821-6.

Hermann, A., Goyal, R. and Jeltsch, A. (2004). "The Dnmt1 DNA-(cytosine-C5)-methyltransferase methylates DNA processively with high preference for hemimethylated target sites." J Biol Chem 279(46): 48350-9.

Herrmann, M. and Corbett_Research (2002). "An explanation of the comparative quantification technique used in the Rotor-Gene analysis software." Corbett Research: 1-4.

Holler, M., Westin, G., Jiricny, J. and Schaffner, W. (1988). "Sp1 transcription factor binds DNA and activates transcription even when the binding site is CpG methylated." Genes Dev 2(9): 1127-35.

Holst, C. R., Nuovo, G. J., Esteller, M., Chew, K., Baylin, S. B., Herman, J. G. and Tlsty, T. D. (2003). "Methylation of p16(INK4a) promoters occurs in vivo in histologically normal human mammary epithelia." Cancer Res 63(7): 1596-601.

Hou, M., Wang, X., Popov, N., Zhang, A., Zhao, X., Zhou, R., Zetterberg, A., Bjorkholm, M., Henriksson, M., Gruber, A. and Xu, D. (2002). "The histone deacetylase inhibitor trichostatin A derepresses the telomerase reverse transcriptase (hTERT) gene in human cells." Exp Cell Res 274(1): 25-34.

Issa, J. P. (1999). "Aging, DNA methylation and cancer." Crit Rev Oncol Hematol 32(1): 31-43.

Jackson, J. P., Johnson, L., Jasencakova, Z., Zhang, X., PerezBurgos, L., Singh, P. B., Cheng, X., Schubert, I., Jenuwein, T. and Jacobsen, S. E. (2004). "Dimethylation of histone H3 lysine 9 is a critical mark for DNA methylation and gene silencing in Arabidopsis thaliana." Chromosoma 112(6): 308-15.

Jaenisch, R. and Bird, A. (2003). "Epigenetic regulation of gene expression: how the genome integrates intrinsic and environmental signals." Nat Genet 33 Suppl: 245-54.

Jenuwein, T. and Allis, C. D. (2001). "Translating the histone code." Science 293(5532): 1074-80.

Johnson, L., Cao, X. and Jacobsen, S. (2002). "Interplay between two epigenetic marks. DNA methylation and histone H3 lysine 9 methylation." Curr Biol 12(16): 1360-7.

Jones, P. A. and Laird, P. W. (1999). "Cancer epigenetics comes of age." Nat Genet 21(2): 163-7.

Jones, P. L., Veenstra, G. J., Wade, P. A., Vermaak, D., Kass, S. U., Landsberger, N., Strouboulis, J. and Wolffe, A. P. (1998). "Methylated DNA and MeCP2 recruit histone deacetylase to repress transcription." Nat Genet 19(2): 187-91.

Karlseder, J., Rotheneder, H. and Wintersberger, E. (1996). "Interaction of Sp1 with the growth- and cell cycle-regulated transcription factor E2F." Mol Cell Biol 16(4): 1659-67.

Kaufmann, J. and Smale, S. T. (1994). "Direct recognition of initiator elements by a component of the transcription factor IID complex." Genes Dev 8(7): 821-9.

Kavurma, M. M. and Khachigian, L. M. (2004). "Vascular smooth muscle cell-specific regulation of cyclin-dependent kinase inhibitor p21(WAF1/Cip1) transcription by Sp1 is mediated via distinct cis-acting positive and negative regulatory elements in the proximal p21(WAF1/Cip1) promoter." J Cell Biochem 93(5): 904-16.

Khokhlatchev, A., Rabizadeh, S., Xavier, R., Nedwidek, M., Chen, T., Zhang, X. F., Seed, B. and Avruch, J. (2002). "Identification of a novel Ras-regulated proapoptotic pathway." Curr Biol 12(4): 253-65.

Kimura, H. and Shiota, K. (2003). "Methyl-CpG-binding protein, MeCP2, is a target molecule for maintenance DNA methyltransferase, Dnmt1." J Biol Chem 278(7): 4806-12.

Kondo, Y., Shen, L. and Issa, J. P. (2003). "Critical role of histone methylation in tumor suppressor gene silencing in colorectal cancer." Mol Cell Biol 23(1): 206-15.

Kudo, S. (1998). "Methyl-CpG-binding protein MeCP2 represses Sp1-activated transcription of the human leukosialin gene when the promoter is methylated." Mol Cell Biol 18(9): 5492-9.

Lagger, G., Doetzlhofer, A., Schuettengruber, B., Haidweger, E., Simboeck, E., Tischler, J., Chiocca, S., Suske, G., Rotheneder, H., Wintersberger, E. and Seiser, C. (2003). "The tumor suppressor p53 and histone deacetylase 1 are antagonistic regulators of the cyclin-dependent kinase inhibitor p21/WAF1/CIP1 gene." Mol Cell Biol 23(8): 2669-79.

Laird, P. W. (1999). DNA Methylation. Development: Genetics, Epigenetics and Environmental Regulation. D. C. V.E.A. Russo, L. Edgar, R. Jaenisch, F. Salamini, Ed.: 395-405.

Latchman, D. S. (1995). "The DNA mobilty-shift assay." Methods in molecular and cellular biology. 5: 137-144.

Lehnertz, B., Ueda, Y., Derijck, A. A., Braunschweig, U., Perez-Burgos, L., Kubicek, S., Chen, T., Li, E., Jenuwein, T. and Peters, A. H. (2003). "Suv39h-mediated histone H3 lysine 9 methylation directs DNA methylation to major satellite repeats at pericentric heterochromatin." Curr Biol 13(14): 1192-200.

Lewis, A., Mitsuya, K., Umlauf, D., Smith, P., Dean, W., Walter, J., Higgins, M., Feil, R. and Reik, W. (2004). "Imprinting on distal chromosome 7 in the placenta involves repressive histone methylation independent of DNA methylation." Nat Genet 36(12): 1291-5.

Lewis, C. M., Cler, L. R., Bu, D. W., Zochbauer-Muller, S., Milchgrub, S., Naftalis, E. Z., Leitch, A. M., Minna, J. D. and Euhus, D. M. (2005). "Promoter hypermethylation in benign breast epithelium in relation to predicted breast cancer risk." Clin Cancer Res 11(1): 166-72.

Li, J., Wang, F., Protopopov, A., Malyukova, A., Kashuba, V., Minna, J. D., Lerman, M. I., Klein, G. and Zabarovsky, E. (2004). "Inactivation of RASSF1C during in vivo tumor growth identifies it as a tumor suppressor gene." Oncogene 23(35): 5941-9.

Litt, M. D., Simpson, M., Gaszner, M., Allis, C. D. and Felsenfeld, G. (2001). "Correlation between histone lysine methylation and developmental changes at the chicken beta-globin locus." Science 293(5539): 2453-5.

Liu, L., Tommasi, S., Lee, D. H., Dammann, R. and Pfeifer, G. P. (2003). "Control of microtubule stability by the RASSF1A tumor suppressor." Oncogene 22(50): 8125-36.

Loo, D. T., Fuquay, J. I., Rawson, C. L. and Barnes, D. W. (1987). "Extended culture of mouse embryo cells without senescence: inhibition by serum." Science 236(4798): 200-2.

Macleod, D., Charlton, J., Mullins, J. and Bird, A. P. (1994). "Sp1 sites in the mouse aprt gene promoter are required to prevent methylation of the CpG island." Genes Dev 8(19): 2282-92.

Maehara, K., Uekawa, N. and Isobe, K. (2002). "Effects of histone acetylation on transcriptional regulation of manganese superoxide dismutase gene." Biochem Biophys Res Commun 295(1): 187-92.

Mancini, D. N., Singh, S. M., Archer, T. K. and Rodenhiser, D. I. (1999). "Site-specific DNA methylation in the neurofibromatosis (NF1) promoter interferes with binding of CREB and SP1 transcription factors." Oncogene 18(28): 4108-19.

Marin, M., Karis, A., Visser, P., Grosveld, F. and Philipsen, S. (1997). "Transcription factor Sp1 is essential for early embryonic development but dispensable for cell growth and differentiation." Cell 89(4): 619-28.

Martin, A. M., Pouchnik, D. J., Walker, J. L. and Wyrick, J. J. (2004). "Redundant roles for histone H3 N-terminal lysine residues in subtelomeric gene repression in Saccharomyces cerevisiae." Genetics 167(3): 1123-32.

Mathon, N. F., Malcolm, D. S., Harrisingh, M. C., Cheng, L. and Lloyd, A. C. (2001). "Lack of replicative senescence in normal rodent glia." Science 291(5505): 872-5.

Matsuo, K., Silke, J., Georgiev, O., Marti, P., Giovannini, N. and Rungger, D. (1998). "An embryonic demethylation mechanism involving binding of transcription factors to replicating DNA." Embo J 17(5): 1446-53.

Matsushita, K., Hagihara, M. and Sugiura, Y. (1998). "Participation of oligomerization through C-terminal D domain region of Sp1 in DNA binding." Biol Pharm Bull 21(10): 1094-7.

Maxam, A. M. and Gilbert, W. (1977). "A new method for sequencing DNA." Proc Natl Acad Sci U S A 74(2): 560-4.

Meeker, A. K., Hicks, J. L., Gabrielson, E., Strauss, W. M., De Marzo, A. M. and Argani, P. (2004). "Telomere shortening occurs in subsets of normal breast epithelium as well as in situ and invasive carcinoma." Am J Pathol 164(3): 925-35.

Mermoud, J. E., Popova, B., Peters, A. H., Jenuwein, T. and Brockdorff, N. (2002). "Histone H3 lysine 9 methylation occurs rapidly at the onset of random X chromosome inactivation." Curr Biol 12(3): 247-51.

Millar, D. S., Paul, C. L., Molloy, P. L. and Clark, S. J. (2000). "A distinct sequence (ATAAA)n separates methylated and unmethylated domains at the 5'-end of the GSTP1 CpG island." J Biol Chem 275(32): 24893-9.

Milutinovic, S., Brown, S. E., Zhuang, Q. and Szyf, M. (2004). "DNA methyltransferase 1 knock down induces gene expression by a mechanism independent of DNA methylation and histone deacetylation." J Biol Chem 279(27): 27915-27.

Muller, H. M., Widschwendter, A., Fiegl, H., Ivarsson, L., Goebel, G., Perkmann, E., Marth, C. and Widschwendter, M. (2003). "DNA methylation in serum of breast cancer patients: an independent prognostic marker." Cancer Res 63(22): 7641-5.

Mummaneni, P., Yates, P., Simpson, J., Rose, J. and Turker, M. S. (1998). "The primary function of a redundant Sp1 binding site in the mouse aprt gene promoter is to block epigenetic gene inactivation." Nucleic Acids Res 26(22): 5163-9.

Mutskov, V. and Felsenfeld, G. (2004). "Silencing of transgene transcription precedes methylation of promoter DNA and histone H3 lysine 9." Embo J 23(1): 138-49.

Ng, H. H., Zhang, Y., Hendrich, B., Johnson, C. A., Turner, B. M., Erdjument-Bromage, H., Tempst, P., Reinberg, D. and Bird, A. (1999). "MBD2 is a transcriptional repressor belonging to the MeCP1 histone deacetylase complex." Nat Genet 23(1): 58-61.

Nguyen, C. T., Weisenberger, D. J., Velicescu, M., Gonzales, F. A., Lin, J. C., Liang, G. and Jones, P. A. (2002). "Histone H3-lysine 9 methylation is associated with aberrant gene silencing in cancer cells and is rapidly reversed by 5-aza-2'-deoxycytidine." Cancer Res 62(22): 6456-61.

Nielsen, S. J., Schneider, R., Bauer, U. M., Bannister, A. J., Morrison, A., O'Carroll, D., Firestein, R., Cleary, M., Jenuwein, T., Herrera, R. E. and Kouzarides, T. (2001). "Rb targets histone H3 methylation and HP1 to promoters." Nature 412(6846): 561-5.

Olsen, C. L., Gardie, B., Yaswen, P. and Stampfer, M. R. (2002). "Raf-1-induced growth arrest in human mammary epithelial cells is p16-independent and is overcome in immortal cells during conversion." Oncogene 21(41): 6328-39.

Ortiz-Vega, S., Khokhlatchev, A., Nedwidek, M., Zhang, X. F., Dammann, R., Pfeifer, G. P. and Avruch, J. (2002). "The putative tumor suppressor RASSF1A homodimerizes and heterodimerizes with the Ras-GTP binding protein Nore1." Oncogene 21(9): 1381-90.

Osley, M. A. (2004). "H2B ubiquitylation: the end is in sight." Biochim Biophys Acta 1677(1-3): 74-8.

Peters, A. H., Mermoud, J. E., O'Carroll, D., Pagani, M., Schweizer, D., Brockdorff, N. and Jenuwein, T. (2002). "Histone H3 lysine 9 methylation is an epigenetic imprint of facultative heterochromatin." Nat Genet 30(1): 77-80.

Philipsen, S. and Suske, G. (1999). "A tale of three fingers: the family of mammalian Sp/XKLF transcription factors." Nucleic Acids Res 27(15): 2991-3000.

Pugh, B. F. and Tjian, R. (1990). "Mechanism of transcriptional activation by Sp1: evidence for coactivators." Cell 61(7): 1187-97.

Qu, G. Z. and Ehrlich, M. (1999). "Demethylation and expression of methylated plasmid DNA stably transfected into HeLa cells." Nucleic Acids Res 27(11): 2332-8.

Rabizadeh, S., Xavier, R. J., Ishiguro, K., Bernabeortiz, J., Lopez-Ilasaca, M., Khokhlatchev, A., Mollahan, P., Pfeifer, G. P., Avruch, J. and Seed, B. (2004). "The scaffold protein CNK1 interacts with the tumor suppressor RASSF1A and augments RASSF1A-induced cell death." J Biol Chem 279(28): 29247-54.

Ramirez, R. D., Morales, C. P., Herbert, B. S., Rohde, J. M., Passons, C., Shay, J. W. and Wright, W. E. (2001). "Putative telomere-independent mechanisms of replicative aging reflect inadequate growth conditions." Genes Dev 15(4): 398-403.

Reuben, M. and Lin, R. (2002). "Germline X chromosomes exhibit contrasting patterns of histone H3 methylation in Caenorhabditis elegans." Dev Biol 245(1): 71-82.

Rhee, I., Bachman, K. E., Park, B. H., Jair, K. W., Yen, R. W., Schuebel, K. E., Cui, H., Feinberg, A. P., Lengauer, C., Kinzler, K. W., Baylin, S. B. and Vogelstein, B. (2002). "DNMT1 and DNMT3b cooperate to silence genes in human cancer cells." Nature 416(6880): 552-6.

Robertson, K. D. (2002). "DNA methylation and chromatin - unraveling the tangled web." Oncogene 21(35): 5361-79.

Robertson, K. D., Ait-Si-Ali, S., Yokochi, T., Wade, P. A., Jones, P. L. and Wolffe, A. P. (2000). "DNMT1 forms a complex with Rb, E2F1 and HDAC1 and represses transcription from E2F-responsive promoters." Nat Genet 25(3): 338-42.

Romanov, S. R., Kozakiewicz, B. K., Holst, C. R., Stampfer, M. R., Haupt, L. M. and Tlsty, T. D. (2001). "Normal human mammary epithelial cells spontaneously escape senescence and acquire genomic changes." Nature 409(6820): 633-7.

Rong, R., Jin, W., Zhang, J., Sheikh, M. S. and Huang, Y. (2004). "Tumor suppressor RASSF1A is a microtubule-binding protein that stabilizes microtubules and induces G2/M arrest." Oncogene 23(50): 8216-30.

Rougeulle, C., Chaumeil, J., Sarma, K., Allis, C. D., Reinberg, D., Avner, P. and Heard, E. (2004). "Differential histone H3 Lys-9 and Lys-27 methylation profiles on the X chromosome." Mol Cell Biol 24(12): 5475-84.

Rountree, M. R., Bachman, K. E. and Baylin, S. B. (2000). "DNMT1 binds HDAC2 and a new co-repressor, DMAP1, to form a complex at replication foci." Nat Genet 25(3): 269-77.

Rountree, M. R., Bachman, K. E., Herman, J. G. and Baylin, S. B. (2001). "DNA methylation, chromatin inheritance, and cancer." Oncogene 20(24): 3156-65.

Sambrook, J., Fritsch, E. F. and T., M. (1989). Molecular cloning. A laboratory manual, Cold Spring Harbor, New York, Cold Spring Harbor Laboratory Press.

Samson, S. L. and Wong, N. C. (2002). "Role of Sp1 in insulin regulation of gene expression." J Mol Endocrinol 29(3): 265-79.

Sandhu, C., Donovan, J., Bhattacharya, N., Stampfer, M., Worland, P. and Slingerland, J. (2000). "Reduction of Cdc25A contributes to cyclin E1-Cdk2 inhibition at senescence in human mammary epithelial cells." Oncogene 19(47): 5314-23.

Santoro, R., Li, J. and Grummt, I. (2002). "The nucleolar remodeling complex NoRC mediates heterochromatin formation and silencing of ribosomal gene transcription." Nat Genet 32(3): 393-6.

Sarraf, S. A. and Stancheva, I. (2004). "Methyl-CpG binding protein MBD1 couples histone H3 methylation at lysine 9 by SETDB1 to DNA replication and chromatin assembly." Mol Cell 15(4): 595-605.

Schneeberger, C., Speiser, P., Kury, F. and Zeillinger, R. (1995). "Quantitative detection of reverse transcriptase-PCR products by means of a novel and sensitive DNA stain." PCR Methods Appl 4(4): 234-8.

Seguin, C. and Hamer, D. H. (1987). "Regulation in vitro of metallothionein gene binding factors." Science 235(4794): 1383-7.

Sherr, C. J. (1996). "Cancer cell cycles." Science 274(5293): 1672-7.

Shiloh, Y. and Kastan, M. B. (2001). "ATM: genome stability, neuronal development, and cancer cross paths." Adv Cancer Res 83: 209-54.

Shivakumar, L., Minna, J., Sakamaki, T., Pestell, R. and White, M. A. (2002). "The RASSF1A tumor suppressor blocks cell cycle progression and inhibits cyclin D1 accumulation." Mol Cell Biol 22(12): 4309-18.

Song, J. Z., Stirzaker, C., Harrison, J., Melki, J. R. and Clark, S. J. (2002). "Hypermethylation trigger of the glutathione-S-transferase gene (GSTP1) in prostate cancer cells." Oncogene 21(7): 1048-61.

Song, M. S., Song, S. J., Ayad, N. G., Chang, J. S., Lee, J. H., Hong, H. K., Lee, H., Choi, N., Kim, J., Kim, H., Kim, J. W., Choi, E. J., Kirschner, M. W. and Lim, D. S. (2004). "The tumour suppressor RASSF1A regulates mitosis by inhibiting the APC-Cdc20 complex." Nat Cell Biol 6(2): 129-37.

Stampfer, M. R. and Yaswen, P. (2003). "Human epithelial cell immortalization as a step in carcinogenesis." Cancer Lett 194(2): 199-208.

Stirzaker, C., Song, J. Z., Davidson, B. and Clark, S. J. (2004). "Transcriptional gene silencing promotes DNA hypermethylation through a sequential change in chromatin modifications in cancer cells." Cancer Res 64(11): 3871-7.

Su, R. C., Brown, K. E., Saaber, S., Fisher, A. G., Merkenschlager, M. and Smale, S. T. (2004). "Dynamic assembly of silent chromatin during thymocyte maturation." Nat Genet 36(5): 502-6.

Suske, G. (1999). "The Sp-family of transcription factors." Gene 238(2): 291-300.

Suzuki, M., Yamada, T., Kihara-Negishi, F., Sakurai, T. and Oikawa, T. (2003). "Direct association between PU.1 and MeCP2 that recruits mSin3A-HDAC complex for PU.1-mediated transcriptional repression." Oncogene 22(54): 8688-98.

Suzuki, T., Kimura, A., Nagai, R. and Horikoshi, M. (2000). "Regulation of interaction of the acetyltransferase region of p300 and the DNA-binding domain of Sp1 on and through DNA binding." Genes Cells 5(1): 29-41.

Tamaru, H. and Selker, E. U. (2001). "A histone H3 methyltransferase controls DNA methylation in Neurospora crassa." Nature 414(6861): 277-83.

Tanese, N., Saluja, D., Vassallo, M. F., Chen, J. L. and Admon, A. (1996). "Molecular cloning and analysis of two subunits of the human TFIID complex: hTAFII130 and hTAFII100." Proc Natl Acad Sci U S A 93(24): 13611-6.

Tang, D. G., Tokumoto, Y. M., Apperly, J. A., Lloyd, A. C. and Raff, M. C. (2001). "Lack of replicative senescence in cultured rat oligodendrocyte precursor cells." Science 291(5505): 868-71.

Tatematsu, K. I., Yamazaki, T. and Ishikawa, F. (2000). "MBD2-MBD3 complex binds to hemi-methylated DNA and forms a complex containing DNMT1 at the replication foci in late S phase." Genes Cells 5(8): 677-88.

Tlsty, T. D., Romanov, S. R., Kozakiewicz, B. K., Holst, C. R., Haupt, L. M. and Crawford, Y. G. (2001). "Loss of chromosomal integrity in human mammary epithelial cells subsequent to escape from senescence." J Mammary Gland Biol Neoplasia 6(2): 235-43.

Tomatsu, S., Orii, K. O., Bi, Y., Gutierrez, M. A., Nishioka, T., Yamaguchi, S., Kondo, N., Orii, T., Noguchi, A. and Sly, W. S. (2004). "General implications for CpG hot spot mutations: methylation patterns of the human iduronate-2-sulfatase gene locus." Hum Mutat 23(6): 590-8.

Tommasi, S., Dammann, R., Zhang, Z., Wang, Y., Liu, L., Tsark, W. M., Wilczynski, S. P., Li, J., You, M. and Pfeifer, G. P. (2005). "Tumor susceptibility of Rassf1a knockout mice." Cancer Res 65(1): 92-8.

Tommasi, S. and Pfeifer, G. P. (1995). "In vivo structure of the human cdc2 promoter: release of a p130-E2F-4 complex from sequences immediately upstream of the transcription initiation site coincides with induction of cdc2 expression." Mol Cell Biol 15(12): 6901-13.

Torigoe, T., Izumi, H., Wakasugi, T., Niina, I., Igarashi, T., Yoshida, T., Shibuya, I., Chijiiwa, K., Matsuo, K. I., Itoh, H. and Kohno, K. (2004). "DNA topoisomerase II poison TAS-103 transactivates GC-box-dependent transcription via acetylation of Sp1." J Biol Chem.

Turner, J. and Crossley, M. (1999). "Mammalian Kruppel-like transcription factors: more than just a pretty finger." Trends Biochem Sci 24(6): 236-40.

Vos, M. D., Ellis, C. A., Bell, A., Birrer, M. J. and Clark, G. J. (2000). "Ras uses the novel tumor suppressor RASSF1 as an effector to mediate apoptosis." J Biol Chem 275(46): 35669-72.

Vos, M. D., Martinez, A., Elam, C., Dallol, A., Taylor, B. J., Latif, F. and Clark, G. J. (2004). "A role for the RASSF1A tumor suppressor in the regulation of tubulin polymerization and genomic stability." Cancer Res 64(12): 4244-50.

Wang, T. C., Cardiff, R. D., Zukerberg, L., Lees, E., Arnold, A. and Schmidt, E. V. (1994). "Mammary hyperplasia and carcinoma in MMTV-cyclin D1 transgenic mice." Nature 369(6482): 669-71.

Won, J., Yim, J. and Kim, T. K. (2002). "Sp1 and Sp3 recruit histone deacetylase to repress transcription of human telomerase reverse transcriptase (hTERT) promoter in normal human somatic cells." J Biol Chem 277(41): 38230-8.

Wu, J., Issa, J. P., Herman, J., Bassett, D. E., Jr., Nelkin, B. D. and Baylin, S. B. (1993). "Expression of an exogenous eukaryotic DNA methyltransferase gene induces transformation of NIH 3T3 cells." Proc Natl Acad Sci U S A 90(19): 8891-5.

Xiong, Z. and Laird, P. W. (1997). "COBRA: a sensitive and quantitative DNA methylation assay." Nucleic Acids Res 25(12): 2532-4.

Yan, P. S., Shi, H., Rahmatpanah, F., Hsiau, T. H., Hsiau, A. H., Leu, Y. W., Liu, J. C. and Huang, T. H. (2003). "Differential distribution of DNA methylation within the RASSF1A CpG island in breast cancer." Cancer Res 63(19): 6178-86.

Yaswen, P. and Stampfer, M. R. (2002). "Molecular changes accompanying senescence and immortalization of cultured human mammary epithelial cells." Int J Biochem Cell Biol 34(11): 1382-94.

Yokota, T., Matsuzaki, Y., Miyazawa, K., Zindy, F., Roussel, M. F. and Sakai, T. (2004). "Histone deacetylase inhibitors activate INK4d gene through Sp1 site in its promoter." Oncogene 23(31): 5340-9.

Zhang, Y. and Dufau, M. L. (2002). "Silencing of transcription of the human luteinizing hormone receptor gene by histone deacetylase-mSin3A complex." J Biol Chem 277(36): 33431-8.

Zhu, W. G., Srinivasan, K., Dai, Z., Duan, W., Druhan, L. J., Ding, H., Yee, L., Villalona-Calero, M. A., Plass, C. and Otterson, G. A. (2003). "Methylation of adjacent CpG sites affects Sp1/Sp3 binding and activity in the p21(Cip1) promoter." Mol Cell Biol 23(12): 4056-65.

Zipper, H., Brunner, H., Bernhagen, J. and Vitzthum, F. (2004). "Investigations on DNA intercalation and surface binding by SYBR Green I, its structure determination and methodological implications." Nucleic Acids Res 32(12): e103.

7   Supplementary data

Table 7-1. Expression of *RASSF1A* and *RASSF1C* in the different human tissues

	RASSF1A		*RASSF1C*	
	Average	Standard deviation	Average	Standard deviation
Heart	56.92%	7.68%	42.45%	5.16%
Brain	3.29%	0.52%	7.11%	1.01%
Placenta	26.42%	13.62%	26.04%	0.00%
Lung	43.75%	5.16%	58.72%	8.65%
Liver	67.66%	0.00%	41.15%	8.12%
Sk. Muscle	1.30%	0.98%	2.58%	0.72%
Kidney	8.98%	2.02%	30.13%	5.91%
Pancreas	100.00%	24.00%	100.00%	1.10%

Table 7-2. Analysis of the *RASSF1A* and *RASSF1C* expressions in the different cell lines

	RASSF1A		*RASSF1C*	
	Average	Standard deviation	Average	Standard deviation
PBMC	197.28%	6.79%	146.74%	7.61%
HeLa	115.93%	3.12%	67.12%	4.07%
HF	100.00%	2.74%	100.00%	4.95%
Mammary gland	8.16%	1.54%	7.88%	3.93%
pre-stasis	15.81%	1.86%	155.42%	52.08%
stasis	6.65%	2.03%	904.25%	1431.44%
post-stasis	3.71%	1.95%	260.02%	361.78%
T47D	0.21%	0.20%	110.57%	5.92%
T47D Aza	2.54%	0.94%	91.78%	0.40%
ZR75-1	0.72%	0.63%	336.61%	29.97%
ZR75-1 Aza	3.22%	0.34%	277.66%	36.46%
MCF7	0.00%	0.00%	99.19%	11.49%
MCF7 Aza	3.42%	0.47%	190.25%	18.16%

Table 7-3. Analysis of the *RASSF1A* and *RASSF1C* expressions in HMEC-184 and HMEC-48R

	RASSF1A		*RASSF1C*	
	Average	Standard deviation	Average	Standard deviation
184 p3	16.85%	0.81%	207.22%	71.97%
184 p6	14.83%	1.29%	174.81%	11.17%
184 stasis	8.89%	0.79%	2557.12%	489.56%
184 p7	2.88%	0.64%	187.42%	28.19%
184 p8	2.27%	0.32%	32.44%	10.29%
48R p3	17.47%	1.69%	105.55%	16.87%
48R p4	13.02%	0.82%	195.15%	36.20%
48R stasis	4.93%	0.97%	70.58%	0.31%
48R p6	5.74%	1.10%	207.31%	42.48%
48R p8	3.02%	0.69%	95.81%	11.63%
48R p12	3.01%	0.57%	178.78%	12.28%
48R p16	1.98%	0.79%	83.93%	0.68%

Table 7-4. The *RASSF1A* and *RASSF1C* expressions in HMEC-184 passage13 after 5-Aza-CdR treatment.

	RASSF1A		*RASSF1C*	
	Average	Standard deviation	Average	Standard deviation
Control	100.00%	0.00%	100.00%	0.00%
Aza treatment	393.00%	32.19%	115.00%	7.81%

Table 7-5. The *p16*^{INK4} expression pattern in HMEC-141 and HMEC-219.

	Average	Standard deviation
HeLa	100.00%	0.00%
HF	3.81%	0.08%
HMEC-141 p2	26.10%	6.36%
HMEC-141 stasis	87.80%	17.41%
HMEC-219 p7	0.52%	0.20%
HMEC-219 p11	0.40%	0.17%
HMEC-219 p14	0.38%	0.09%

Table 7-6. Frequency of acetylated histone H3 in the *RASSF1A* and *RASSF1C* promoters.

| | *RASSF1A* | | | | *RASSF1C* | |
| | A2 | | A1 | | C | |
	Average	Standard deviation	Average	Standard deviation	Average	Standard deviation
HeLa	1126.03%	460.81%	778.00%	115.66%	329.38%	140.57%
HMEC p6	281.34%	27.51%	290.24%	23.86%	285.37%	36.77%
HMEC p12	145.04%	15.50%	121.93%	21.20%	446.18%	91.26%
ZR75-1	38.48%	5.11%	35.35%	3.91%	150.46%	4.39%

Table 7-7. Frequency of trimethylated histone H3 lysine 9 in the *RASSF1A* and *RASSF1C* promoters.

| | *RASSF1A* | | | | *RASSF1C* | |
| | A2 | | A1 | | C | |
	Average	Standard deviation	Average	Standard deviation	Average	Standard deviation
HeLa	5.75%	4.50%	4.97%	4.09%	3.39%	3.50%
HMEC p6	21.19%	1.36%	19.42%	2.08%	10.39%	4.62%
HMEC p12	19.95%	6.44%	42.45%	10.05%	4.40%	3.02%
ZR75-1	1.38%	0.88%	1.71%	1.03%	2.05%	0.62%

Table 7-8. The *Sp1* binding to the *RASSF1A* and *RASSF1C* promoters.

| | *RASSF1A* | | | | *RASSF1C* | |
| | A2 | | A1 | | C | |
	Average	Standard deviation	Average	Standard deviation	Average	Standard deviation
HeLa	3.65%	2.20%	10.32%	3.14%	11.31%	7.39%
HMEC p6	7.70%	1.14%	13.35%	0.30%	13.43%	1.21%
HMEC p12	-0.33%	1.41%	1.78%	0.61%	32.07%	5.59%
ZR75-1	1.27%	0.36%	2.45%	1.49%	21.09%	2.35%

Halle (Saale), den 10. Oktober 2005

Erklärung

Hiermit erkläre ich, Maria Hahn, geb. Strunnikova, die vorliegende Arbeit selbständig und nur unter Verwendung der angegebenen Hilfsmittel angefertigt zu haben.

Maria Hahn, geb. Strunnikova

CURRICULUM VITAE

Name:	Maria, Hahn, geb. Strunnikova
Degree:	Master of Science
Birth date:	01 February 1977
Birth place:	Sankt-Petersburg
Citizenship:	Russia

Education

2001-2005 TG WG, Medical Faculty, Martin-Luther University, Halle (S.), Germany
PhD-student
PhD thesis scientific area: Biology

1999-2001 Individual program: Cytogenetics, Department of Genetics and Selective Breeding, Faculty of Biology and Soil Sciences, St-Petersburg State University, Russia
Degree: **Master of Science**.

1994-1998 Department of Genetics and Selective Breeding, Faculty of Biology and Soil Sciences, St-Petersburg State University, Russia
Degree: **Bachelor**

1992-1994 Small Biological Faculty for school students, St-Petersburg State University, Russia

1984-1994 Physical-mathematical school №239, St-Petersburg, Russia

Publications:

1. *Strunnikova M.*, Schagdarsurengin U., Kehlen A., Garbe J.C., Stampfer M.R. and Dammann R. (2005) Chromatin inactivation precedes de novo DNA methylation during the progressive epigenetic silencing of the RASSF1A promoter. Mol Cell Biol. 2005 May;25(10):3923-33.
2. Dammann R., *Strunnikova M.*, Schagdarsurengin U., Rastetter M., Papritz M., Hofman S., Silber R., Burdach S. and Hansen G. (2005) Aberrant methylation andexpression of tumor associated genes in lung carcinoma. Eur J Cancer. 2005 May;41(8):1223-36
3. Dammann R., Schagdarsurengin U., Seidel C., *Strunnikova M.*, Rastetter M., Baier K,. Pfeifer G.P.(2005) The tumor suppressor RASSF1A in human carcinogenesis: an update. Histol Histopathol. Apr; 20 (2) 645-663.
4. Dammann R, Schagdarsurengin U, *Strunnikova M*, Rastetter M, Seidel C, Liu L, Tommasi S, Pfeifer GP.(2003) Epigenetic inactivation of the Ras-association domain family 1 (*RASSF1A*) gene and its function in human carcinogenesis. Histol Histopathol. Apr;18 (2):665-77.
5. Kisliakova TV, Kustova ME, Lianguzova MS, Malashcheva AB, *Strunnikova MA*, Suchkova IO, Pospelov VA, Patkin EL. (2000) Non induced single strand DNA breaks in F9 teratocarcinoma cells of mouse. Tsytologiia 42(11):1060-8.

Thanks

I would like to tell a lot of thanks to my supervisor Dr. Reinhard Dammann for very interesting project, help at every phase of my PhD work and very interesting scientific discussions.

I am very thankful to Prof. Dr. G. Pfeifer and Prof. Dr. G. Reuter, since they accepted to be reviewers of my PhD thesis.

To all members of my working group, I would like to tell thanks for nice work together.

To my colleagues from Human Genetic Institute, I am very thankful for the nice working atmosphere.

To Usha Dutta, I would like tell thanks for checking English grammar of my PhD thesis.

To my friend, Torsten Hahn, I would like to tell a lot of thanks, since he have done everything that I can perform present study.

I would like to tell a lot of thanks to my big Russian-German family for psychological support and for love, which helped me to perform present research.